Igneous-Rock Hosted Orogenic Gold Deposit at Hog Mountain, Tallapoosa County, Alabama

by

Safak Ozsarac

A thesis submitted to the Graduate Faculty of
Auburn University
in partial fulfillment of the
requirements for the Degree of
Master of Science

Auburn, Alabama
December 10th, 2016

Keywords: Orogenic Gold, Hog Mountain,
Tallapoosa County, Alabama

Approved by

James A. Saunders, Chair, Professor of Geosciences
Mark Steltenpohl Professor of Geosciences
Zeki Billor, Research Fellow of Geosciences

Abstract

The Hog Mountain gold deposit is located in northern Tallapoosa County, Alabama and is part of the historic Goldville mining district. Hog Mountain is geologically located in the eastern Blue Ridge consisting of phyllites, schists, and a Carboniferous tonalite pluton. The Hog Mountain deposit has been mined for gold episodically since 1893 producing ~17,000 troy ounces. Gold at Hog Mountain is hosted in quartz veins within the tonalite pluton and are thought to be orogenic in origin. Sixteen major veins have been identified and successfully mined in the past. Three of these quartz veins, namely the Blue, Kennedy, and Sugar Quartz veins were analyzed for this study. In particular, geochemical studies were carried out on the Blue vein, which is the largest in Hog Mountain. Several quartz textures including planar deformation lamellae, undulose extinction, and polygonal grains were identified using transmitted light microscopy studies. Petrographic studies of the samples were conducted in both reflected and transmitted light. Based on the reflected light studies on polished sections, gold is associated with sulfide minerals including pyrrhotite, pyrite, chalcopyrite, arsenopyrite, and galena. The most dominant sulfide mineral is pyrrhotite, which occurs as big masses, remobilized grains, and filling fractures. Geochemical analyses from the Blue Vein indicate that there are strong correlations between gold (Au) and tellurium (Te), gold (Au) and bismuth (Bi), and bismuth (Bi) and tellurium (Te). Alteration types, geochemistry, and general geologic setting of the Hog Mountain mine have many similarities compared to typical other quartz vein-hosted gold systems including Otago

schist, New Zealand, and Bendigo-Ballarat area of Victoria, Australia. Newmont Mining Corporation did drilling at the property in the early 1980s, but current exploration at Hog Mountain is being conducted by Wellborn Mining Company. More than a hundred core holes have been drilled since 2010 on the property based on magnetic anomalies apparently caused by elevated pyrrhotite. Drilling continues to date at Hog Mountain and as of yet, no decision has been made concerning the economics of actual mining.

Acknowledgments

I would like to thank my thesis advisor, Dr. James Saunders, whose supports was invaluable in every conceivable way. This thesis would never have been written without his efforts and advice. I would also like to thank my other committee members, Dr. Mark Steltenpohl and Dr. M. Zeki Billor, for their welcome contributions to this research.

I would like to thank Mark Whitney, who is a consultant at Wellborn Mining Company, for his aid in planning and carrying out the field work on Hog Mountain, helping me on every stage of core logging. I also like to thank Phil Padgett for his hospitality and vast knowledge of local geology and mining history during the field work at Hog Mountain. I would also thank the Turkish Ministry of National Education for providing me a Master's scholarship. Without this support, this research would have not been possible.

Finally, I would like to send out all of the thanks and appreciation that I can for my family, especially my dad, my brother Vedat, and brother-in-law Caglar. The support they have shown me throughout my life will never be eclipsed, and my gratitude is endless. I also thank all the people who helped me at various times throughout my project. Thank you to Aziz Sen and Yazgan Kirkayak for commenting on microscopic studies of the project, and Enis Baltaci for sampling related to the project. Throughout the project, discussions with many of my fellow graduate students, especially Ziaul Haque

and Jason Fisher helped focus and strengthen this thesis, and to them I am grateful. Thank you so much.

Style manual or journal used: Economic Geology

Computer software used: Microsoft Excel, Microsoft Word, Microsoft PowerPoint, Microsoft Paint, Arcgis 10.

Table of Contents

List of Tables

List of Figures

1. INTRODUCTION

1.1 Orogenic Gold Deposits

Orogenic gold ores are a type of hydrothermal Au deposit that forms during regional tectonism. Orogenic gold deposits are formed at depths of 2 to 20 km (Groves et al., 2003), relatively great pressure (1.5-5 kbar), and typically high-temperatues (300-500 ^{0}C). These Au deposits are alternatively known as "lode Au deposits", "quartz-vein Au deposits", "Au-only deposits" or "mesothermal Au deposits" (Ridley, 2013). Due to the broad depth range of formation, the term 'mesothermal' is not appropriate to this type of deposit. Therefore, according to their depth of formation, the orogenic gold deposits are best subdivided into epizonal (<6 km), mesozonal (6-12 km), and hypozonal (>12 km) classes (Groves et al., 1998) (Fig. 1). Thus, orogenic gold deposits are a distinctive class of mineral deposit that has been the source for much of world gold production (Bohlke, 1982; Groves et al., 1998; Hagemann and Brown, 2000).

Orogenic gold deposits have formed during more than 3 billion years of Earth's history, episodically during the Middle Archean to younger Precambrian, and continuously throughout the Phanerozoic. The orogenic gold deposits are found in three different broad temporal/geologic settings (Goldfarb et al., 2001; Saunders et al., 2014). They are: (1) ores hosted in Late Archean greenstone were mainly formed between 2750 and 2520 Ma in granitoid-greenstone terranes worldwide; (2) ores dated between 2100 and 1730 that Ma hosted by Paleoproterozoic sedimentary and volcanic rocks

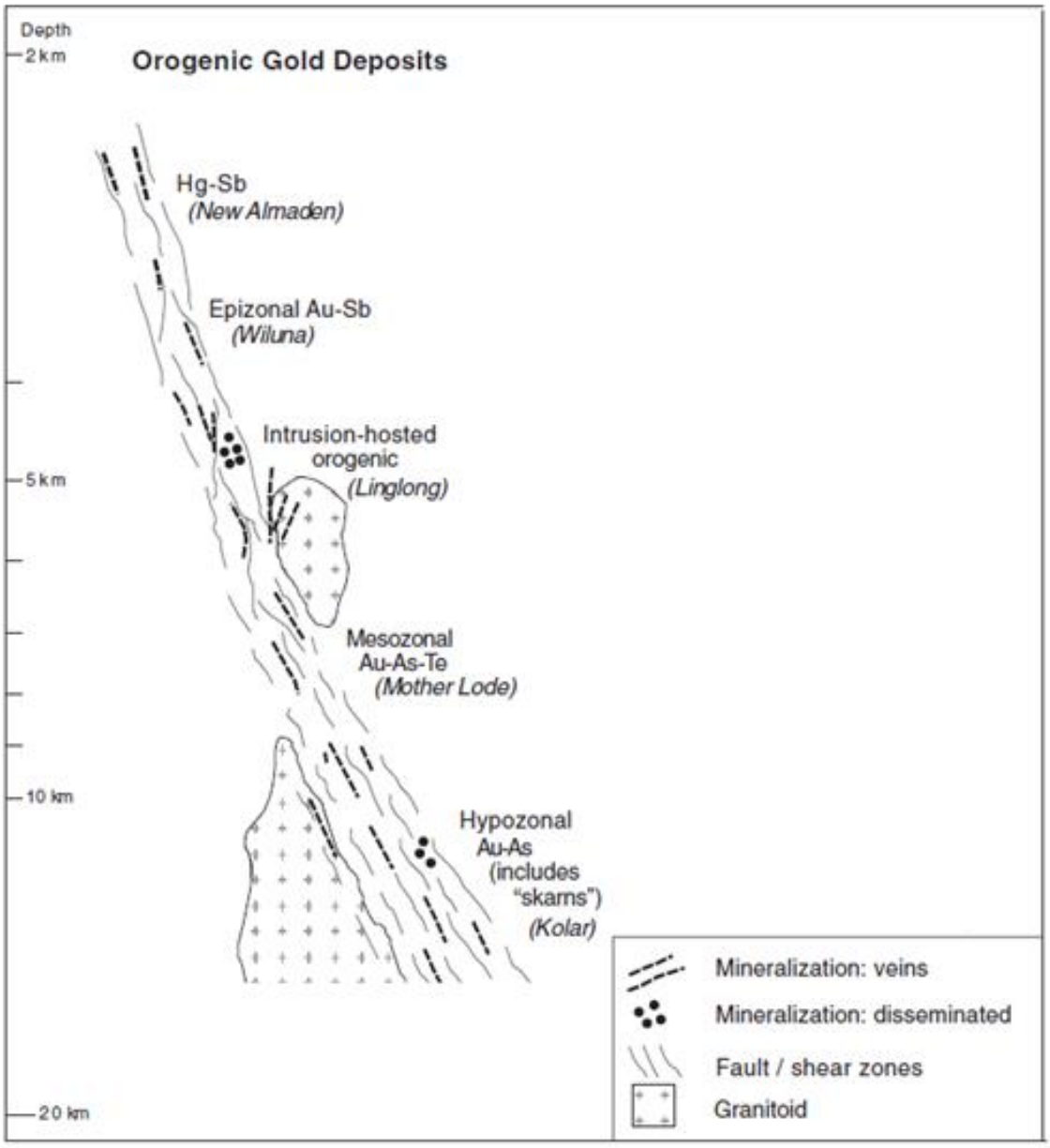

Figure 1: Interpreted settings of orogenic gold types in metamorphic terranes. Epizonal, mesozonal, and hypozonal orogenic gold deposits are associated with regional fluid flow along major deep-crustal fault zone and form at depths of 2 to 20 km. After Groves et al., (2003).

deposited on the margins to the granitoid-greenstone terranes; and (3) ores formed between ~650 and 50 Ma in marine sedimentary rocks (Saunders et al., 2014) (Fig. 2). These gold deposits are associated with deformed and metamorphosed mid-crustal rocks, particularly in spatial association with major crustal structures (Goldfarb et al., 2001)

Orogenic gold deposits are associated with regionally metamorphosed terranes of all ages (Kerrich and Cassidy, 1994) and are spatially linked to subduction-related thermal processes (Kerrich and Wyman, 1990) (Fig. 3). These metal concentrations formed during compressional to transpressional deformation processes at convergent plate margins in accretionary (oceanic-continental plate interaction) and collisional (continental-continental collision) orogens (Bohlke, 1982; Groves et al., 1998; Hagemann and Brown, 2000) (Fig 3).

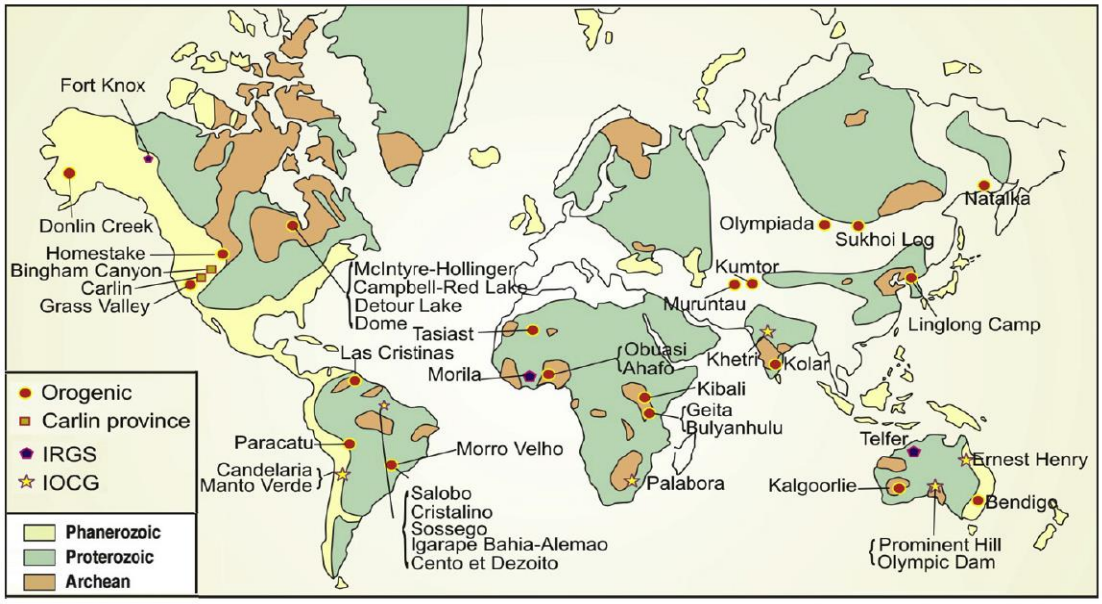

Figure 2: Schematic map of world showing giant orogenic gold, Carlin-type, Intrusion-related gold deposits (IRGD) and Iron oxide copper gold ore deposits(IOCG) (Groves et al., 2015).

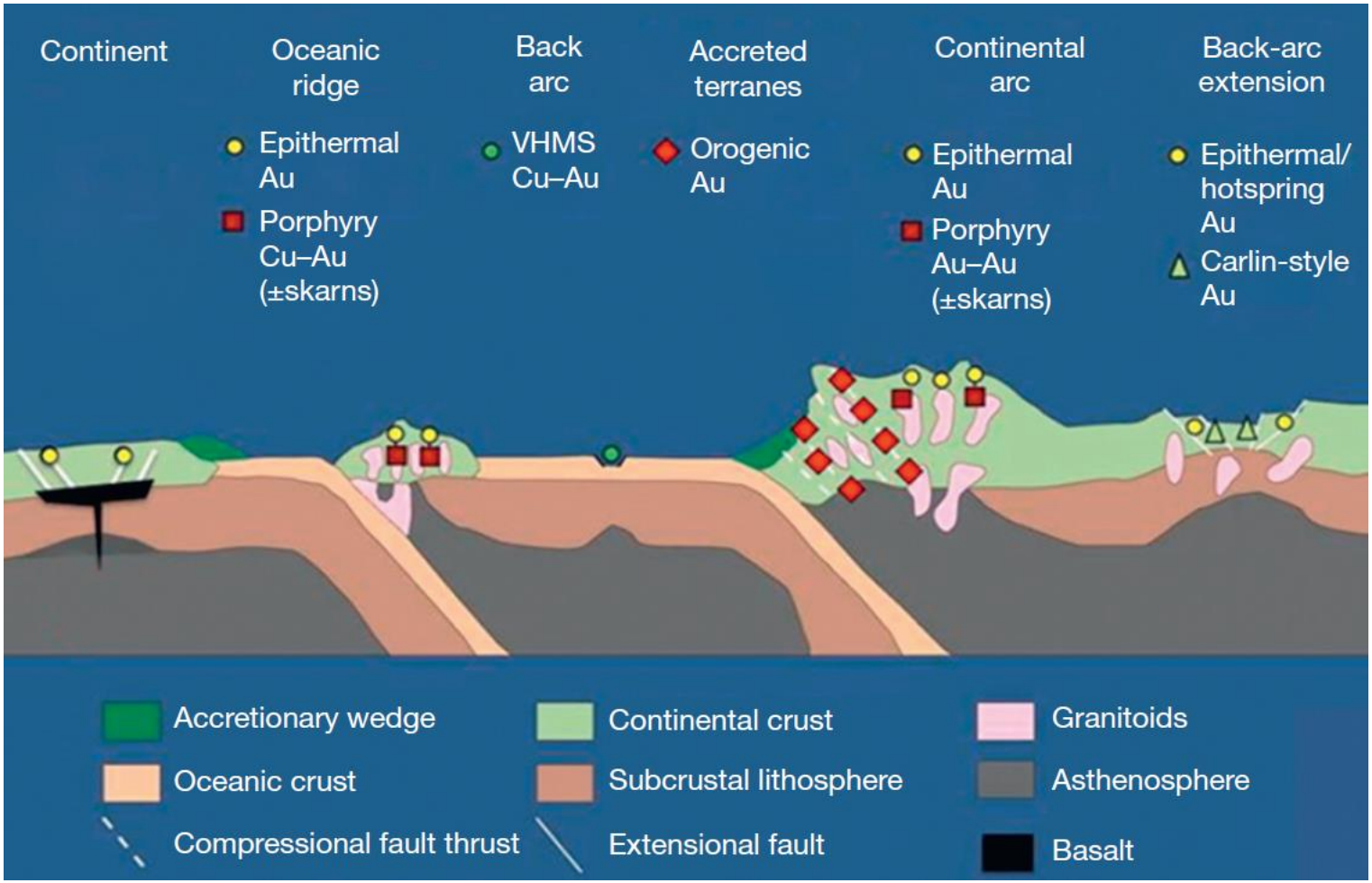

Figure 3: Schematic diagram of different gold deposit classes based on their plate tectonic settings (Groves et al., 1998; Saunders et al., 2014).

1.2 History of Orogenic Gold Deposit Models

In the Early 1980s, 'Mesothermal' is the term that was widely used and adopted for orogenic gold deposits, but it is a term that originally was defined by Lindgren (1933). Workers at the U.S. Geological Survey initially termed the epigenetic, structurally hosted lode gold deposits in metamorphic rocks as orogenic gold deposits (e.g., Bohlke, 1982). However, these deposits were divided into low sulfide gold-bearing quartz (Phanerozoic) and Homestake (Precambrian) gold deposit types in later mineral deposits models (e.g., Berger, 1986; Goldfarb et al., 2005). The orogenic gold deposits are predominant and are recognized to be broadly coincidence with metamorphism, magmatism, and deformation during lithospheric-scale continental-margin orogeny (Groves et al., 1998).

The term orogenic gold deposits was introduced and justified by Gebre-Mariam et al. (1995) and Groves et al. (1998) as a term to replace 'mesothermal'. They mainly pointed out that orogenic gold deposits, whether of Precambrian or Phanerozoic age, had significant features in common including their very late to post-peak metamorphic timing and their tectonic setting most consistently being in a metamorphosed fore-arc or back-arc (Fig. 3). This term has been followed and accepted by Goldfarb et al. (2001, 2005, 2014) and Bierlin et al., (2006). However, there is still some discussion on terminology (e.g., Phillips and Powell, 2015) and a debate on the genesis of orogenic gold deposits (Groves and Santosh, 2015). A review for these genetic models and the various geological, geochemical, isotopic and fluid-inclusion constraints on these models was provided by Goldfarb and Groves (2015) and Groves and Santosh, (2015) (Fig 4).

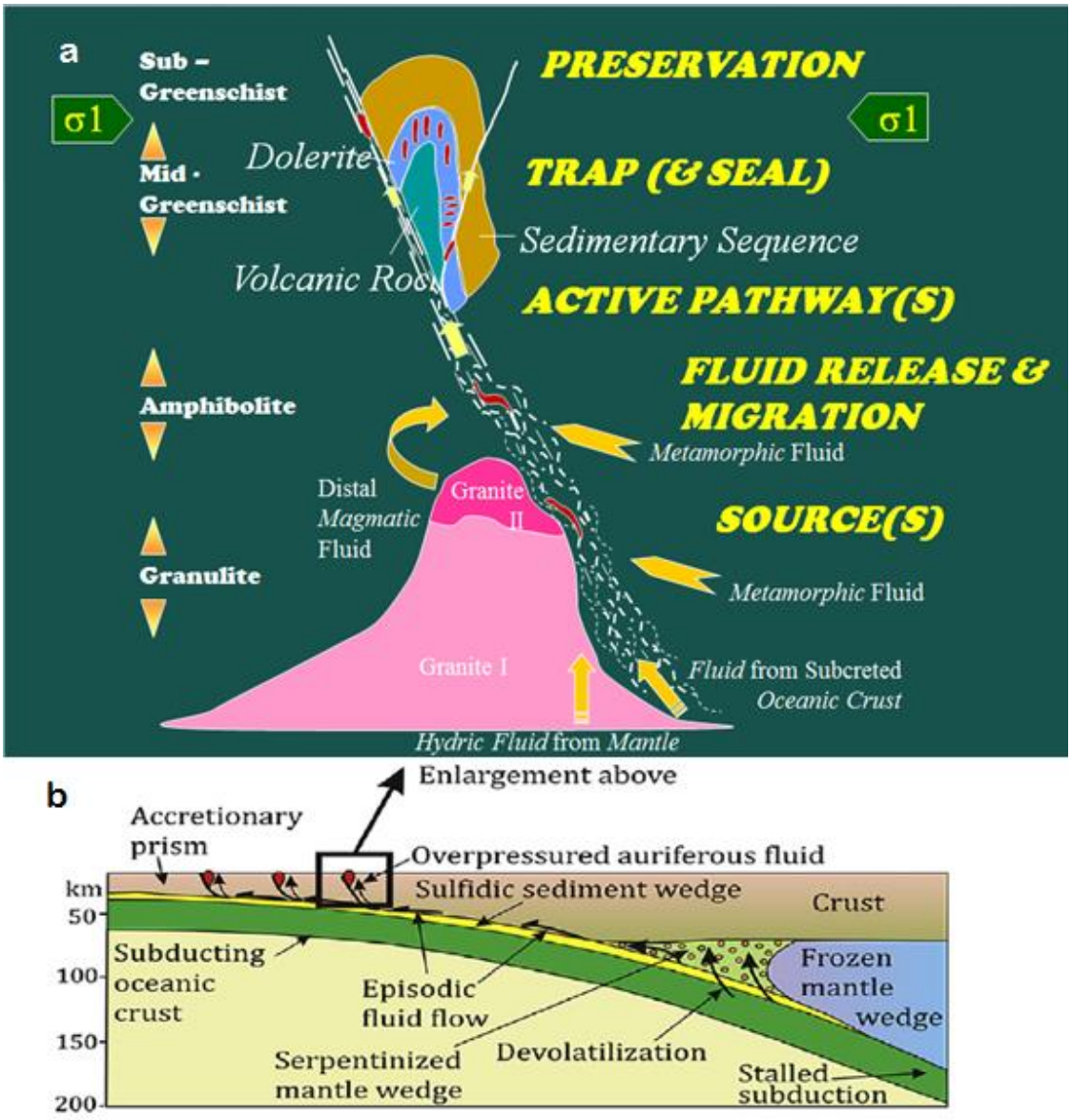

Figure 4: Schematic representation of orogenic gold deposits, including those in high-grade metamorphic rocks, involving a subcrustal fluid and metal source from slab devolatilization. (a) Where these overpressured slab-derived fluids intersect deep-crustal faults, they move upward to form orogenic gold deposits. (b) Fluids released during devolatilization of the subducting slab (Groves and Santosh, 2015).

1.3 Objective of Study

The main objective of this study is to understand the genesis of ores at the Hog Mountain deposit in the Alabama Appalachian Piedmont, which is thought to be an orogenic deposit. The research seeks to better understand the ore and gangue mineralogy and the geochemistry of the veins to help with future exploration. This is accomplished by: (1) describing the gangue mineral textures present in the ore samples from the sulfide-bearing quartz veins; (2) characterizing the ore mineralogy in the quartz veins; and (3) determining the source of gold in the igneous-rock-hosted quartz veins via geochemical analysis. This study will also lead to better understanding of where the gold within the quartz veins was derived.

2. PREVIOUS WORKS

Pardee and Park (1948) observed at least 16 well-defined quartz veins from surface cuts and shallow workings that cut the pluton at Hog Mountain. The thickest two of the veins are called the Blue vein and Barren vein. Pardee and Park (1948) found that the presence and orientation of the veins preclude their origin by the theory of tension cracks formed during the cooling of the tonalite as suggested by Aldrich (1909) and Park (1935). In a few places the veins widen near the contact to form pipe-shaped ore bodies. Aldrich (1909) and Park (1935) also observed that tension fissures, sheeted zones, and joint planes have apparently influenced silicification in many places. The same authors reported total production of gold at Hog Mountain between 1893 and 1915 was 12,500 troy ounces and between 1934 and 1935 another 4,800 troy ounces. The mine was idle between 1916 and 1933, and 1936 to date.

Guthrie and Lesher (1989) described the general geologic setting of lode gold deposits in the Northern Piedmont and Brevard zone. According to their study, lode gold mineralization in Alabama occurs in 13 principal districts in the Northern Piedmont and Brevard zone that can be subdivided into three groups on the basis of host rock lithology: (1) metasediment-hosted deposits (Riddle's Mill, Gold Ridge, Cragford, Goldville, Eagle Creek, and Devil's Backbone districts); (2) mixed metasediment-metavolcanic-hosted deposits (Chilton County, Arbacoochee, Chulafinnee, Coosa County, Idaho, and Turkey Heaven Mountain districts); and (3) granitoid-hosted deposits (Hog Mountain area and Dutch Bend deposits) (Fig 5).

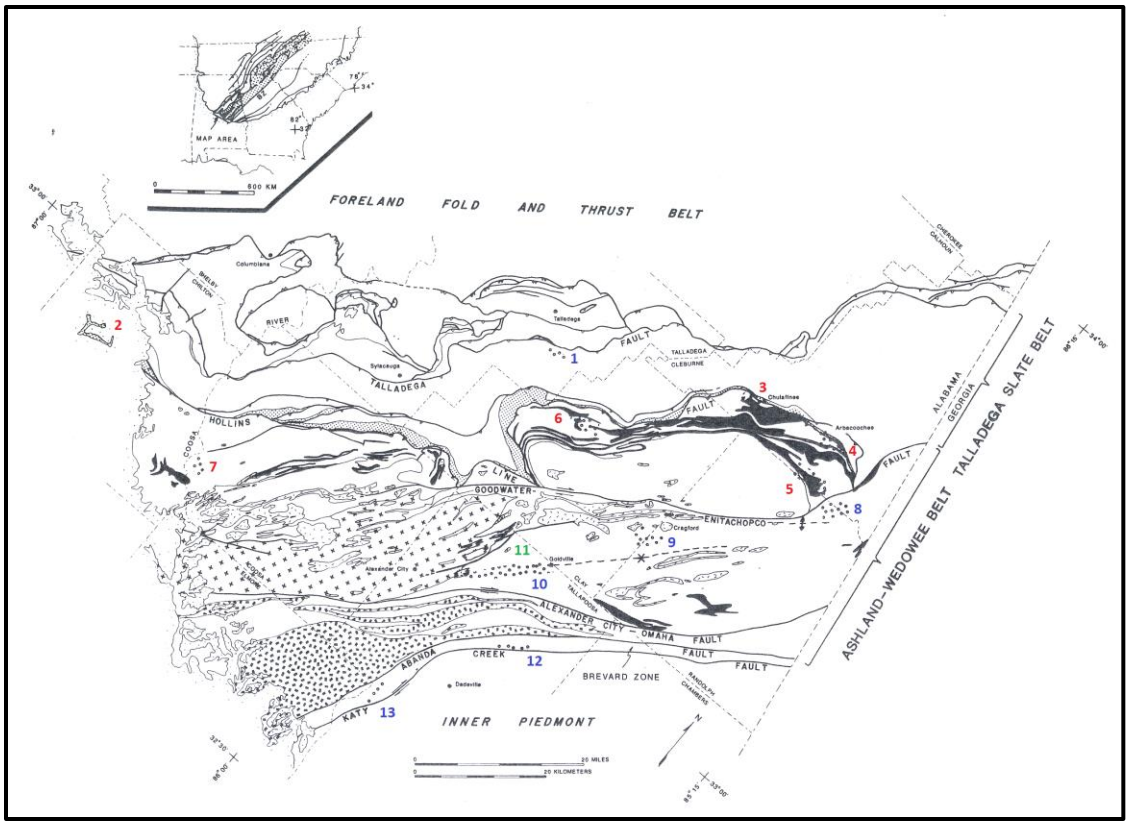

Figure 5: Generalized geologic map of the Northern Piedmont and Brevard zone showing the distribution of gold mining districts (modified after Neathery and Reynolds (1975), Osborne et al. (1988), Guthrie (1989), Guthrie and Dean (1989)). Mining districts: (1) Riddle's Mill; (2) Chilton County; (3) Chulafinnee; (4) Arbacoochee; (5) Turkey Heaven Mountain; (6) Idaho; (7) Coosa County; (8) Gold Ridge; (9) Cragford; (10) Goldville; (11) Hog Mountain; (12) Eagle Creek, and (13) Devil's Backbone. Large random dots = mining districts; small dots = Hillabee Greenstone; black = amphibolites; crosses = Elkahatchee Quartz Diorite Gneiss; random dashes = Devonian to Mississippian granitoids; double dashes = Zana Granite and Kowaliga Gneiss. Blue color numbers indicate metasediment-hosted deposits, red color numbers indicate mixed metasediment-metavolcanic-hosted deposits, and green color numbers granitoid-hosted deposits. (Modified from Guthrie and Lesher (1989)).

Guthrie and Lesher (1989) also mentioned that gold had been mined primarily from weathered zones of quartz ± sulfide ± carbonate ± feldspar veins or from placers associated with these gold deposits. Granitoid-hosted deposits are characterized by extensive quartz-sericite-sulfide wall rock alteration and associated sulfides that include abundant pyrrhotite, pyrite, minor chalcopyrite, sphalerite, and rare arsenopyrite. Guthrie and Lesher's (1989) study shows that mineralization is generally restricted to zones of synkinematic quartz veins within a variety of host rocks, suggesting that most deposits in the area are epigenetic. Wall-rock alteration is extensive in granitoid-hosted deposits. Guthrie and Lesher (1989) found that ore-forming fluids probably were derived from devolatilization reactions deeper in the metamorphic pile and ascended along zones of structurally enhanced permeability and were emplaced into dilatant zones in host rocks during or slightly after peak metamorphism. Their study indicates that gold mineralization at Hog Mountain is associated with early quartz ± sulfide ± carbonate and later calcite-quartz ± sulfide veins. Foliated to massive quartz-sericite-sulfide alteration envelopes and borders all veins and pyrrohotite, chalcopyrite, sphalerite, minor arsenopyrite, and rare molybdenite are the sulfide minerals.

Stowell et al. (1996) provided a detailed fluid inclusion, petrologic, stable isotope data, and whole-rock geochemical data on metavolcanic, metaplutonic, and metasedimentary rock-hosted lode gold mineralization in the southernmost part of the Appalachians. Stowell et al. (1996) aimed to develop a model for gold mineralization by using these data that takes into account the relationship between gold mineralization, host-rock lithology, and metamorphism. Five mines in the Blue Ridge were chosen for their study: Anna Howe and Royal Vindicator mines hosted by metavolcanic rocks of the

Hillabee Greenstone, the Hog Mountain mine hosted by carboniferous tonalite, and the Lowe, Tallapoosa, and Jones vein mines (Goldville district) hosted by metasedimentary rocks of the Wedowee Group (Fig. 6). Stowell et al. (1996) concluded that gold mineralization is: (1) epigenetic, which means the ore fluids were derived from a metasedimentary source deeper in the crust; (2) that veins were emplaced during metamorphism and second and third phases of the regional deformation; and (3) these events occurred during Carboniferous Alleghanian orogenic phase. Their study indicates that metamorphism and mineralization probably occurred during shortening and overthrusting of allochthons over sedimentary rocks of the autochthonous North American margin**.** However, Adams (1930) and Pardee and Park (1948) had interpreted that gold mineralization in the Goldville district formed by igneous activity.

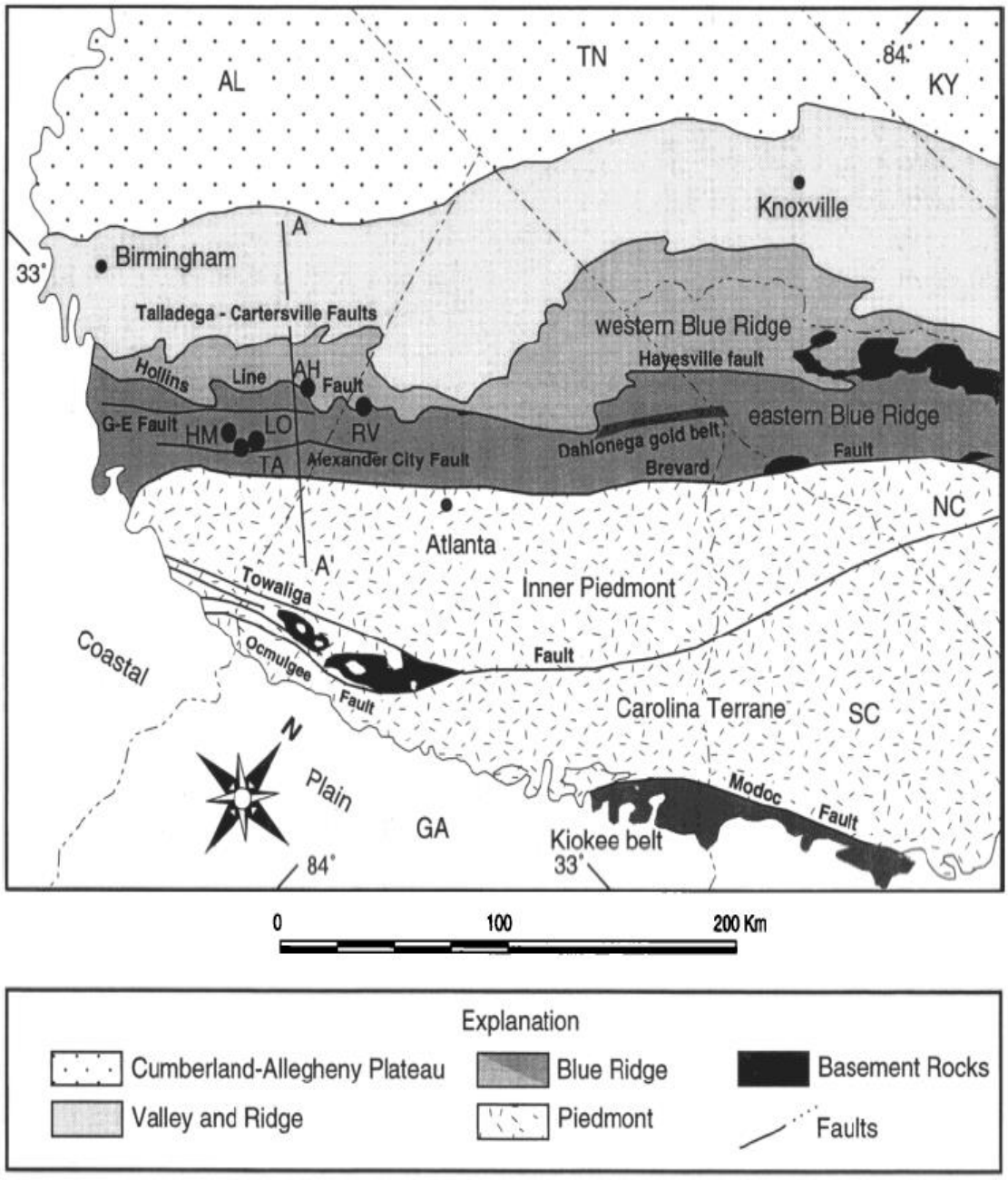

Figure 6: Generalized geologic map of southern Appalachians showing the Anna Howe (AH), Royal Vindicator (RV), Hog Mountain (HM), Tallapoosa (TA), and Lowe (LO) gold mines in the southernmost Blue Ridge. G-E = Goodwater-Enitachopco fault. Tectonic belts and faults are modified from Hooper and Hatcher (1988), Steltenpohl et al. (1995), and Hatcher et al. (1990). From Stowell et al. (1996).

Saunders et al. (2013) described some of the recent exploration and geology of gold occurrences in the most productive part of the Alabama Piedmont. They noted that there is a strong association of gold and arsenic in bedrock, saprolite, and soils, which reflects the mineralogical association of gold with arsenian pyrite and arsenopyrite in mineralized zones (Fig. 7) (Saunders et al., 2013). Polished sections examined in the study of ore from the Blue vein indicate that gold occurs in pyrrhotite, but chalcopyrite is also commonly associated with the gold. The same authors concluded that the general geologic setting of gold deposits in the Alabama-Georgia Appalachian Piedmont has similarities to other quartz vein-hosted gold systems in metasedimentary sequences such as including the Otago schist, South Island, New Zealand, and Bendigo-Ballarat area of Victoria, Australia.

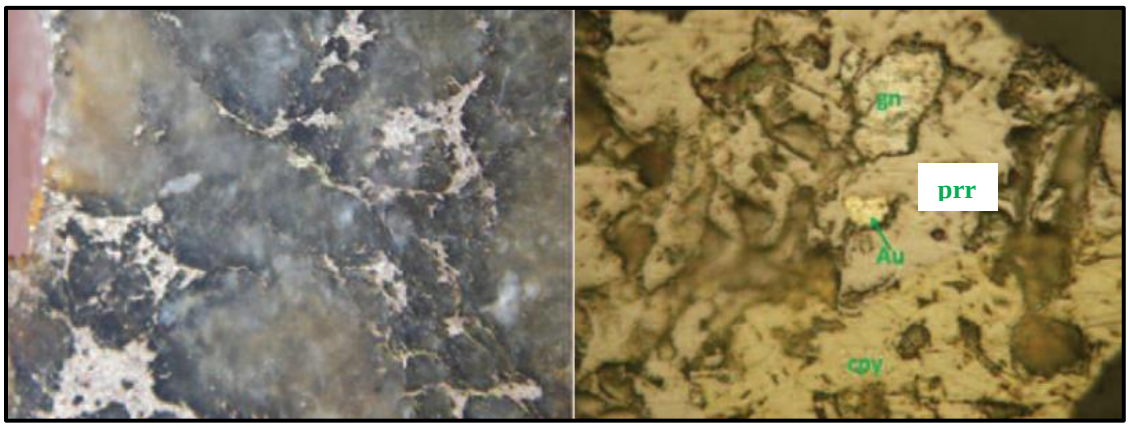

Figure 7: Left: Photograph of a slab of quartz vein containing pyrrhotite, arsenopyrite, and chalcopyrite from Hog Mountain (Blue Vein); field of view is 10 cm. Right: Photomicrograph of a polished section prepared from sample at left showing pyrrhotite (prr), chalcopyrite (cpy), galena (gn), and native gold (Au); field of view is 0.05 mm.

In early 1980s, Newmont Exploration Limited became interested in the Hog Mountain mine. Lambe (1982) provided a detailed report related to the Hog Mountain exploration project. He mentioned that the exploration project was based on the recognition of a large quartz-sericite alteration over the northern two-thirds of the stock and of the existence of a quartz stockwork between major veins. An extensive soil geochemical sampling program indicated that nearly the entire stock was anomalous in gold and these large gold anomalies are present over the northern two-thirds of the stock (Lambe, 1982). These large anomalies are not oriented northeasterly as are major veins. Therefore, the major veins are not the sole control on these anomalies. A resistivitiy-Induced Polarization survey was run using the geochemical soil survey over the Hog Mountain. The survey shows that the east-west lines have only low resistivity, high chargeability of the graphitic Wedowee schist. The north-south lines indicate a shallow, high resistivity zone over a zone of low resistivity. According to these results, a series of twelve vertical diamond drill holes was proposed to evaluate the distribution of gold at the Hog Mountain mine.

Current exploration at the Hog Mountain mine is being held by Wellborn Mining Company. More than one hundred drill cores have been drilled since 2010 on the property based on magnetic anomalies due to pyrrhotite. Because the veins dip steeply, angle core holes are used to intercept the veins at approximately right angles to provide a true thickness. Drilling continues to date at Hog Mountain and as of yet, no mining decision has been made about the economics of actual mining at this time.

3. GEOLOGIC SETTING

3.1 Geology of Eastern Blue Ridge

Hog Mountain (Fig. 8) is located in northern Tallapoosa County, approximately 6 km west of the Goldville district (Guthrie and Lesher, 1989) and 21 km northeast of Alexander City. The Hog Mountain deposit occurs in the eastern Blue Ridge (Russell, 1978; Drummond et al., 1997, Saunders et al., 2013). The eastern Blue Ridge comprises, from northewest to southeast; schist of the Ashland Supergroup, phyllites and schists of the Wedovee Group, and schist and amphibolite of the Emuckfaw Group (Fig. 8). The Ashland Supergroup and Wedowee Group are separated by the Goodwater-Enitachopco normal fault; the Wedowee and Emuckfaw Groups are separated by the Alexander City fault (Stowell et al., 1996). Hog Mountain is underlain by a biotite-muscovite tonalite pluton that intrudes phyllites of the Wedowee Group (Stowell et al., 1996) (Fig. 8). It hosts the gold deposit that is the focus of this research.

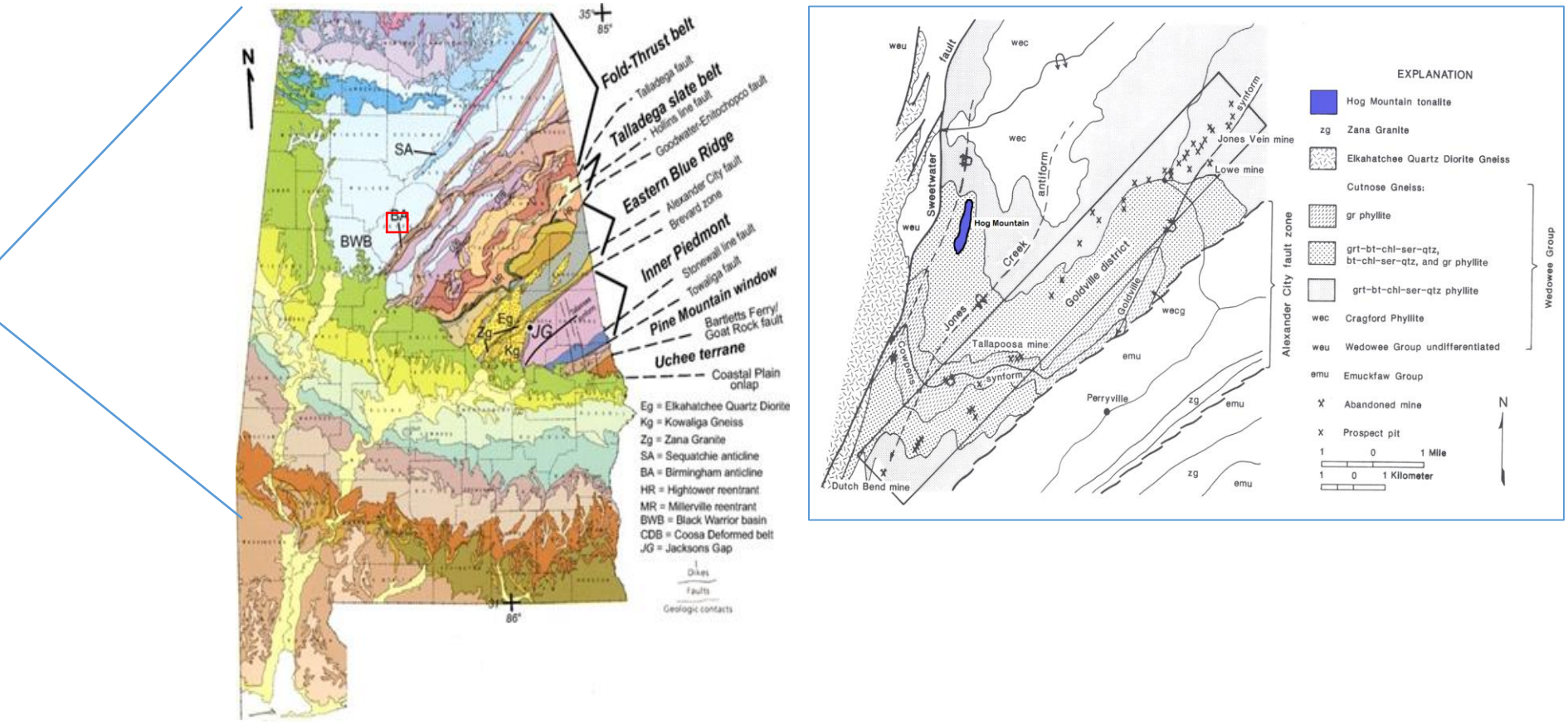

Figure 8: Geologic bedrock map of part of the Alabama eastern Blue Ridge illustrating rock units, rock packages, and faults. Inset map of Alabama is from Sapp and Emplaincourt (1975) and Raymond et al. (1988). Rectangle indicating area of Fig. 9.

3.2 Hog Mountain

The Hog Mountain deposit is hosted by biotite-muscovite tonalite pluton that intrudes phyllites of the Wedowee Group (Stowell et al., 1996) (Fig. 9). Least-altered tonalite of Hog Mountain is white, medium grained,weakly to nonfoliated, and contains minor amounts of biotite, plagioclase, muscovite, ilmenite, apatite, zircon, and garnet; K-feldspar is rare (Green et al., 1988 and Stowell et al., 1996). The spatial association of muscovite and garnet in tonalite with veins and alteration indicates that they are metamorphic in origin (Stowell et al., 1996). The geochemistry of the tonalite suggests that the parental melt was derived by melting of an intermediate composition igneous source (Stowell et al., 1996).

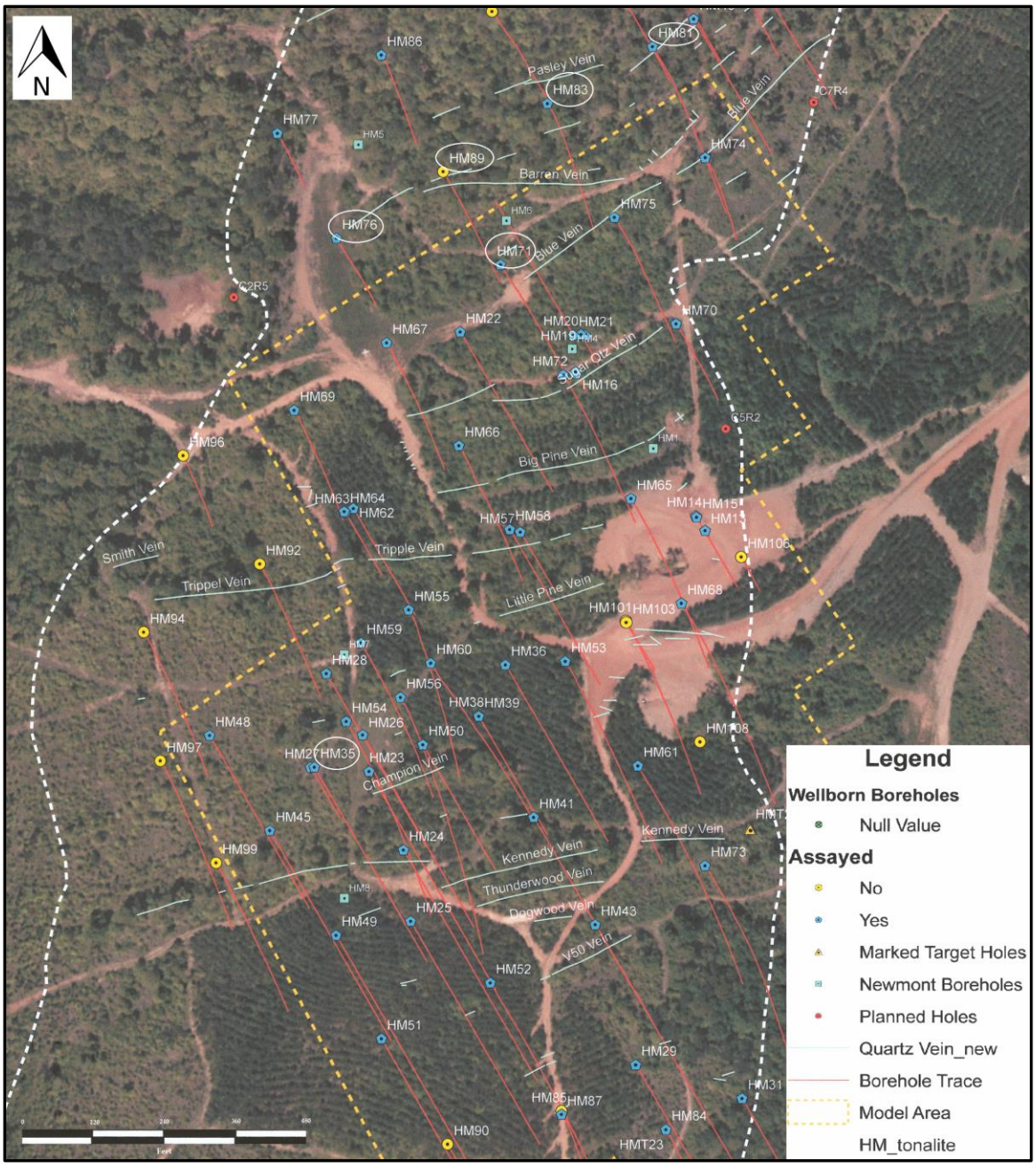

Figure 9: Map, superimposed on a Google Earth image, showing the contact between Hog Mountain tonalite and Wedowee schist-phyllites (white dashed line), and drill holes. Circled drill holes used for this study (source is Wellborn Mining Company).

4. METHODOLOGY

4.1 Field Methods

In February 2015, high-grade sulfide-bearing ore samples were obtained from the Wellborn Mining Company for reflected light studies (Fig 10). These samples are from HM35 drill hole (see Fig. 9 for locations) that cuts Kennedy Vein and HM71 drill hole that cuts Sugar Quartz Vein.

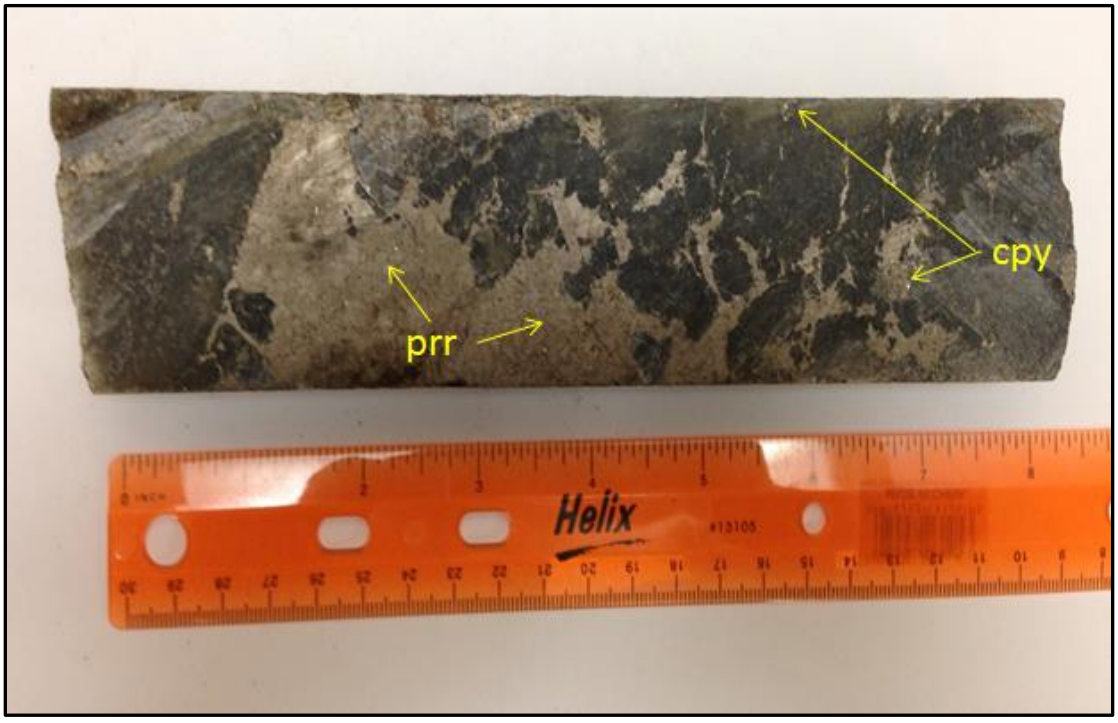

Figure 10: A core sample showing sulfide minerals pyrrhotite (prr) and chalcopyrite (cpy) in blue and smoky colored quartz from the Sugar Quartz Vein.

In May 2015, Blue vein and Barren vein core samples that had already been logged were obtained from the company. These core samples were also cut into suitable size for making thin sections and were sent to Precimat LLC for making polished thin sections.

In July 2015, core logging was done at the Wellborn Mining Company with the assistance of Mark Whitney, who is a consultant of the company. Cores intersect the Blue vein, Barren vein, Aldrich vein, and Sugar Quartz vein. The cores were logged and interpreted in terms of the relationship between the quartz veins and the host rocks, alterations, sulfide mineral types, vein orientations, and structural features (Fig 11).

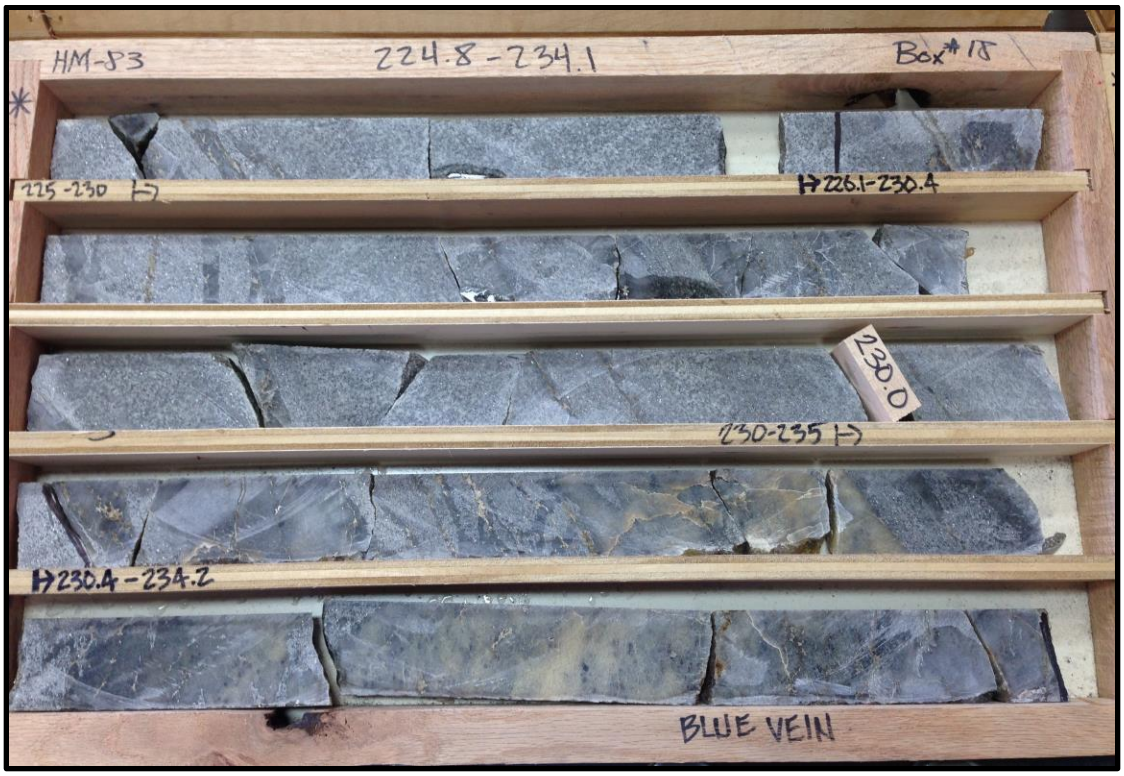

Figure 11: Photograph of HM-83 exploration core from the Blue Vein showing fresh core samples. Disseminated pyrrhotite is present in fractured smoky and blue colored quartz vein.

In August 2015, Dr. Mark Steltenpohl and the author went to Hog Mountain for field work. The field work was completed under the direction and supervision of Wellborn Mining Company at the Hog Mountain located in northern Tallapoosa County, approximately four miles west of Goldville district. The basic goal of the field work was to collect samples and to note structures associated with them. Hand samples were collected from tonalite, schist, and old quartz vein dumps for making thin sections. The contact between Wedowee group schist-phyllites, Blue Vein (Fig. 12), and the Hog Mountain tonalite and its quartz veins were observed with the assistance of Phil Padgett and Mark Whitney.

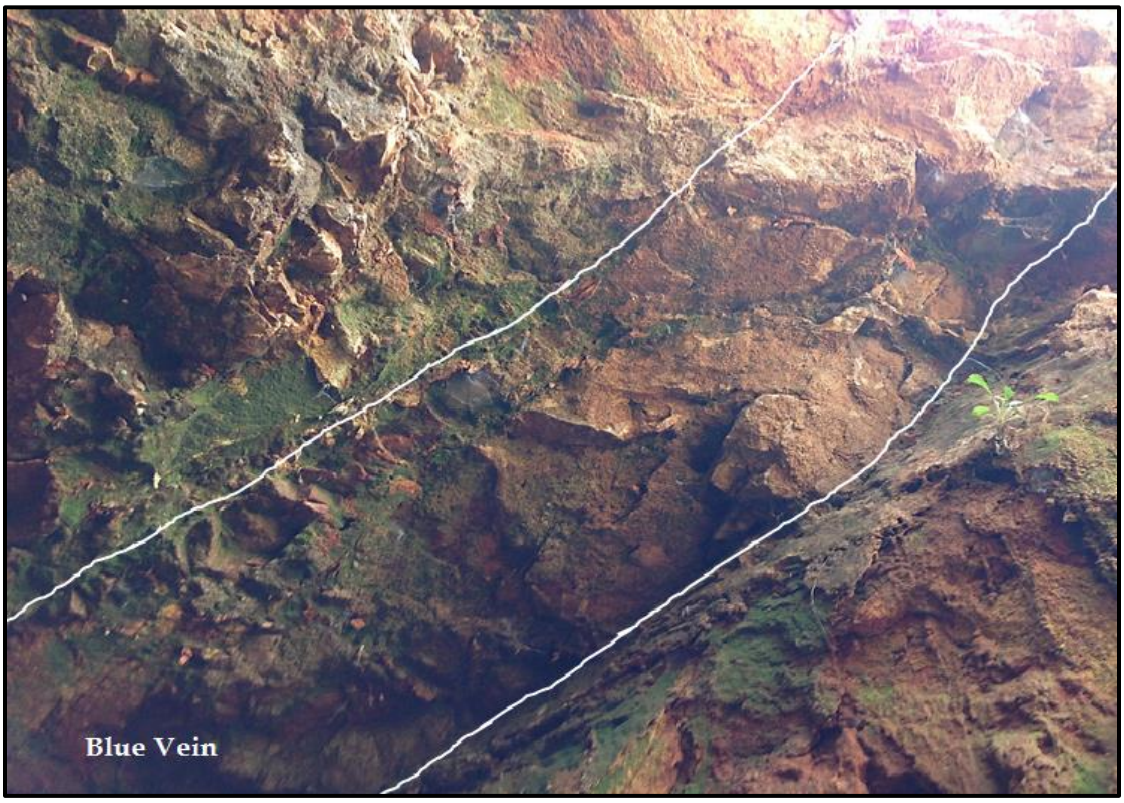

Figure 12: Photograph of the Blue Vein exposed at Hog Mountain.

4.2 Sample Preparation

Samples for polished sections were collected from HM-35 and HM-71 drill cores tha cut the Kennedy vein and Sugar Quartz veins. These samples were selected based on gold assays from the high-grade sulfide mineralization. Polished thin sections were made from ore samples were collected from the HM-46, HM-76, HM-81, HM-83, and HM-89 drill cores that cut the Blue vein. Samples were cut into approximately a size smaller than the 3 cm diameter of the polished sections and into approximately 46x27 mm rectangular shapes with a thickness of 1 cm for polished thin sections. ICP-MS analysis of samples also were chosen from Blue vein samples based upon the Au grade. All of these samples were chosen by using a binocular microscope in Department of Geosciences at Auburn University.

4.3 Ore Petrography

Reflected light microscopy was used to distinguish between the opaque sulfide minerals and to determine their rock and ore textures in polished thick sections. In order to use the reflected light, 14 polished thick sections (Fig. 13) were made. Sulfide-bearing quartz vein samples were cut into small pieces using the ore-trimming saw at Auburn University. Samples selected for making polished sections had a high sulfide percentage and interesting ore textures. Polished sections were made at the Department of Geosciences, Auburn University by setting the samples in 3cm diameter two-piece cylindrical plastic molds by using Buehler EpoKwick Epoxy Resin. Four different sizes of grit (120, 400, 600, and 1000) on a combination of glass plates and polishing wheels (1 and 6 micron) were used for polishing the samples. After the samples were polished, a Nikon Eclipse E400 POL light microscope was used for reflected light studies.

Transmitted light microscopy was used to classify the rock type and to identify the quartz textures and other gangue minerals in ore samples. Transmitted light studies were performed on 7 standard thin sections that were made by Wagner Petrographic LLC and 10 polished thin sections made by Precimat LLC. After the samples were received, a Nikon Eclipse E400 POL light microscope was used for transmitted light microscopy.

Figure 13: Polished thick sections from HM35 drill hole from the Kennedy vein, HM71 drill hole from Sugar Quartz vein, and HM78 drill hole from Blue vein.

4.4 Geochemical Analysis

Geochemical analyses were performed on Sugar Quartz and Blue vein core samples. Geochemical samples were selected for high grade ppm values of Au. A total of 8 samples were weighed (each sample was between 70 – 100 g) and sent to Acme Analytical Laboratories Ltd. in Vancouver, Canada for whole rock geochemical analysis. Core samples crushed and pulverized to 200 mesh by using the PRP70-250 procedure code. Sample splits of 0.5 g each were leached in hot modified Aqua Regia for ICP-ES/MS analysis. Using the AQ200 package (Fig.14), samples were analyzed by ICP-ES/MS for 36 elements with upper and lower detection limits indicated in figure 14. Moreover, assay results of 96 samples showing Appendix 1 that selected from 12 different drill holes obtained from Wellborn Mining Company. These samples came from veins and from tonalite containing narrow veins. Results of these 96 samples are thought to be representative the entire property of the Hog Mountain prospect.

	ELEMENT	AQ200 DETECTION	UPPER LIMIT
Standard Package	Ag	0.1 ppm	100 ppm
	Al	0.01 %	10 %
	As	0.5 ppm	10000 ppm
	Au	0.5 ppb	100000 ppb
	B*	20 ppm	2000 ppm
	Ba	1 ppm	10000 ppm
	Bi	0.1 ppm	2000 ppm
	Ca	0.01 %	40 %
	Cd	0.1 ppm	2000 ppm
	Co	0.1 ppm	2000 ppm
	Cr	1 ppm	10000 ppm
	Cu	0.1 ppm	10000 ppm
	Fe	0.01 %	40 %
	Ga	1 ppm	1000 ppm
	Hg	0.01 ppm	50 ppm
	K	0.01 %	10 %
	La	1 ppm	10000 ppm
	Mg	0.01 %	30 %
	Mn	1 ppm	10000 ppm
	Mo	0.1 ppm	2000 ppm
	Na	0.001 %	5 %
	Ni	0.1 ppm	10000 ppm
	P	0.001 %	5 %
	Pb	0.1 ppm	10000 ppm
	S	0.05 %	10 %
	Sb	0.1 ppm	2000 ppm
	Sc	0.1 ppm	100 ppm
	Se	0.5 ppm	100 ppm
	Sr	1 ppm	10000 ppm
	Te	0.2 ppm	1000 ppm
	Th	0.1 ppm	2000 ppm
	Ti	0.001 %	5 %
	Tl	0.1 ppm	1000 ppm
	V	2 ppm	10000 ppm
	W	0.1 ppm	100 ppm
	Zn	1 ppm	10000 ppm

Figure 14: AQ200 package detection limits from Acme Analytical Laboratories.

5. RESULTS

5.1 Geochemical Analysis

The geochemical analyses by ICP-MS were conducted for the following 36 elements for the HM-71 drill hole sample from the Sugar Quartz vein and HM-46, HM-76 (2 samples), HM-81, HM-83, HM-89 (2 samples) drill hole samples from the Blue vein: Mo, Cu, Pb, Zn, Ag, Ni, Co, Mn, Fe, As, Au, Th, Sr, Cd, Sb, Bi, V, Ca, P, La, Cr, Mg, Ba, Ti, B, Al, Na, K, W, Hg, Sc, Tl, S, Ga, Se, and Te. A Pearson's correlation matrix was generated using Microsoft Excel for a subset of these 36 elements that were detected in all the 8 different drill core samples. These elements were used for the correlation matrix. The results for the correlation matrix are shown in Table 1. Any correlation value that higher than 0.5 is considered to have a strongly positive correlation. Any correlation value that lower than -0.5 is considered to have a strongly negative correlation.

Table 1: Pearson's Correlation Matrix of Geochemical Data for Blue vein drill hole samples.

	Mo	*Cu*	*Pb*	*Zn*	*Ag*	*Ni*	*Co*	*Mn*	*Fe*	*As*	*Au*	*Sb*	*Bi*	*Cr*	*Ba*	*W*	*S*	*Se*	*Te*
Mo	1																		
Cu	-0.19621	1																	
Pb	-0.04677	-0.38402	1																
Zn	-0.20263	0.983139	-0.22297	1															
Ag	0.185821	0.704248	0.111923	0.795327	1														
Ni	0.98072	-0.04843	-0.01699	-0.04034	0.349725	1													
Co	0.9587	0.047623	-0.03121	0.055242	0.418674	0.990245	1												
Mn	-0.38833	0.492664	-0.56986	0.405292	-0.08034	-0.35974	-0.37409	1											
Fe	0.947488	0.060632	0.006441	0.076307	0.450643	0.988741	0.997948	-0.3771	1										
As	0.948631	-0.3812	0.174408	-0.34608	0.158384	0.924066	0.873028	-0.48574	0.872024	1									
Au	0.605707	0.410088	0.08597	0.484299	0.87635	0.718668	0.76608	-0.36662	0.784359	0.572648	1								
Sb	-0.04565	-0.73087	0.648467	-0.61712	-0.21402	-0.10207	-0.199	-0.41615	-0.17936	0.265759	-0.13381	1							
Bi	0.462649	0.303417	0.37751	0.427604	0.882204	0.581898	0.622072	-0.47414	0.651994	0.513125	0.946563	0.102872	1						
Cr	-0.43727	-0.13421	-0.57824	-0.24958	-0.63063	-0.52712	-0.59571	0.705747	-0.61932	-0.44122	-0.74116	2.86E-17	-0.82493	1					
Ba	0.838763	-0.10518	-0.37336	-0.1452	0.152875	0.816592	0.757994	-0.0104	0.745141	0.812041	0.49274	6.94E-17	0.301869	0	1				
W	0.45018	-0.26537	0.340213	-0.21457	0.056171	0.379337	0.415595	-0.60456	0.388771	0.432517	0.294237	0.087365	0.337119	-0.56541	0.069892	1			
S	0.722349	0.437685	-0.05183	0.458649	0.710677	0.834057	0.886727	-0.24544	0.901454	0.597502	0.880733	-0.41412	0.746396	-0.6927	0.534705	0.192099	1		
Se	0.946646	0.066062	0.012336	0.0811	0.443182	0.986543	0.997731	-0.36734	0.998973	0.865753	0.773559	-0.19571	0.641878	-0.62383	0.731672	0.410701	0.898775	1	
Te	0.574936	0.509154	0.026914	0.571641	0.882271	0.684384	0.750055	-0.29167	0.76132	0.49616	0.976507	-0.2735	0.906094	-0.73935	0.432174	0.384956	0.876213	0.758677	1

Note: Any correlation value higher than 0.5 is considered to have a strongly positive correlation (highlighted with yellow color). Any correlation value lower than -0.5 is considered to have a strongly negative correlation (highlighted with red color).

The ore samples from the Blue vein have an Au grade up to 16.7 ppm, a Bi grade up to 321.3 ppm, a Se grade up to 13.7 ppm, a Te grade up to 46.9 ppm, an Ag grade up to 2.2 ppm, and the S grade more than 10% . Moreover, the ore samples from the Blue Vein contain significant amount of Mo (between 1.2 - 6.1 ppm) and Pb (between 0.4 - 3.3 ppm). A core sample (HM71) from the Sugar Quartz vein (Fig. 15) contains 64.7 ppm gold, 1318 ppm Bi, 5.2 ppm Se, 186.6 ppm Te, 5 ppm Ag, and % 9.65 S grade (Table 2).

Figure 15: Photograph of a core sample from Sugar Quartz Vein at Hog Mountain showing the disseminated pyrrhotite in smoky colored quartz.

Table 2: Selected Geochemical Data for the Hog Mountain Ore Samples of the Blue Vein.

Sample	Drill Core Location / Depth(ft)	Mo ppm 0.1	Cu ppm 0.1	Pb ppm 0.1	Zn ppm 1	Ag ppm 0.1	Ni ppm 0.1	Co ppm 0.1	Mn ppm 1	Fe % 0.01	As ppm 0.5	Au ppb 0.5	Th ppm 0.1	Sr ppm 1	Cd ppm 0.1	Sb ppm 0.1	Bi ppm 0.1	V ppm 2	Ca % 0.01
Core 1	**HM46/261.5-261.8**	1.2	235.6	3.3	3	1	4.5	14.6	51	6.97	1.6	6477.5	<0.1	1	<0.1	0.3	213.6	<2	0.03
Core 2	**HM71/265.4-266.2**	2.4	1403.3	7.8	8	5	8.2	46.6	66	16.46	3.7	64702.3	<0.1	2	0.3	1.6	1317.9	<2	0.03
Core 3	**HM76/118.3-119.1**	1.6	366.4	0.4	1	0.1	3.2	3.5	69	1.33	1.2	63.9	<0.1	<1	<0.1	0.2	1.7	<2	0.02
Core 4	**HM76/132.5-133.0**	1.4	965.6	1.7	5	0.5	3.6	23.4	52	7.22	<0.5	3330.5	<0.1	1	0.2	<0.1	86.1	<2	0.03
Core 5	**HM81/253.0-253.7**	1.2	89.9	2.6	2	1	2	5.4	44	2.29	1.4	8079.1	<0.1	1	<0.1	0.3	235.3	<2	0.02
Core 6	**HM83/237.5-237.9**	1.4	2943.3	0.9	17	2.2	6.8	42.4	63	13.79	0.7	15142.7	<0.1	<1	1.1	0.1	304.1	<2	<0.01
Core 7	**HM89/195.7-196.0**	1.5	448.2	0.8	2	0.7	4.1	18.2	47	6.07	1.1	6989.1	0.2	<1	0.1	0.2	141.2	<2	0.01
Core 8	**HM89/196.1-196.9**	6.1	286.3	1.7	2	1.3	24.3	137.4	43	>40	4.6	16665.9	<0.1	1	<0.1	0.2	321.3	<2	0.02

Table 2: Cont. Selected Geochemical Data for the Hog Mountain Ore Samples of the Blue Vein.

Sample	Drill Core Location / Depth(ft)	P % 0.001	La ppm 1	Cr ppm 1	Mg % 0.01	Ba ppm 1	Ti % 0.001	B ppm 20	Al % 0.01	Na % 0.001	K % 0.01	W ppm 0.1	Hg ppm 0.01	Sc ppm 0.1	Tl ppm 0.1	S % 0.05	Ga ppm 1	Se ppm 0.5	Te ppm 0.2
Core 1	**HM46/261.5-261.8**	<0.001	<1	2	<0.01	2	<0.001	<20	0.01	<0.001	<0.01	0.1	<0.01	<0.1	<0.1	3.68	<1	2.3	13.1
Core 2	**HM71/265.4-266.2**	<0.001	<1	2	<0.01	2	<0.001	<20	0.01	0.001	<0.01	0.1	0.02	<0.1	<0.1	9.65	<1	5.2	186.6
Core 3	**HM76/118.3-119.1**	<0.001	<1	5	<0.01	4	<0.001	<20	0.03	0.001	0.02	0.2	<0.01	0.5	<0.1	0.65	<1	<0.5	<0.2
Core 4	**HM76/132.5-133.0**	<0.001	<1	2	<0.01	1	<0.001	<20	<0.01	<0.001	<0.01	1.9	<0.01	<0.1	<0.1	4.03	<1	2.8	14.4
Core 5	**HM81/253.0-253.7**	<0.001	<1	2	<0.01	2	<0.001	<20	0.01	<0.001	<0.01	2.7	<0.01	<0.1	<0.1	1.35	<1	0.8	24.1
Core 6	**HM83/237.5-237.9**	<0.001	<1	2	<0.01	3	<0.001	<20	0.02	<0.001	<0.01	0.4	0.01	<0.1	<0.1	7.8	<1	4.7	46.5
Core 7	**HM89/195.7-196.0**	<0.001	<1	3	<0.01	3	<0.001	<20	0.02	<0.001	0.01	<0.1	<0.01	<0.1	<0.1	3.7	<1	1.7	15.2
Core 8	**HM89/196.1-196.9**	<0.001	<1	1	<0.01	6	<0.001	<20	0.02	<0.001	0.01	2.4	0.01	<0.1	<0.1	>10	<1	13.7	46.9

To clarify the geochemical relationships, a statistical method called Pearson's correlation matrix was applied to the Blue vein geochemical dataset. The Pearson's correlation matrix shown in Table 1 was calculated in Microsoft Excel using the geochemical data set belong to the Blue vein fresh drill hole samples (HM46, HM76, HM81, HM83, and HM89). There are strong positive correlations between Au:Bi, Au:S, Au:Te, Au:Ag, and Au:Se. Furthermore, there are very strong correlations (higher than 0.90) between other elements such as Ni:Mo, Co:Ni, Zn:Cu, As:Mo, Mo:Se, Ag:Bi, Ni:Co, Fe:Ni, Se:Ni, Co:Fe, Co:Se, Fe:Se, S:Fe, Se:As, Bi:Te (Table 1).

In addition to the correlation matrix of the Blue vein, the Pearsons's correlation matrix was applied to another much larger data set that represents the entire property of the Hog Mountain, which was provided by Wellborn Mining Company. According to that correlation matrix, there are strong correlations between Au:Bi (0.82), Au:Te (0.86), Bi:Te (0.98), and Cd:Zn (0.99) (Table 3). To better understand the change of Au, Bi, and Te depending on the depth, the element contents are plotted on a diagram (Fig. 16). The element contents change depending on the depth for Cd and Zn elements plotted on a different diagram (Fig. 17).

There are several limitations with the Blue vein statistical analysis of the geochemical data set and also for the entire property of the Hog Mountain. The number of the samples chosen for the Blue vein geochemical study was limited, and thus the Pearson's correlation matrix calculated may not be representative of a larger sample set. Another limitation for both data sets is that some of the elements having values below the detection limits (such as As, Na, and K) or above the upper detection limits (such as Fe).

For these cases where the geochemical data were either above or below the detection limit, statistical analysis was done by assigning numerical values to those samples equaling the detection limit.

Table 3: Pearson's Correlation Matrix of Geochemical Data provided by Wellborn Mining Company for the entire property of the Hog Mountain drill hole samples.

	Au	Ag	Al	As	Ba	Bi	Ca	Cd	Co	Cr	Cu	Fe	Ga	K	Li	Mg	Mn	Mo	Na	Ni	P	Pb	Rb	S	Sb	Se	Sn	Sr	Te	Ti	U	W	Zn
Au	1.00																																
Ag	0.29	1.00																															
Al	-0.68	-0.38	1.00																														
As	-0.02	0.38	-0.02	1.00																													
Ba	-0.39	-0.26	0.74	0.02	1.00																												
Bi	0.82	0.37	-0.77	-0.01	-0.45	1.00																											
Ca	-0.51	-0.16	0.57	-0.04	0.08	-0.56	1.00																										
Cd	-0.03	0.05	-0.04	0.01	0.01	0.07	-0.04	1.00																									
Co	0.60	0.17	-0.56	0.24	-0.30	0.52	-0.46	0.02	1.00																								
Cr	0.60	0.23	-0.80	-0.06	-0.55	0.65	-0.54	-0.03	0.49	1.00																							
Cu	0.58	0.22	-0.54	-0.03	-0.21	0.58	-0.54	0.02	0.78	0.54	1.00																						
Fe	0.61	0.22	-0.59	0.02	-0.36	0.54	-0.44	0.06	0.90	0.52	0.85	1.00																					
Ga	-0.45	-0.35	0.82	0.01	0.89	-0.55	0.21	-0.09	-0.33	-0.57	-0.25	-0.36	1.00																				
K	-0.30	-0.19	0.60	0.09	0.84	-0.36	-0.04	-0.03	-0.16	-0.35	-0.03	-0.18	0.86	1.00																			
Li	-0.58	-0.25	0.79	0.04	0.45	-0.67	0.54	-0.06	-0.49	-0.57	-0.44	-0.43	0.65	0.57	1.00																		
Mg	-0.53	-0.34	0.74	-0.07	0.23	-0.65	0.69	-0.15	-0.41	-0.55	-0.42	-0.36	0.51	0.30	0.83	1.00																	
Mn	-0.53	-0.12	0.60	0.06	0.03	-0.61	0.76	-0.05	-0.48	-0.56	-0.54	-0.47	0.22	0.03	0.71	0.81	1.00																
Mo	0.17	0.02	-0.14	-0.05	0.15	0.19	-0.34	-0.05	0.20	0.24	0.35	0.21	0.06	0.28	-0.06	-0.18	-0.35	1.00															
Na	-0.59	-0.32	0.73	-0.09	0.24	-0.65	0.72	0.02	-0.58	-0.73	-0.67	-0.62	0.29	-0.08	0.47	0.62	0.72	-0.44	1.00														
Ni	0.00	-0.02	-0.02	-0.06	-0.14	-0.03	0.05	-0.05	0.03	-0.04	0.10	0.11	-0.02	-0.08	0.04	0.12	0.12	0.16	-0.01	1.00													
P	-0.30	-0.22	0.53	0.03	0.34	-0.36	0.36	-0.08	-0.16	-0.37	-0.22	-0.19	0.48	0.39	0.51	0.60	0.38	0.12	0.30	0.02	1.00												
Pb	-0.09	0.73	0.01	0.45	-0.02	0.02	0.05	0.07	-0.13	-0.13	-0.07	-0.13	-0.04	0.04	0.10	-0.07	0.22	-0.14	-0.01	-0.03	-0.09	1.00											
Rb	-0.26	-0.09	0.46	0.10	0.68	-0.31	-0.15	-0.03	-0.15	-0.26	0.03	-0.15	0.73	0.94	0.53	0.24	0.03	0.27	-0.20	-0.02	0.29	0.14	1.00										
S	0.62	0.29	-0.64	0.07	-0.27	0.59	-0.43	0.08	0.85	0.55	0.81	0.92	-0.34	-0.08	-0.49	-0.50	-0.60	0.25	-0.75	0.02	-0.27	-0.08	-0.06	1.00									
Sb	0.05	0.31	-0.12	0.36	-0.06	0.15	-0.12	-0.02	0.14	0.18	0.32	0.11	-0.04	-0.01	-0.12	-0.09	-0.07	0.07	-0.17	0.22	-0.09	0.39	0.04	0.10	1.00								
Se	0.63	0.28	-0.61	0.05	-0.29	0.58	-0.41	0.09	0.81	0.52	0.76	0.88	-0.39	-0.13	-0.44	-0.43	-0.52	0.31	-0.67	0.01	-0.17	-0.10	-0.12	0.90	0.16	1.00							
Sn	-0.15	0.20	0.22	0.33	0.36	-0.14	-0.08	0.09	-0.10	-0.11	0.05	-0.08	0.34	0.64	0.49	0.13	0.16	0.23	-0.24	-0.05	0.07	0.38	0.74	0.03	0.19	0.01	1.00						
Sr	-0.58	-0.32	0.70	-0.09	0.12	-0.66	0.83	-0.05	-0.54	-0.65	-0.63	-0.55	0.27	-0.10	0.58	0.76	0.80	-0.40	0.92	0.07	0.38	-0.03	-0.21	-0.70	-0.13	-0.61	-0.23	1.00					
Te	0.86	0.39	-0.80	0.01	-0.51	0.98	-0.54	0.05	0.53	0.66	0.56	0.55	-0.59	-0.41	-0.65	-0.62	-0.57	0.18	-0.65	-0.02	-0.35	0.01	-0.34	0.59	0.13	0.61	-0.15	-0.64	1.00				
Ti	-0.51	-0.34	0.74	-0.09	0.21	-0.64	0.70	-0.14	-0.40	-0.57	-0.44	-0.36	0.48	0.23	0.79	0.98	0.82	-0.22	0.68	0.10	0.65	-0.09	0.15	-0.53	-0.13	-0.45	0.03	0.81	-0.60	1.00			
U	-0.51	-0.28	0.72	-0.05	0.79	-0.52	0.19	0.01	-0.42	-0.60	-0.35	-0.49	0.74	0.62	0.37	0.25	0.15	0.01	0.37	-0.07	0.44	-0.01	0.51	-0.44	-0.01	-0.44	0.20	0.29	-0.60	0.25	1.00		
W	0.24	0.05	0.00	-0.03	0.23	0.30	-0.25	0.03	0.12	0.03	0.21	0.11	0.15	0.25	-0.08	-0.15	-0.22	0.00	-0.17	-0.04	-0.01	-0.02	0.23	0.14	0.04	0.21	0.16	-0.27	0.28	-0.15	0.01	1.00	
Zn	-0.09	0.02	0.03	-0.01	0.01	0.00	0.05	0.99	-0.06	-0.09	-0.06	-0.02	-0.06	-0.02	0.04	-0.05	0.05	-0.08	0.11	-0.03	-0.04	0.06	-0.02	-0.01	-0.04	0.01	0.10	0.05	-0.02	-0.04	0.03	-0.01	1.00

Note: Any correlation value that higher than 0.5 is considered to have a strongly positive correlation (highlighted with yellow color). Any correlation value that lower than -0.5 is considered to have a strongly negative correlation (highlighted with red color).

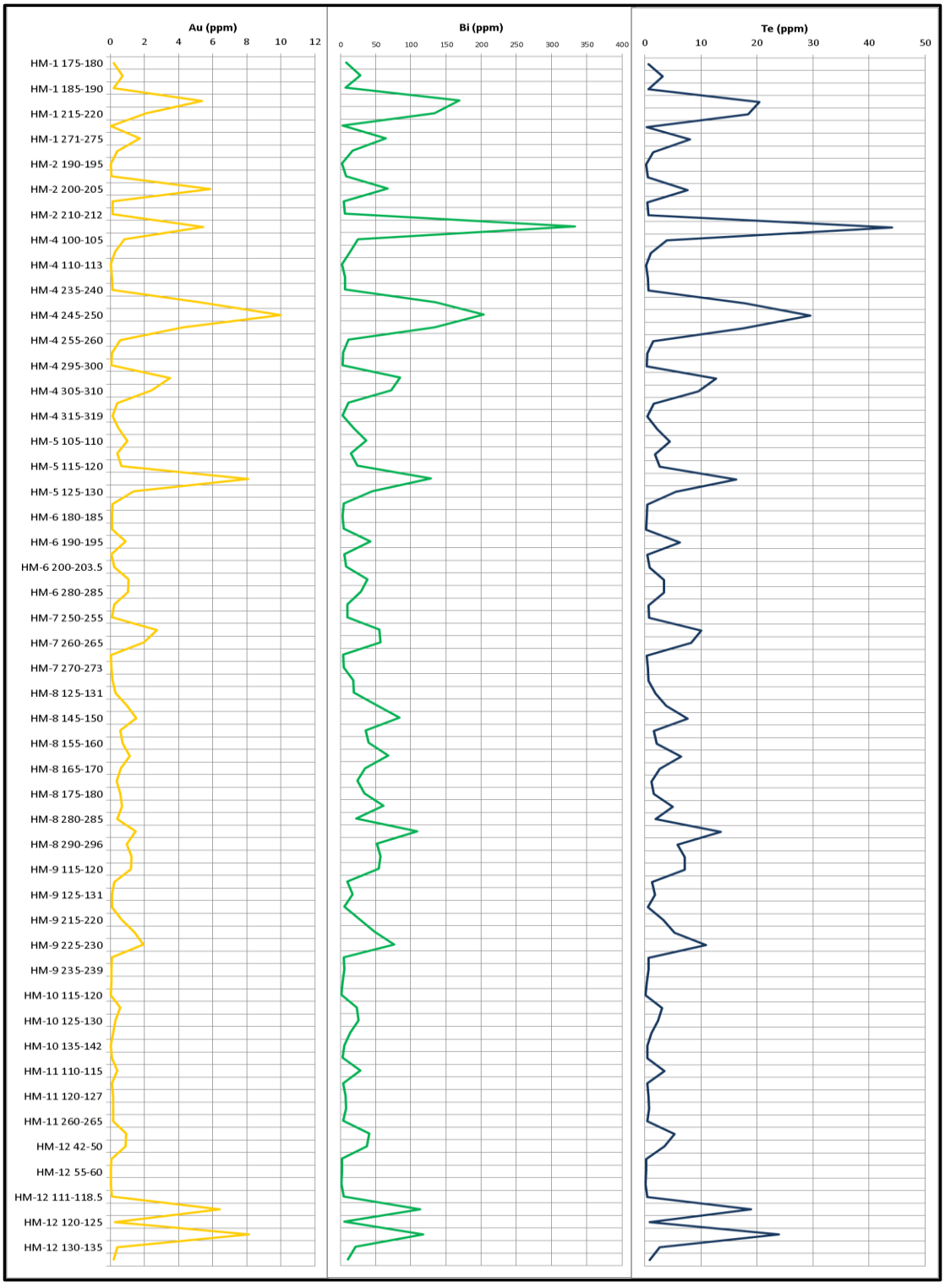

Figure 16: Gold (Au), bismuth (Bi), and tellurium (Te) contents plotted with the depth down for 12 drill holes.

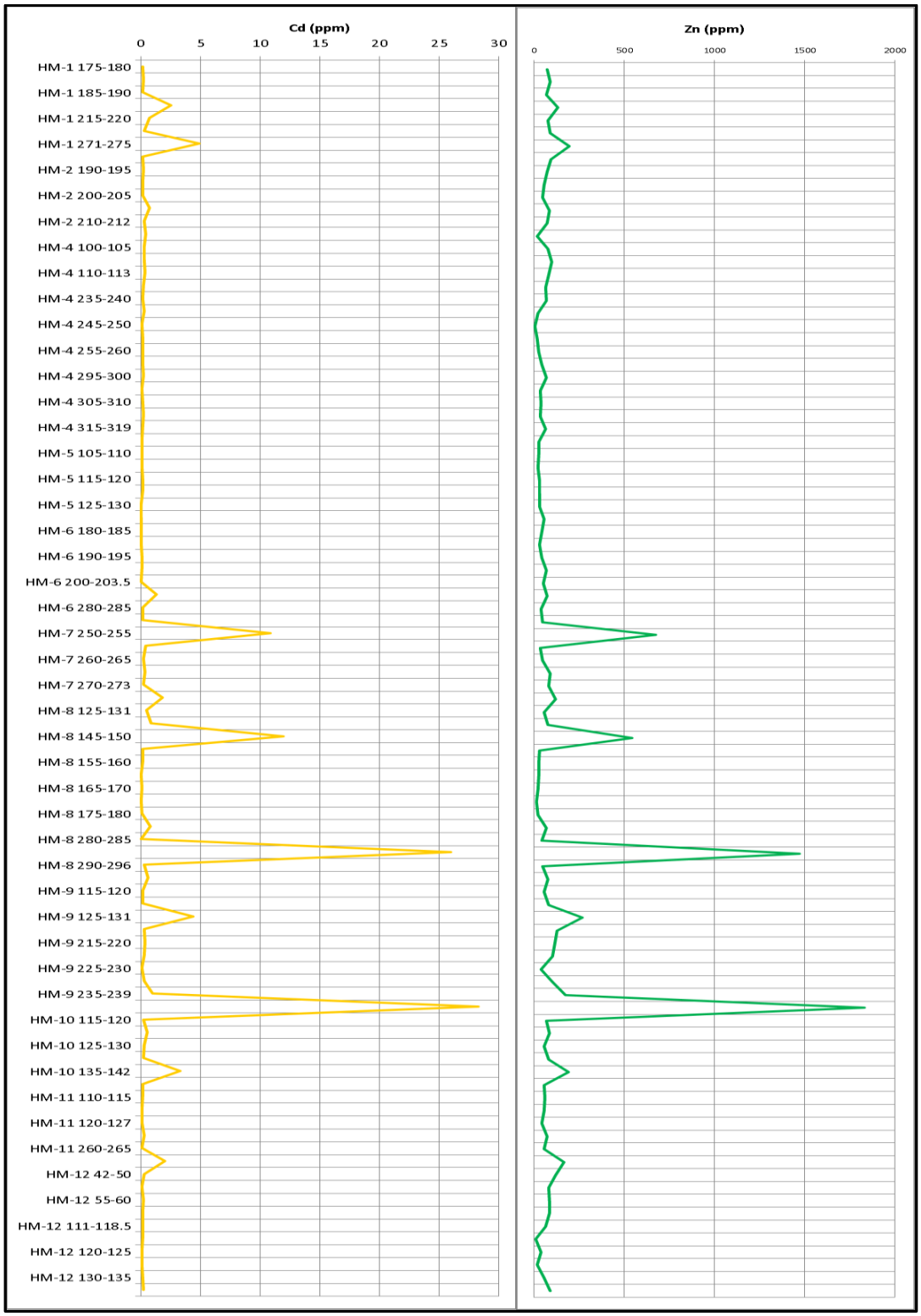

Figure 17: Cadmium (Cd) and zinc (Zn) contents plotted with the depth down for 12 drill holes. Strong correlations can be seen between these two elements.

5.2 Reflected Light Microscopy

Reflected light studies were conducted on polished sections to characterize rock and ore textures and their relationships within quartz veins. There are several distinctive textures that were observed in polished sections of ore samples from the Sugar Quartz vein and Kennedy vein described below.

Quartz is the dominant gangue mineral in polished sections. Sulfide mineral assemblages in ore samples consist of pyrite (FeS_2), chalcopyrite ($CuFeS_2$), pyrrhotite ($Fe_{1-x}S$), arsenopyrite (FeAsS), sphalerite (ZnS), and galena (PbS). Pyrrhotite is the dominant sulfide mineral; pyrite and chalcopyrite are also locally common minerals. Sphalerite, arsenopyrite, and galena are other, less-abundant, sulfide minerals in polished sections.

5.2.1 Mineralized Veinlets / Irregular Fractures

Mineralized veinlets that occur in quartz veins are typically filled with sulfide minerals. Pyrrhotite, pyrite, and sphalerite are the minerals that fill these veinlets. Pyrite and pyrrhotite veinlets occur in quartz and are generally wider in comparison to the sphalerite veinlets. In one of the ore samples in (Fig. 18), the veinlet filled with pyrite in massive quartz gangue. Sphalerite veinlets appear to be thinner compared to the other sulfide mineral veinlets and occur in pyrrhotite matrix and in other sulfide minerals. In some cases, these sphalerite veinlets are surrounded by quartz gangue (Fig. 19). Irregularly oriented fractures are common in Kennedy vein ore samples (Fig. 20). These fractures are mostly filled by pyrite and rarely pyrrhotite. They typically occur in quartz gangue and fractures and are sub-parallel to each other.

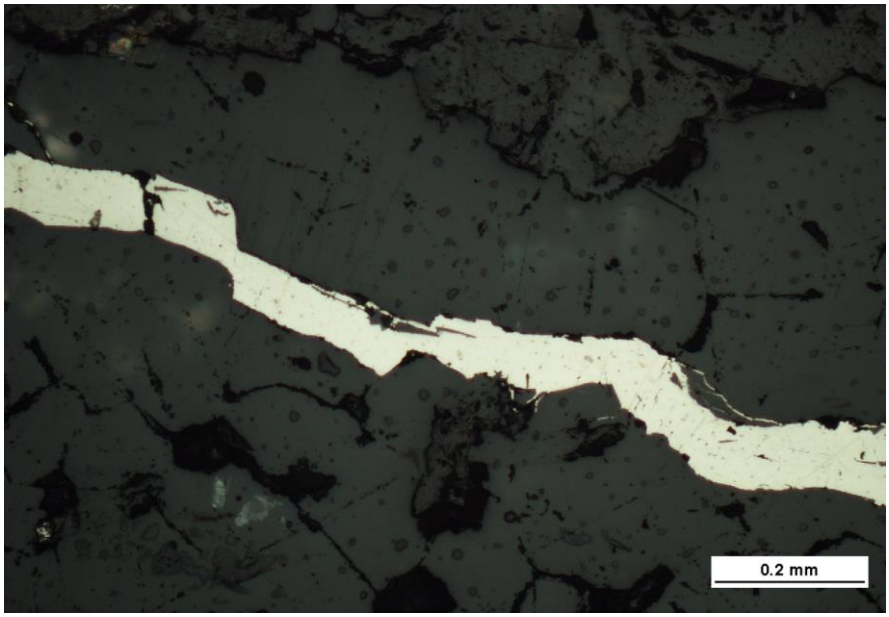

Figure 18: Photomicrograph showing the pyrite veinlets in quartz (dark color) under the reflected light.

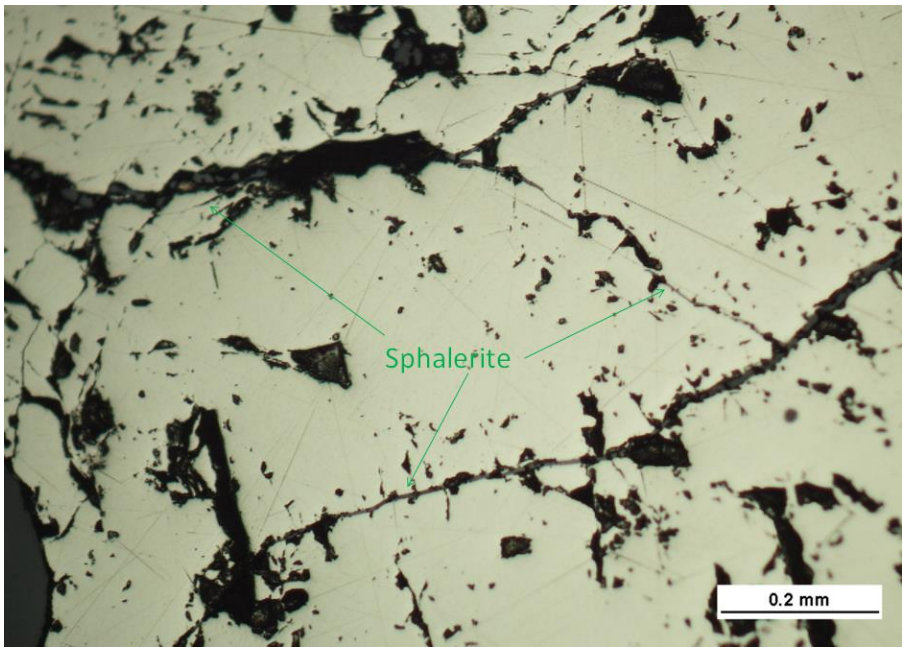

Figure 19: Photomicrograph of sphalerite veinlets in pyrrhotite matrix under the reflected light.

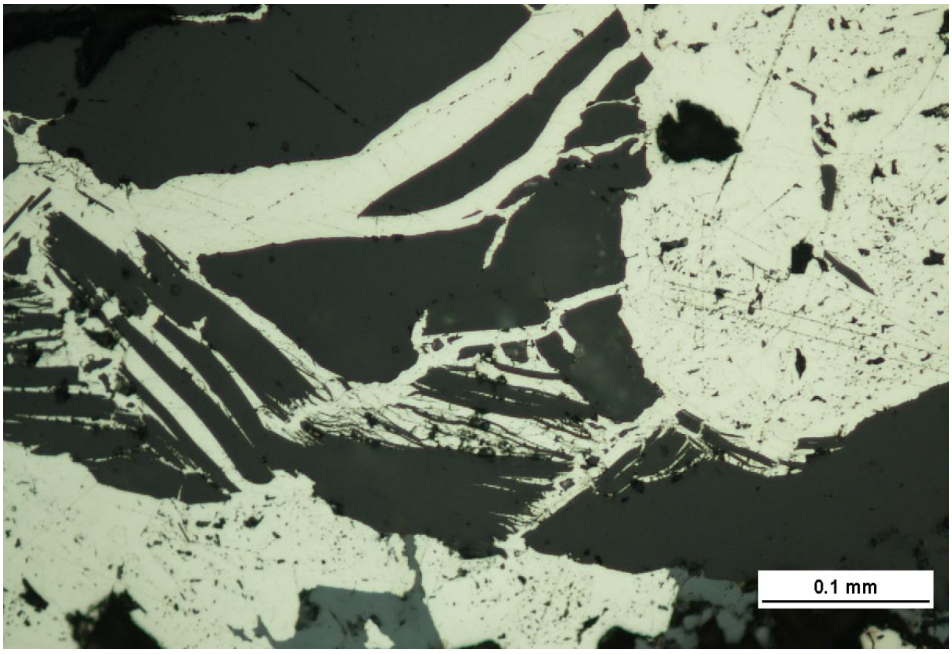

Figure 20: Photomicrograph showing irregular fractures of quartz gangue filled by pyrite under the reflected light. Gray-colored minerals are sphalerite. Quartz is dark colored.

5.2.2 Massive Pyrrhotite / Disseminated Pyrrhotite

Pyrrhotite is the most common sulfide mineral of ore samples from the Sugar Quartz vein and the Kennedy vein. In polished sections, massive pyrrhotite appears to be subhedral to anhedral grains and these grains tend to appear larger compared to the other sulfides (up to 2 cm length). In hand samples, it appears to be much larger grains up to 10 cm length (Fig. 21). A portion of this sample was used for geochemical analysis and contained up to 64.7 ppm gold. This indicates that massive pyrrhotite likely is related to the gold mineralization in the Sugar Quartz vein. However, there is no visible gold observed in the hand sample. Disseminated pyrrhotite is also common in ore samples and it occurs in quartz gangue (Fig. 22).

Figure 21: Photograph of massive pyrrhotite in a core sample from Sugar Quartz vein.

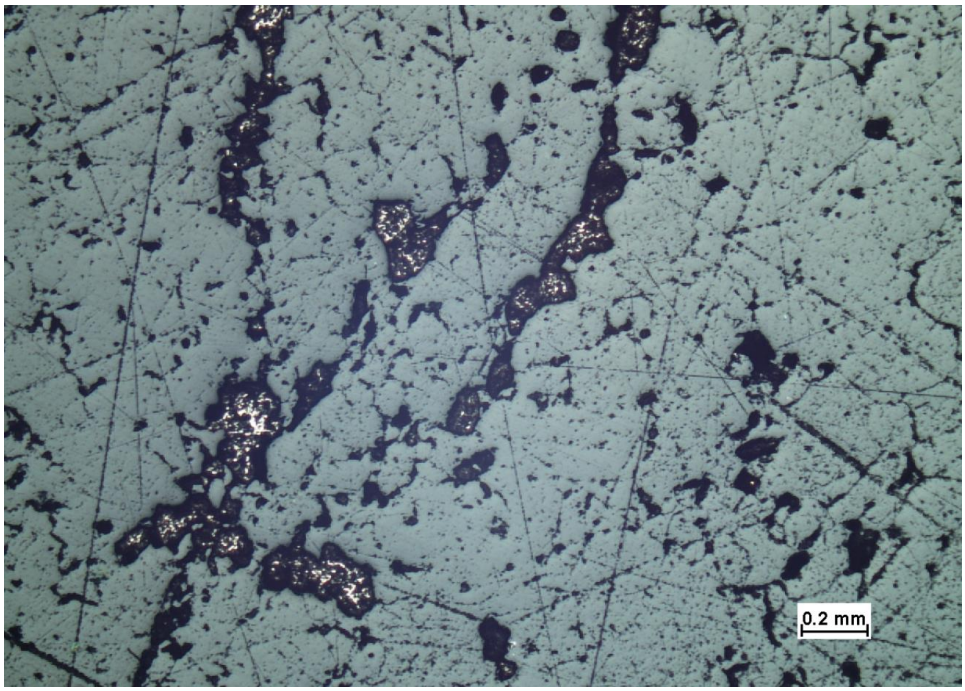

Figure 22: Photomicrograph of disseminated pyrrhotite in polished section from Sugar Quartz vein under the reflected light.

5.2.3 Altered Pyrite

Pyrite is the most common sulfide mineral after pyrrhotite in polished sections. Pyrite is associated with the gold mineralization in both the Sugar Quartz and Kennedy veins. Pyrite minerals occur as euhedral to anhedral grains. The most common occurrence of pyrite is as abundant euhedral grains in quartz gangue or as filling fractures (smaller than 0.2 mm length). In some cases, these pyrite grains are altered and formed as "finger like" structures that are parallel to each other (Fig. 23). These altered pyrite grains have either sphalerite inclusions or replacing the host rock tonalite (Fig. 24). Their parallel structures suggest that the precursor mineral might have been tonalite.

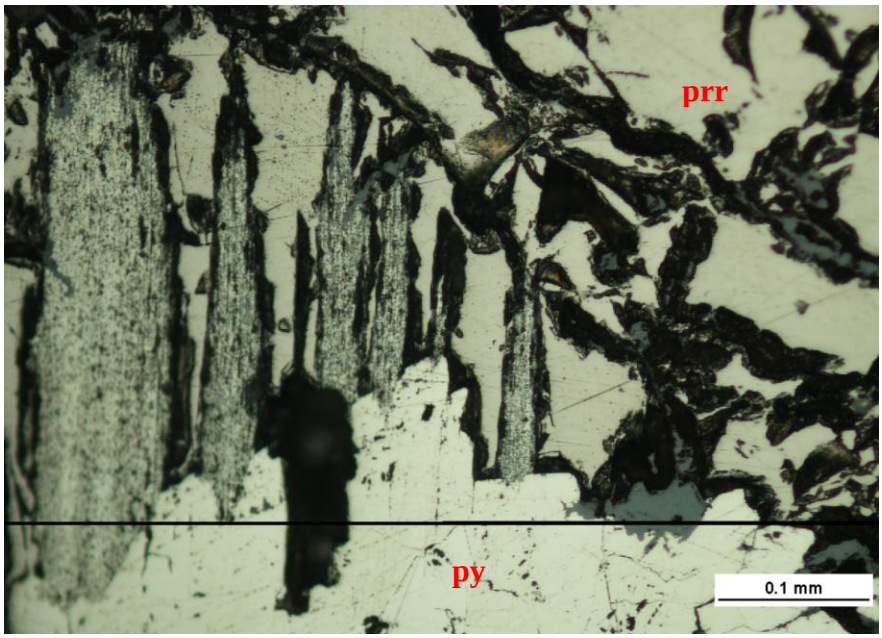

Figure 23: Photomicrograph hosted by pyrite (py) and pyrrhotite (prr) showing altered parallel pyrite (py) grains of a sample from the Kennedy vein under reflected light.

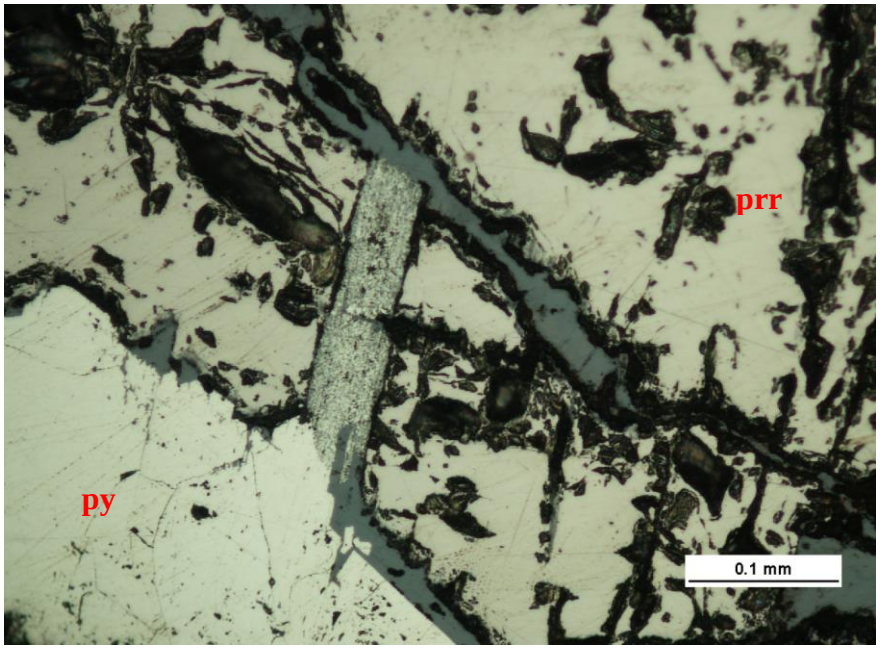

Figure 24: Photomicrograph hosted by pyrite (py) and pyrrhotite (prr) showing an altered pyrite grain is being replaced by sphalerite (gray color) and the veinlet of sphalerite under the reflected light.

5.2.4 Euhedral Arsenopyrite

Fine-grained euhedral arsenopyrite grains were identified in several polished sections from the Sugar Quartz vein. These euhedral arsenopyrite grains are fractured and generally smaller than 0.1 mm. These fractures filled by quartz gangue and the grains are enclosed by pyrrhotite. In orogenic gold deposits, arsenopyrite has been identified as an important indicator for gold (Cook et al., 2012). These euhedral arsenopyrite grains that were identified on polished sections from Sugar Quartz vein are closely associated with gold occurrences (Fig. 25).

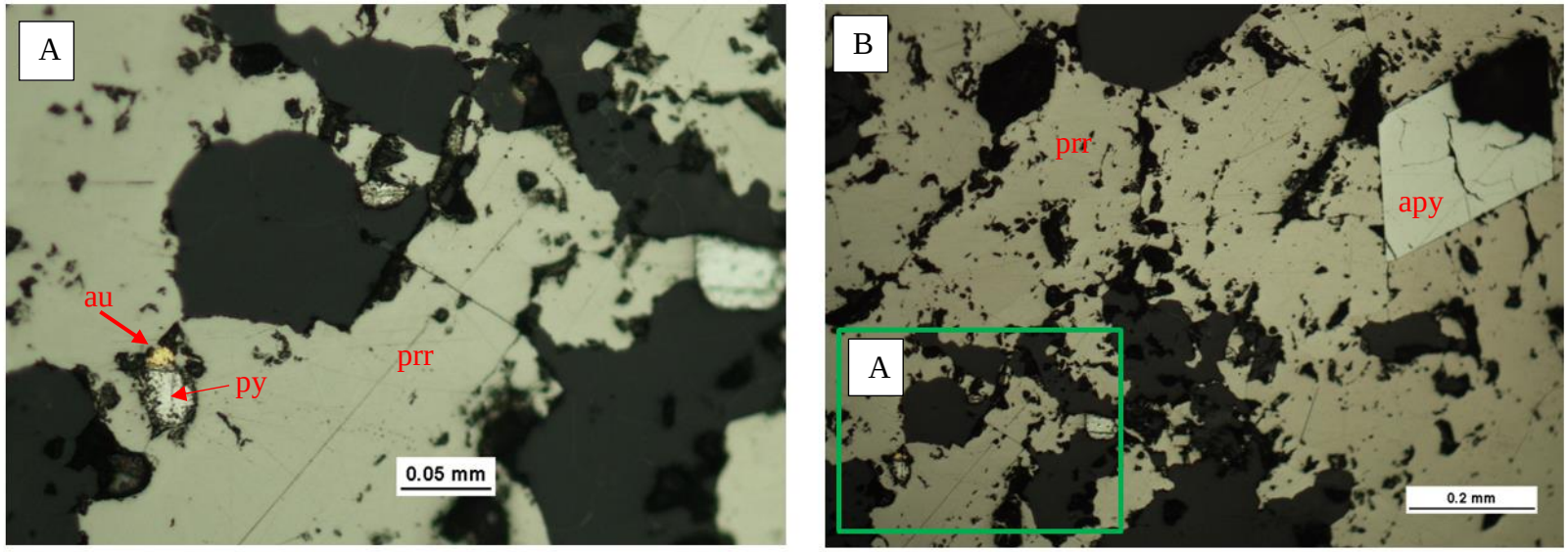

Figure 25: (A) Photomicrograph of gold (au) and pyrite (py) enclosed by pyrrhotite (prr) (green box from photomicrograph B). (B) Photomicrograph of a characteristic rhombic crystal of fractured arsenopyrite (apy) in pyrrhotite (prr) under reflected light.

5.2.5 Gold

Gold is generally found with pyrite and rarely arsenopyrite in Sugar Quartz vein and Kennedy vein ore samples (Figs. 26, 27 and 28). Most of the gold grains are anhedral, very fine grained (<0.05 mm). The largest gold grain size is 0.2 mm size on a polished section from HM 71 drill core (Fig. 26). There was no visible gold observed in Sugar Quartz or Kennedy vein ore samples. However, in a polished section from the HM 71 drill hole, more than 15 gold grains were observed under the microscope.

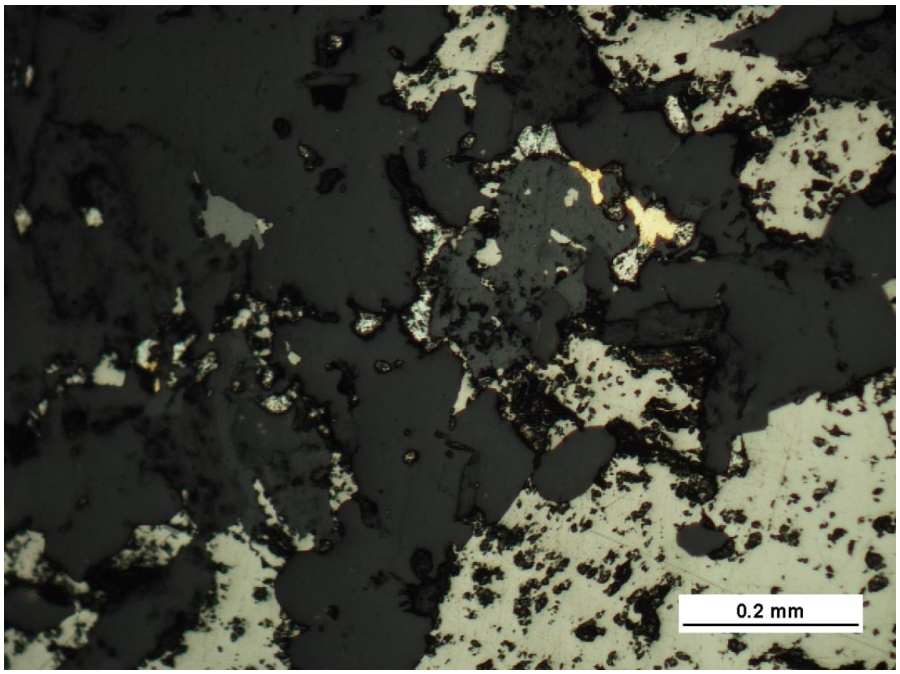

Figure 26: Photomicrograph showing gold grains (bright yellow color) in a sample from HM 71 drill core under the reflected light. Pyrrhotite is light yellow colored and the dark portion is the quartz gangue.

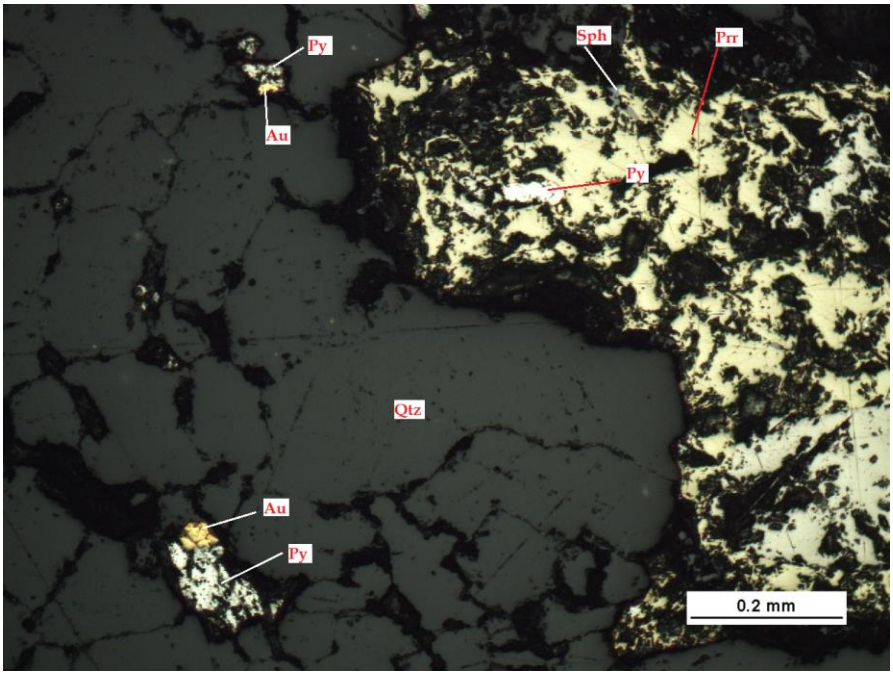

Figure 27: Photomicrograph of HM 71 drill core illustrating the relationship of gold and pyrite grains under the reflected light.

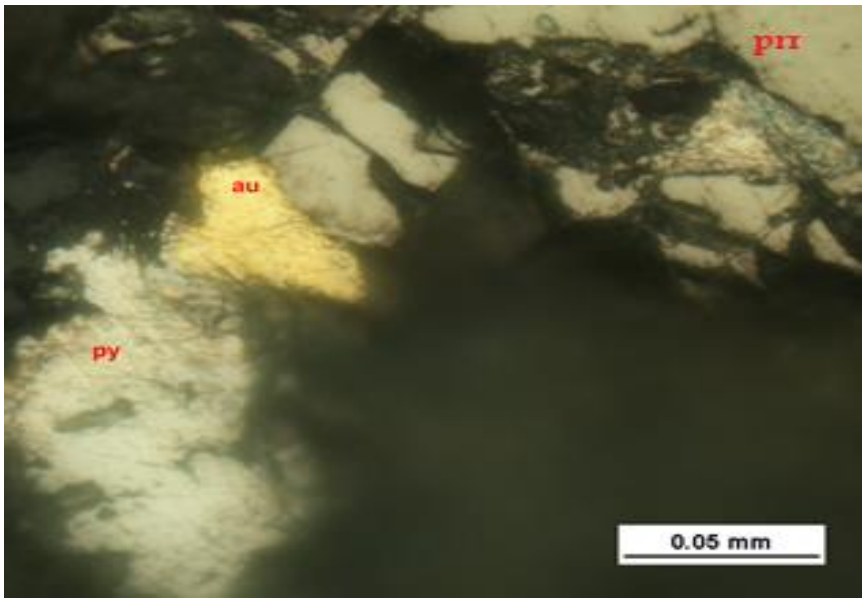

Figure 28: Photomicrograph of gold (au), pyrite (py), and pyrrhotite (prr) minerals of a sample from HM 71 drill core under the reflected light. Gold grain has a contact with pyrite and fractured pyrrhotite. Dark colored area is quartz gangue.

5.2.6 Paragenesis of Sugar Quartz Vein

Based upon reflected light studies of polished sections and the relationships of sulfide minerals, the general paragenesis of the Sugar Quartz vein is resolvable. Sulfide mineral assemblages in ore samples of the Sugar Quartz vein consist of pyrite, chalcopyrite, pyrrhotite, arsenopyrite, sphalerite, and galena. Pyrite is generally associated with pyrrhotite and chalcopyrite (Fig. 29). Pyrite was replaced by other sulfide minerals. In another polished section, sphalerite intrudes into the pyrite grain (Fig. 30). Sphalerite also intrudes into pyrrhotite and chalcopyrite within the same polished section (Figs. 31 and 32). These grain relationships were also observed in other polished sections. In some cases, such as in figure 29, it is hard to distinguish which sulfide mineral was deposited first. Galena is a rare sulfide mineral in the the Sugar Quartz vein (Fig. 33). It generally has a contact with pyrrhotite. According to the observed relationships between the sulfide minerals, the generalized paragenetic sequence is as follows: Pyrite appears to be early and is followed in progressive order by chalcopyrite, pyrrhotite, gold, arsenopyrite, and galena.

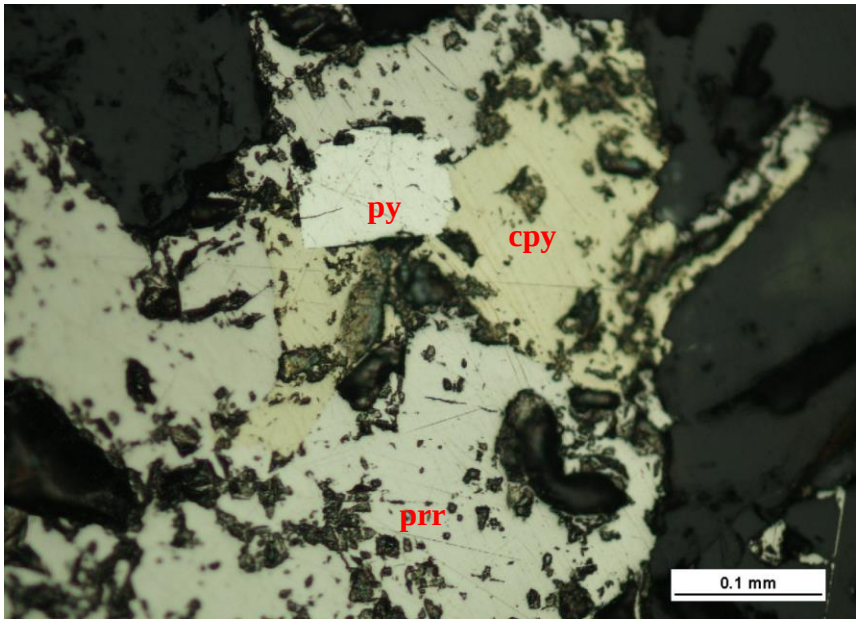

Figure 29: Photomicrograph of an euhedral pyrite (py) grain (center) and chalcopyrite (cpy) in pyrrhotite (prr) matrix. Dark colored portion is quartz.

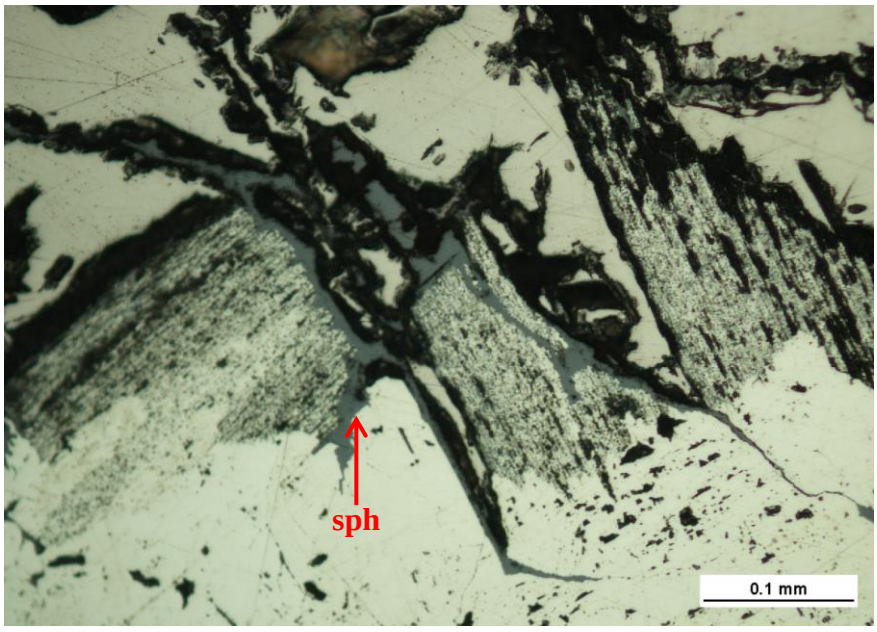

Figure 30: Photomicrograph of sphalerite (sph) intrudes into pyrite.

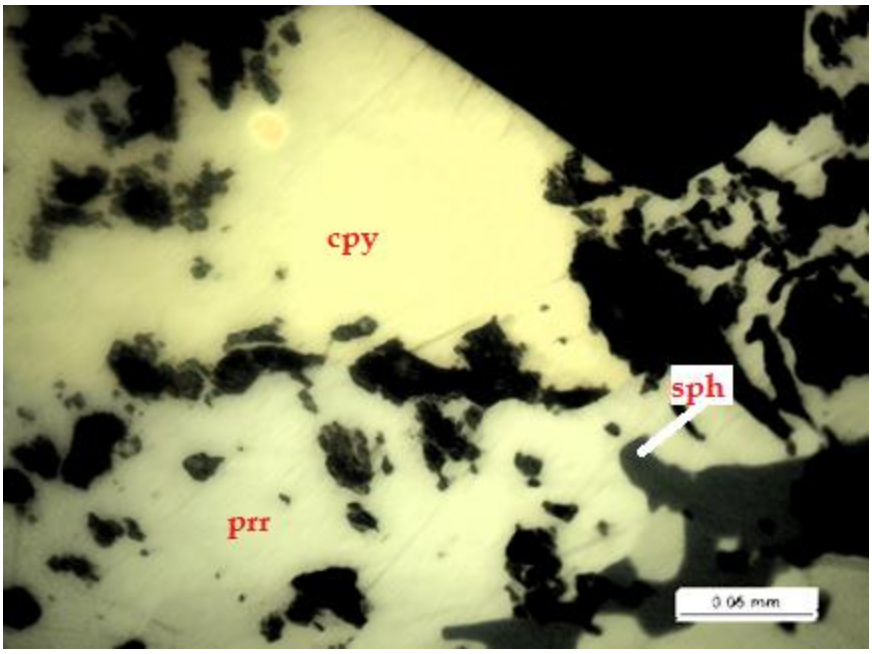

Figure 31: Photomicrograph of sphalerite (bottom right) embaying into pyrrhotite.

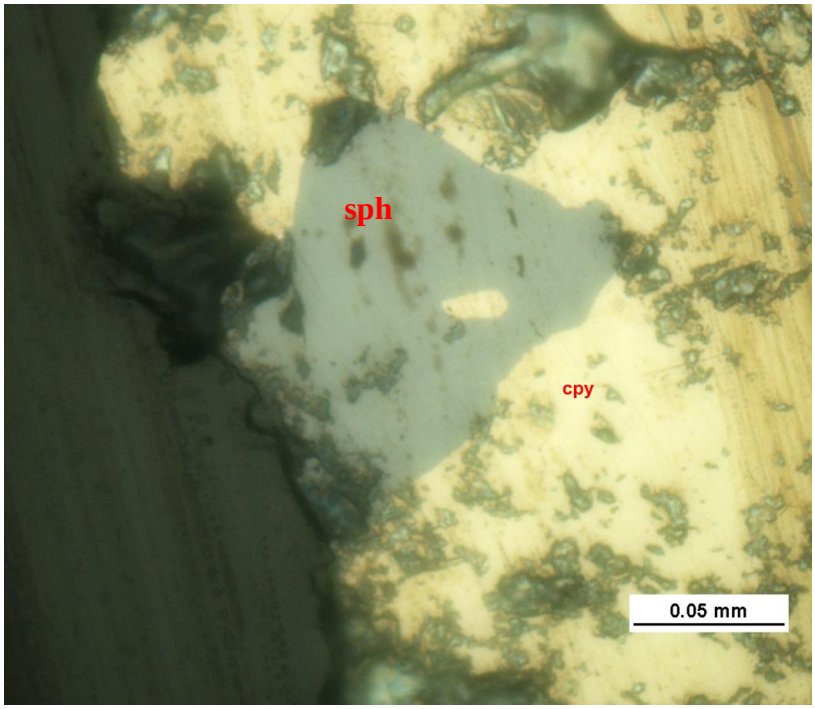

Figure 32: Photomicrograph showing sphalerite (sph) embaying chalcopyrite (cpy).

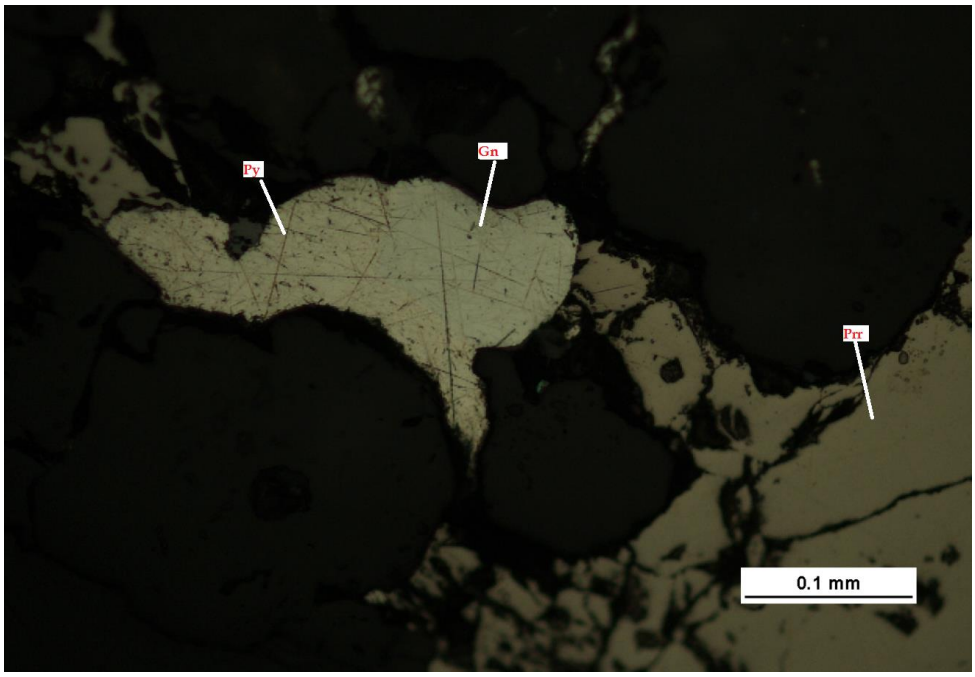

Figure 33: Photomicrograph documenting the relationship of galena (gn) with other sulfide minerals pyrite (py) and pyrrhotite (prr).

5.3 Transmitted Light Microscopy

In order to fully characterize the ore samples obtained from Blue vein and Barren vein, polished thin sections and standard thin sections were made and used to identify the alteration types and to characterize the gangue mineral textures. Samples were examined using a Nikon Eclipse E400 petrographic microscope to identify the minerals for alterations and to classify the textures of quartz.

5.3.1 Alterations

The alteration assemblage was characterized on thin sections from HM 83 drill hole that cuts the Blue vein and HM53 drill hole samples. Both potassic alteration and phyllic alteration were identified. In wall-rock alteration zones of phyllic alteration the dominant alteration is along the vein edges. On the Blue vein, phyllic alteration is typical

for the assemblage quartz-sericite and is characterized by the complete substitution of the plagioclase feldspars by sericite (Fig. 34). The characteristic minerals of potassic alteration are K-feldspar, biotite, and sericite. In the HM 53 drill hole potassic alteration assemblage is characterized by the replacement of biotite by muscovite (Fig 35).

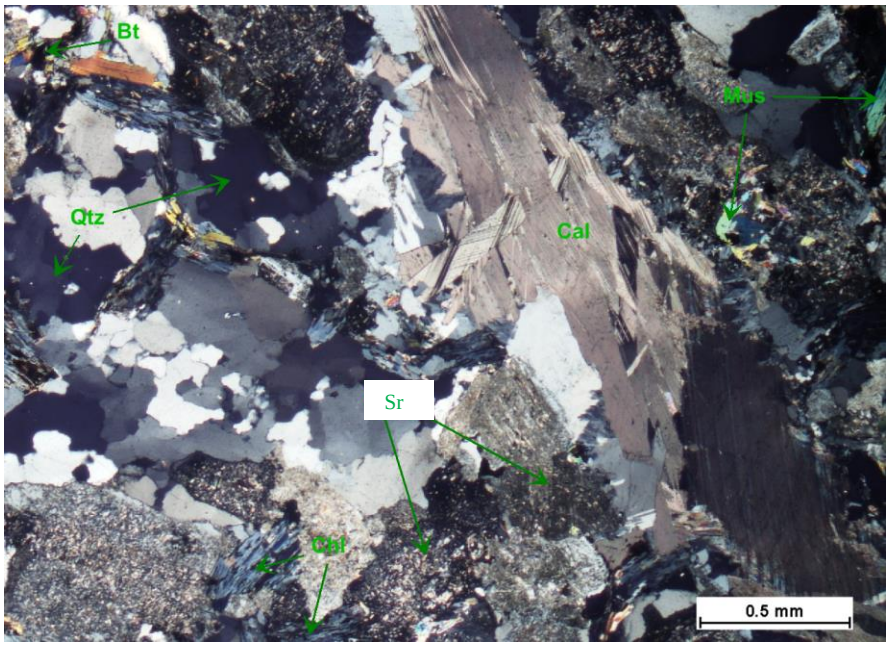

Figure 34: Photomicrograph (crossed polars) showing a mineral assemblage of potassic alteration. Quartz (qtz), muscovite (mus), sericite (sr), calcite (cal) and chlorite (chl).

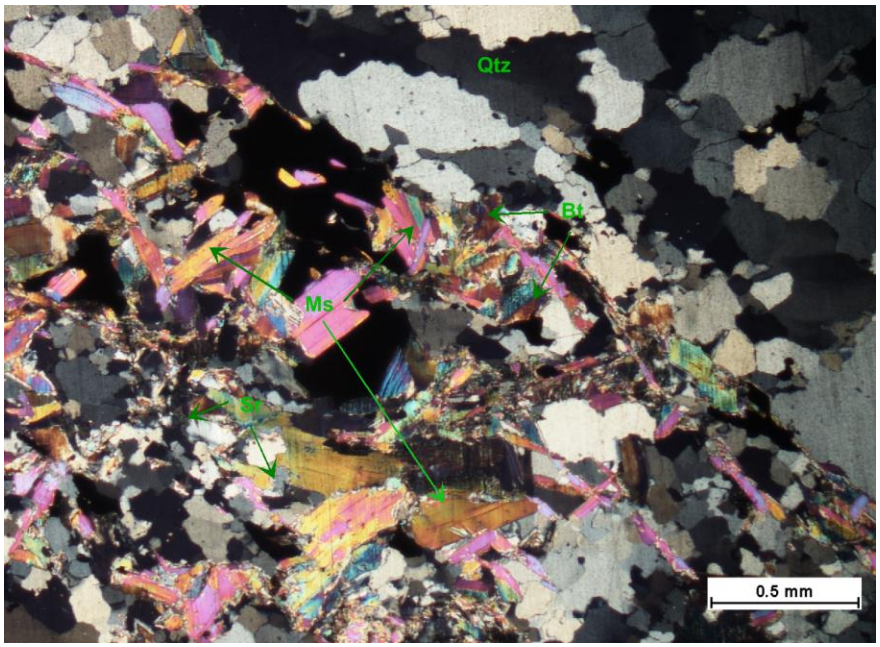

Figure 35: Photomicrograph (crossed polars) illustrating mineral assemblage of phyllic alteration. Quartz vein (top right), muscovite (Ms), biotite (Bt), and sericite (Sr) under cross polarized light.

5.3.2 Textures of Quartz

Based on transmitted light studies of Blue vein thin sections, planar deformation microstructures in quartz, saccharoidal quartz textures, pseudo-feathery quartz, strained quartz, ribbon quartz, and polygonal quartz texture (triple-point junctions) were observed.

Planar deformation features are optically recognizable microscopic features of quartz consisting of very narrow planes of glassy material arranged in parallel sets that have distinct orientations with respect to the grain's crystal structure. Planar deformation features (PDF) that were caused by a meteorite are only produced by extreme shock strains at the strain rate of meteorite impacts (Goltrant et al., 1991). These features are also called shock lamellae or planar lamellae. The occurrence of PDFs in quartz plays an

important role in the establishment of impact structures. The PDFs observed in HM 89 drill core samples are indicated in figure 36 and figure 37.

Saccharoidal quartz texture is one of the most common textures observed in Blue vein samples. This type of quartz texture is characterized with fine grained, subhedral anhedral, randomly distributed quartz grains (Fig. 38). Pseudo-feathery quartz texture is also common in thin sections. This type of texture is characterized by individual quartz crystals having a feathery appearance seen only as slight optical differences in maximum extinction position under cross polarized lights (Adams, 1920). These quartz crystals also have abundant inclusions (Figs. 39 and 40). Another common quartz texture is strained quartz texture. Quartz grains never go fully extinct as a crystal and these grains display undulose extinction under cross polarized lights. This type of texture is common when the grain size is larger than 0.5 mm in Blue vein samples (Figs. 41 and 42). Ribbon quartz texture is quite similar to the strained quartz texture type. The quartz grains have undulose extinction. However, crystal size is smaller compared to the strained quartz grains and the grains are elongated (Figs. 43 and 44). Both strained quartz texture and ribbon quartz texture is related to strong mylonitic deformation. Polygonal quartz texture (triple junctions) is another quartz texture observed in Blue vein ore sample thin sections. This type of texture is characterized by straight quartz grain boundary contacts. Some of these grains have perfectly straight 6 grain boundaries and these grains intersect at 120^0 angle (Fig. 45).

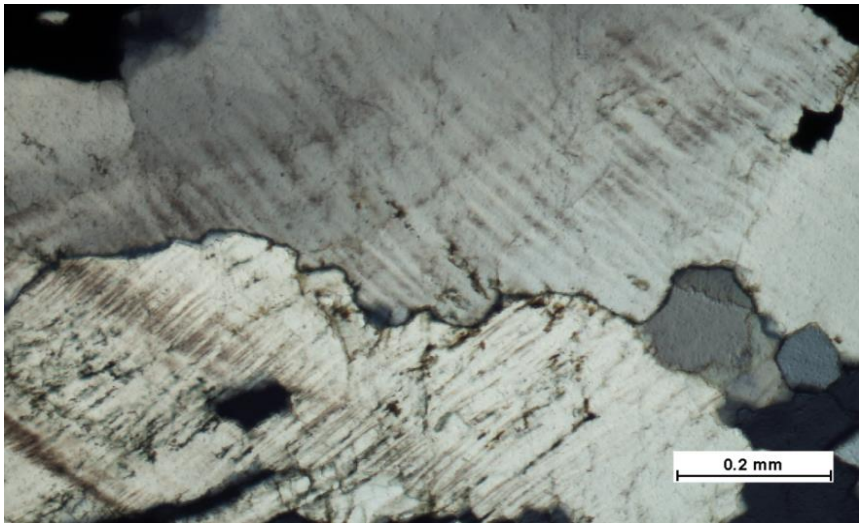

Figure 36: Photomicrograph showing planar deformation features quartz crystals. Parallel lamelles are in different direction for different two crystals.

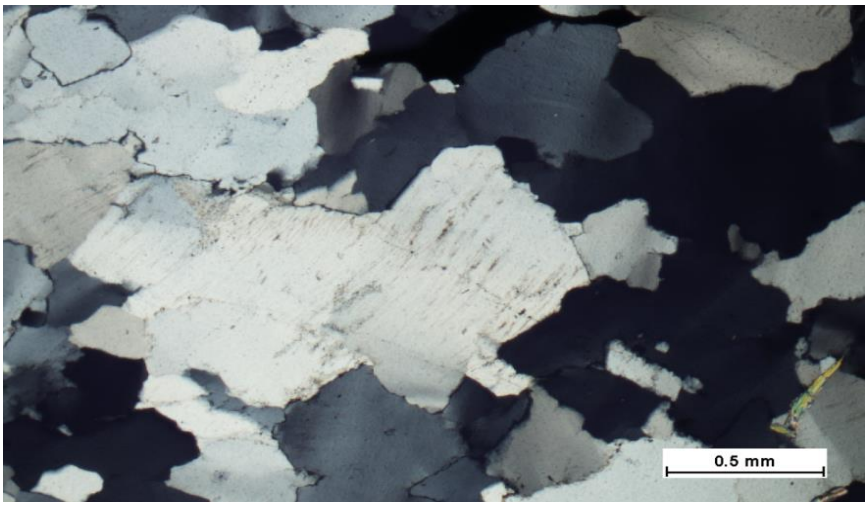

Figure 37: Photomicrograph showing planar deformation features of quartz crystals a sample from HM 89 drill core.

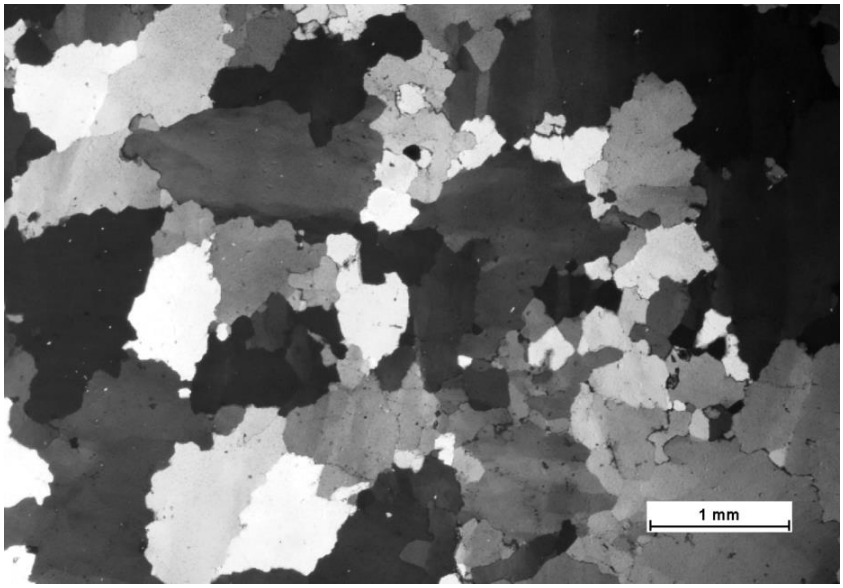

Figure 38: Photomicrograph showing saccharoidal quartz texture.

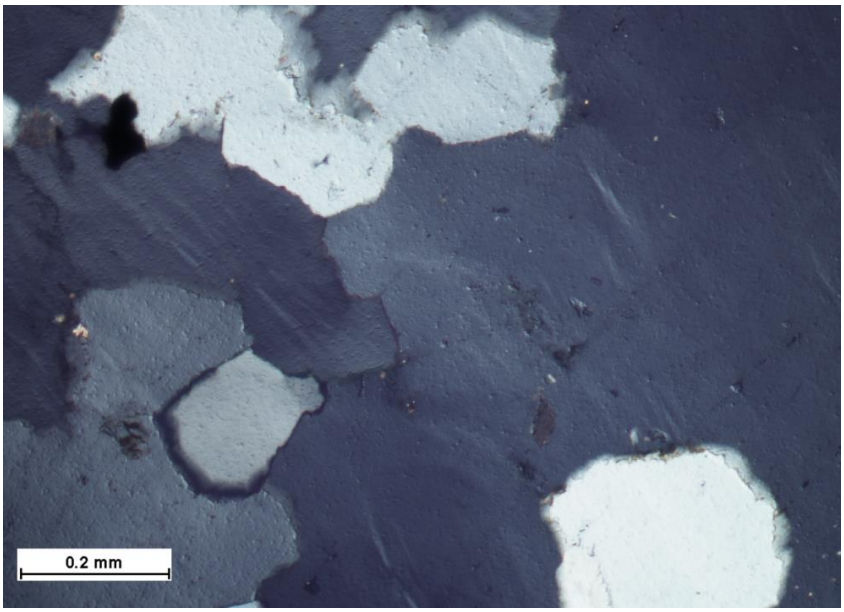

Figure 39: Photomicrograph showing pseudo-feathery quartz texture.

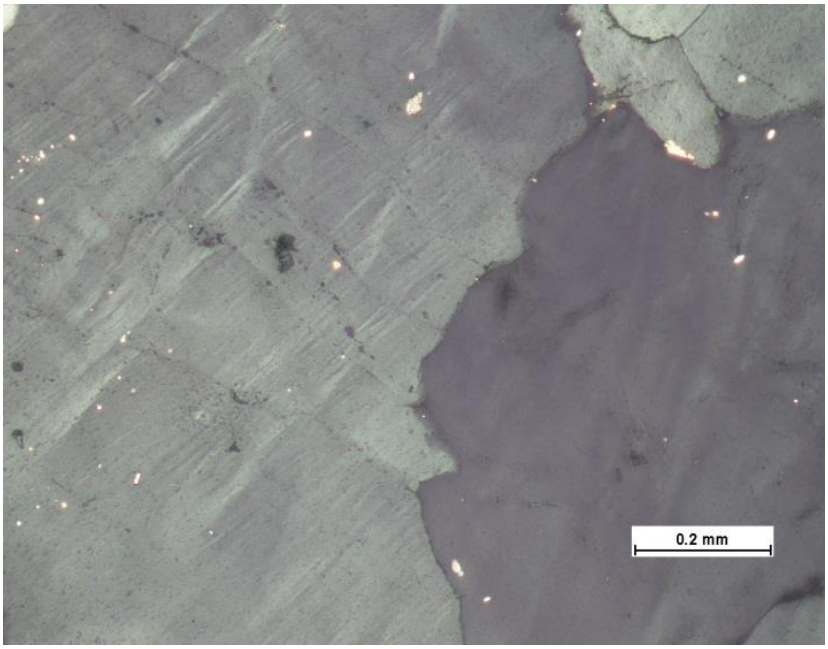

Figure 40: Photomicrograph showing pseudo-feathery quartz texture and inclusions.

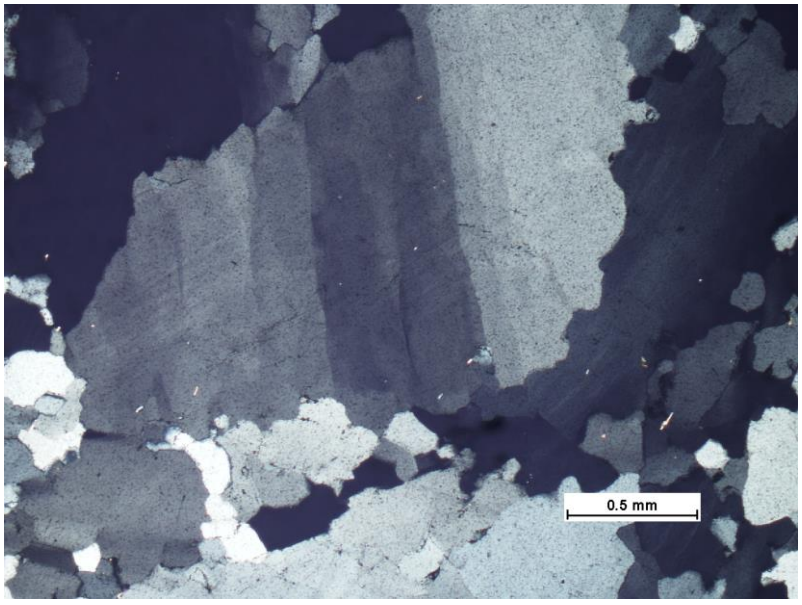

Figure 41: Photomicrograph showing deformation bands in strained quartz texture from HM81-2 drill core.

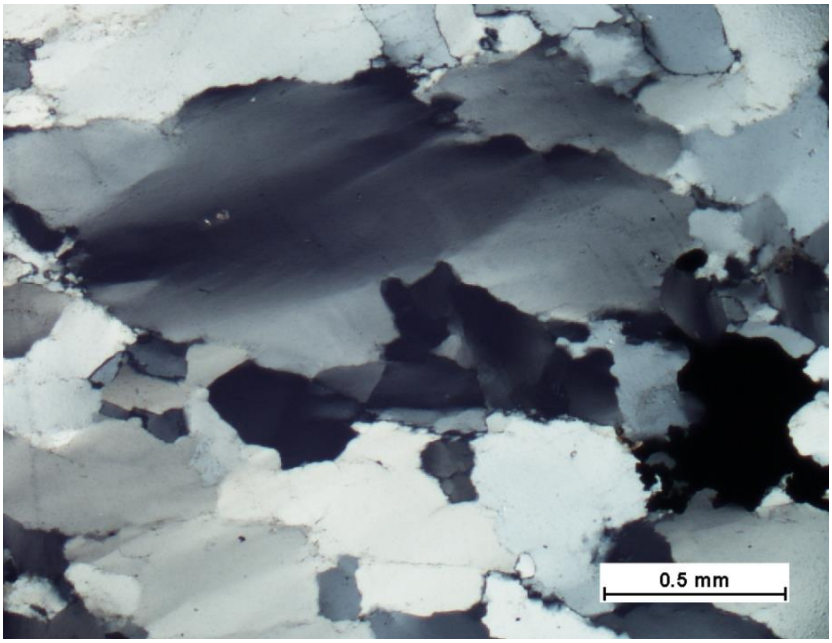

Figure 42: Photomicrograph showing undulose extinction and sutured grain boundaries in quartz.

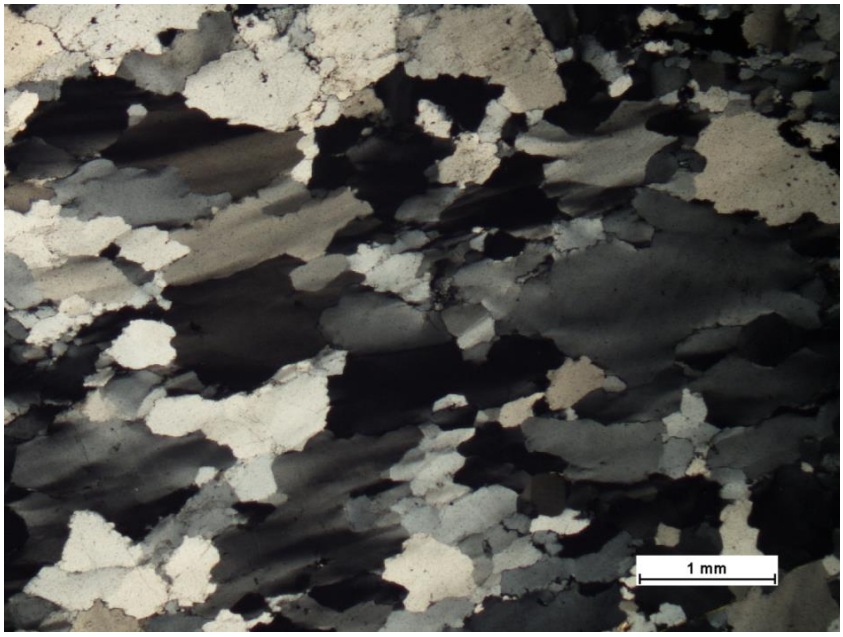

Figure 43: Photomicrograph of ribbon quartz texture with undulose extinction.

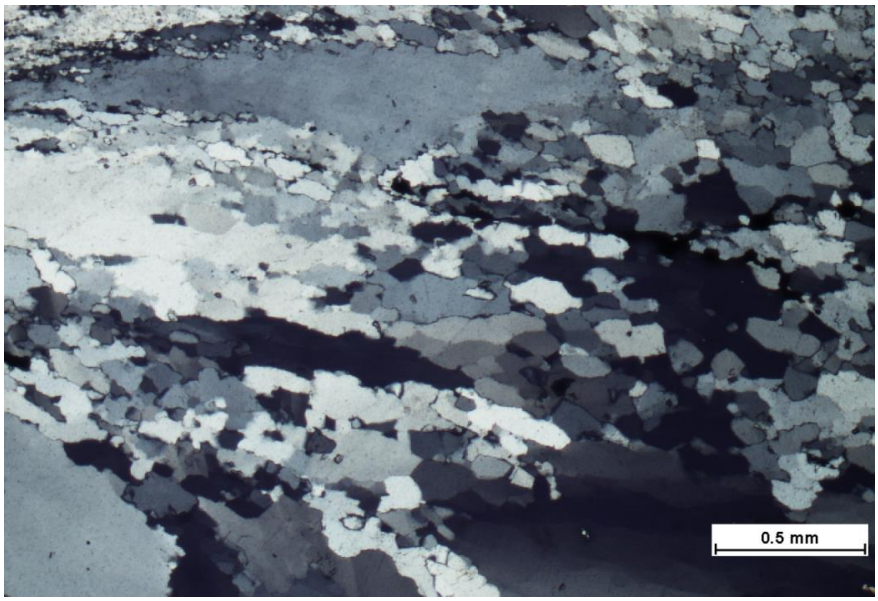

Figure 44: Photomicrograph showing ribbon quartz texture on elongated parallel quartz crystals.

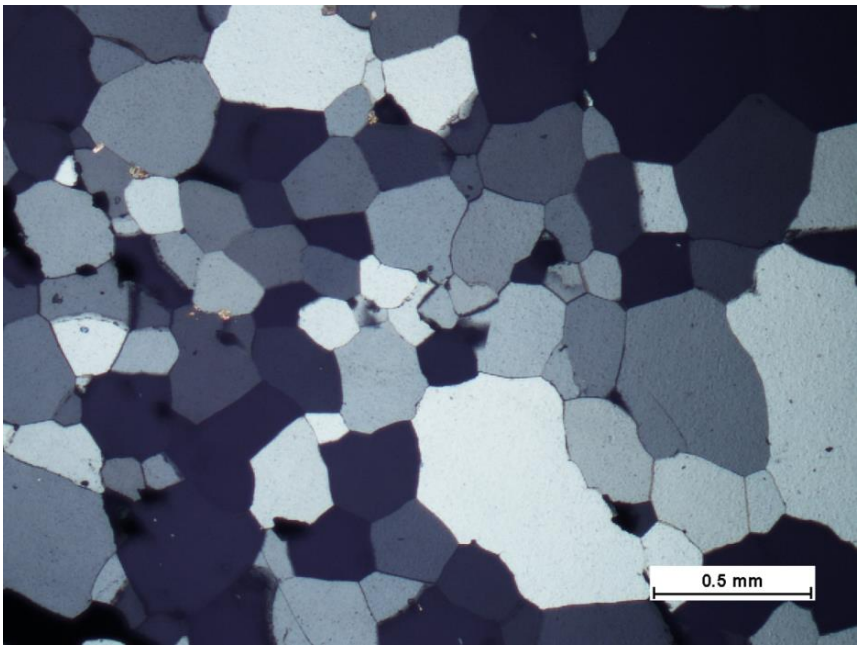

Figure 45: Photomicrograph showing polygonal quartz texture (triple junctions).

6. DISCUSSION

Pyrrhotite and pyrite are the most common sulfide minerals in igneous-rock hosted orogenic gold deposit (Groves et al., 1998). Sulfide mineral assemblages in ore samples from the Sugar Quartz vein and Kennedy vein at Hog Mountain consist of pyrite, chalcopyrite, pyrrhotite, arsenopyrite, sphalerite, and galena. Pyrrhotite is the dominant sulfide mineral; pyrite and chalcopyrite are also locally common minerals. Sphalerite, arsenopyrite, and galena are other less-abundant sulfide minerals. Saunders et al., (2013) reported that veins at Hog Mountain mine comprise predominantly quartz, minor plagioclase and muscovite, and as much as 10% sulfide minerals consisting of pyrrhotite, chalcopyrite, and arsenopyrite. The sulfide mineral assemblage at Hog Mountain mine is similar to other quartz-vein hosted gold deposits such as Otago schist (New Zealand) and Queensland (Australia).

Equigranular, medium-fine grained tonalite at Hog Mountain is typically composed of plagioclase, quartz, and potassium feldspar. Hydrothermal wallrock alteration products at Hog Mountain include carbonate minerals (calcite), sulfide minerals (pyrrhotite, pyrite, chalcopyrite, and arsenopyrite), silicate minerals (sericite, potassium feldispar,and albite), and chlorite. Eilu et al. (1999) mentioned that the hydrothermal wallrock alteration assemblage in orogenic deposits in metamorphic terranes typically consist of silicification and sericification; these are similar to the alteration assemblage of the Hog Mountain tonalite. The alteration assemblage characterized from the Blue vein samples at Hog Mountain mine for this study is similar

to those of Stowell et al. (1996) and Guthrie and Lesher (1989). Potassic alteration and phyllic alteration were identified from this study and phyllic alteration is the dominant alteration along the vein edges in wall rock alteration zones. Quartz-sericite is typical for phyllic alteration and chlorite and sericite replace biotite on the Blue vein. Stowell et al. (1996) characterized that silicification is the main alteration type at Hog Mountain mine and chlorite, sericite, and pyrrhotite replace the plagioclase.

The geochemistry of the Blue vein has similarities and differences compared to the entire property of Hog Mountain. Au has a good correlation with Bi, Co, Cr, Cu, Fe, S, Se, and Te elements in both geochemistry results. Au also has a good correlation with As, Mo, and Ni elements in the Blue vein. However, these elements do not have a correlation at the entire property of the Hog Mountain. Gold is more abundant in the ore samples compared to silver and Au:Ag ratios of the Blue vein and the entire property of Hog Mountain are highly variable but typically between 2 and 5. Robert et al. (1997) reported that the Au:Ag ratios of the quartz-vein hosted gold deposits are typically between 1 and 10.

The origin of the blue quartz in not fully understood. However, blue quartz has distinguished features from other types of quartz. These are: (1) blue quartz grains contain abundant nano-inclusions of rutile; (2) blue quartz contains significant numbers of submicron mica-group mineral inclusions; (3) blue quartz is generally of igneous origin; and (4) blue quartz is generally Ti-rich and formed at high temperatures ($> 700^0$C) (Seifert et al., 2011). Based on transmitted light studies of Blue vein thin sections, light to dark blue colored quartz grains in hand samples were observed in thin sections. These quartz grains have a grain contacts with rutile (TiO_2) and they have mica inclusions (Fig

46). The features of blue quartz grains in Blue vein are similar to quartz grains were studied by Seifert et al., (2011).

Covariant plots for the geochemical data set for the entire property of the Hog Mountain provided by Wellborn Mining Company reveal element-element correlations in more detail. A covariant plot for Au, Bi, and Te (Fig. 47) shows a strong positive correlation between these three elements (Au:Bi, Au:Te, and Bi:Te), which supports the results from the Pearson's correlation matrix. In addition to these plots, a covariant plot between Au and metalloids indicate that there is no correlation between Au and As. However, Ge and Sb concentrations are generally less than 1 ppm and these values are independent from Au concentrations (Fig. 48).

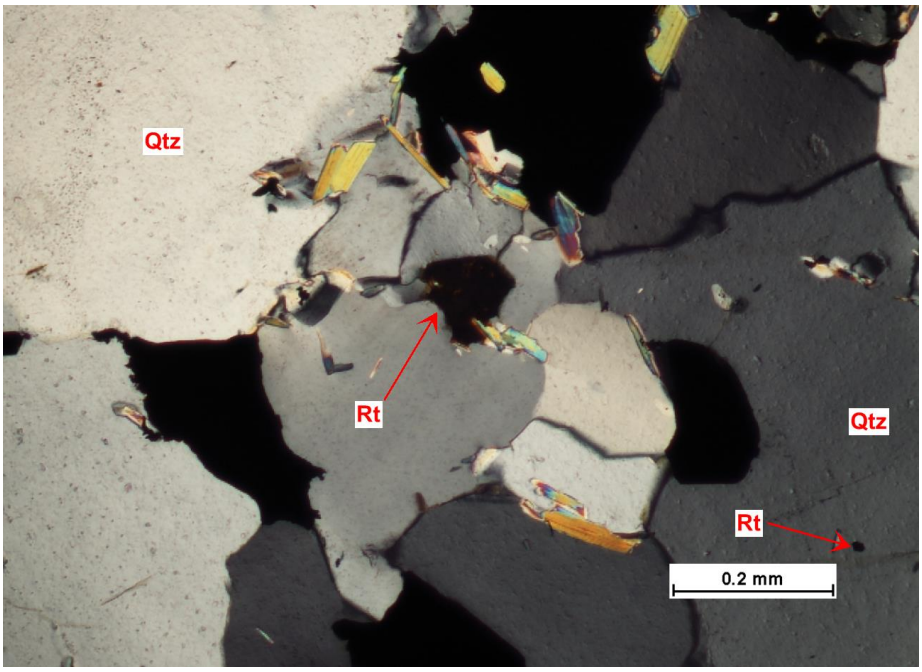

Figure 46: Photomicrograph of blue quartz grains under cross polarized light. Quartz (Qtz) and rutile (Rt).

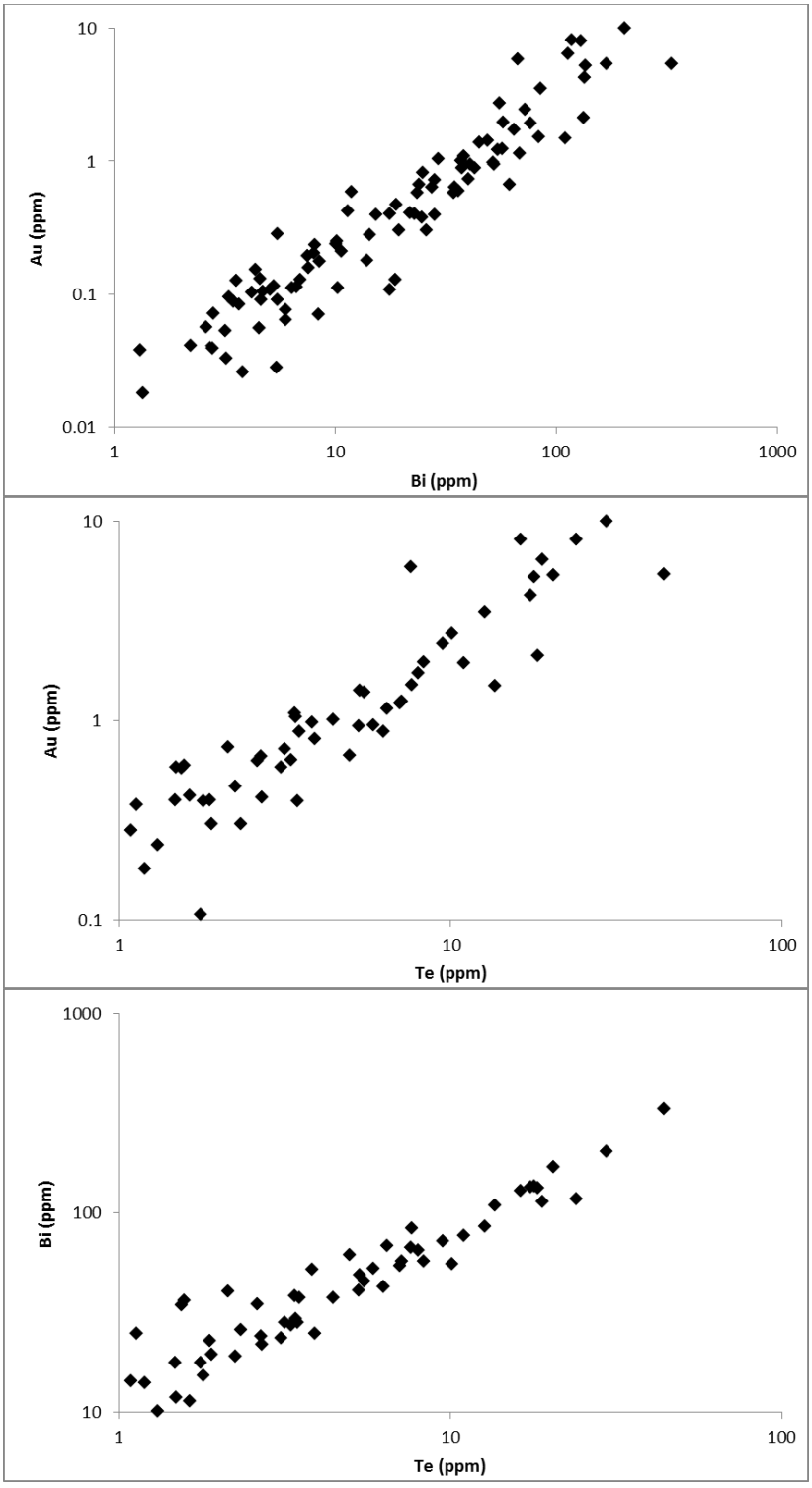

Figure 47: Covariant plots of geochemical data for Au, Bi, and Te for the entire property of the Hog Mountain.

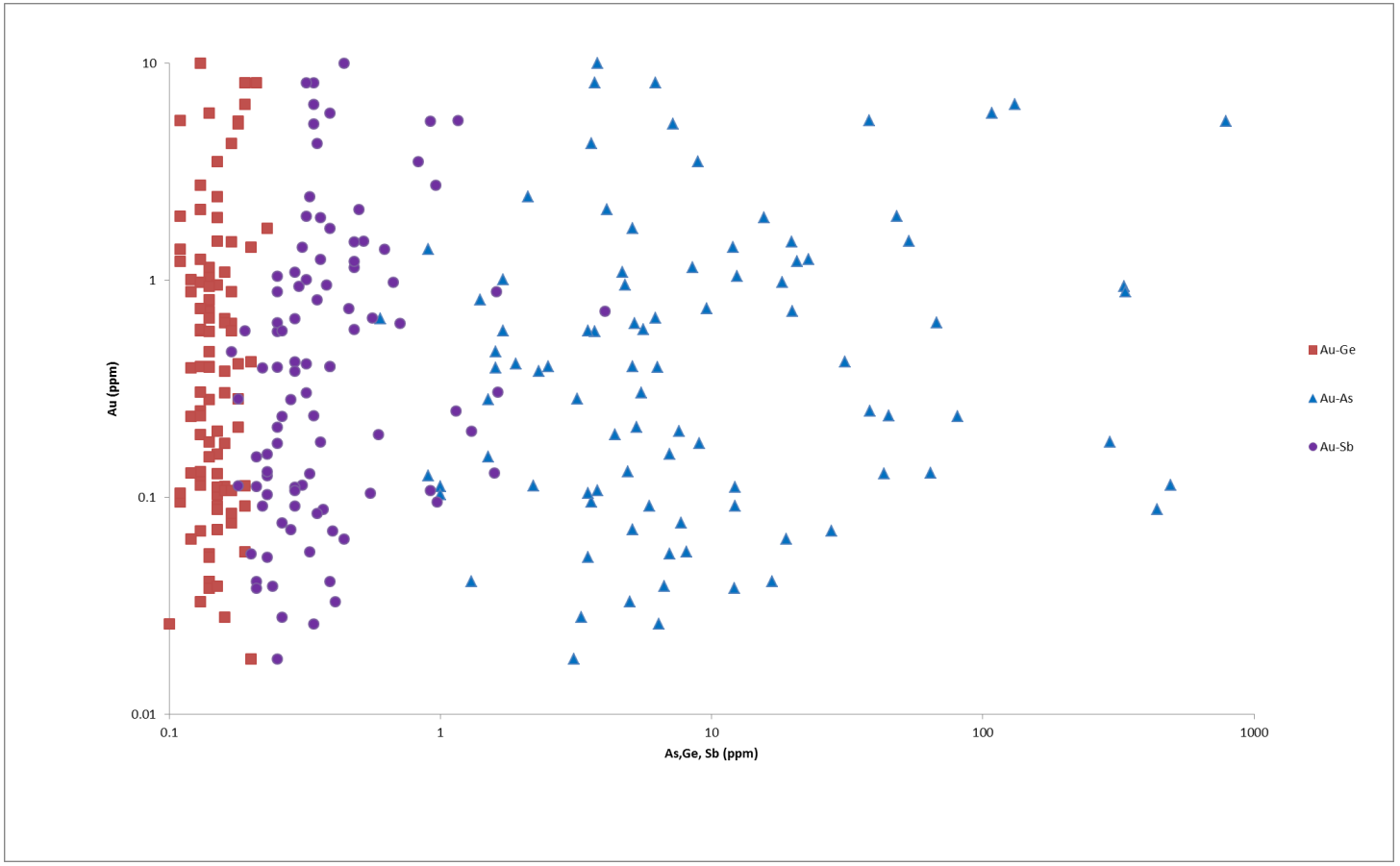

Figure 48: Covariant plots of geochemical data for Au vs metalloids (Ge, As, and Sb)

7. CONCLUSIONS

In general, the Hog Mountain deposit quartz veins are similar in many respects, especially sulfide-mineral assemblages to other quartz vein-hosted gold systems in metasedimentary sequences including the Otago schist, New Zealand, and the Bendigo-Ballarat area of Victoria, Australia.

1. Overall, the ore mineral assemblage of the Sugar Quartz vein is similar to the Kennedy vein except for the greater amount of pyrrhotite in Sugar Quartz vein.

2. The most abundant sulfide mineral is pyrrhotite in both the Sugar Quartz vein and Kennedy vein. It occurs as large masses, remobilized, and filling the fractures. Other sulfide minerals are, in relative order of abundance, chalcopyrite, pyrite, sphalerite, arsenopyrite, and galena.

3. Reflected light studies from the Sugar Quartz vein and Kennedy vein document that gold occurs with pyrite, chalcopyrite, and pyrrhotite. Ninety-five percent of the gold grains identified from Sugar Quartz vein and Kennedy vein have a grain contact with pyrite grains indicating that gold in both veins is found associated with pyrite. Moreover, yellow color and reflectance indicate that it is essentially pure gold.

4. Geochemical analysis from the Blue vein and the entire property of Hog Mountain indicate that there are highly strong correlations between Au and Te, Au and Bi, and Bi and Te.

5. Geochemical analysis and polished section studies documents that the highest gold grade in Sugar Quartz vein is found between 265.00-268.00 feet in drill core HM 71.

6. Mica-group mineral inclusions and rutile grains and its inclusions may be the reason for the origin of the blue color of quartz in the Blue vein.

7. Gangue mineral textures especially planar deformation features in quartz support that quartz grains experienced mylonitic strains under high pressure and high temperature crustal condition.

8. Potassic alteration and phyllic alteration are the main alteration assemblages in wall-rock alteration zones. Along the quartz vein edges, most of the biotite minerals are converted to muscovite.

9. Further research at the Hog Mountain mine is needed to better characterize veins via geochemical analyses such as detailed geochemical analysis for each veins. Detailed microprobe analyses would help to better characterize the composition of gold and other ore minerals, especially, pyrrhotite which could be hosting Fe, Se, Co, Ni, Bi, and Te in the veins. Microprobe analyses could also aid in characterizing the origin of the blue color of the quartz in the Blue vein.

REFERENCES

Adams, G.I., 1930, Gold deposits of Alabama, and occurences of copper, pyrite, arsenic, and tin: Alabama Geological Survey Bulletin 40, 91 p.

Adams, S.F., 1920, A microscopic study of vein quartz: Economic Geology, v. 15, p. 623-664.

Aldrich, T.H., Jr., 1909, The treatment of the gold ores of Hog Mountain, Alabama: American Institute of Mining and Metallurgical Engineers Transactions, v. 39, p. 578.

Berger, B.R., 1986, Descriptive model of low-sulphide Au-quartz veins: U.S. Geological Survey Bulletin 1963, p. 183-186.

Bierlin, F.P., Groves, D.I., Goldfarb, R.J., and Dube, B., 2006, Lithospheric controls on the formation of giant orogenic gold deposits: Mineralium Deposita, v. 40, p. 874-886.

Bohlke, J.K., 1982, Orogenic (metamorphic-hosted) gold-quartz veins: U.S. Geological Survey, Open-File Report 82-795, p. 70-76.

Cook, N.J., Ciobanu, C.L., Meria, D., Silcock, D., and Wade, B., 2012, Arsenopyrite-Pyrite association in an orogenic gold ore: Tracing mineralization history from textures and trace elements: Economic Geology, v. 108, p. 1273-1283.

Drummond, M.S., Neilson, M.J., Allison, D.T., and Tull, J.F., 1997, Igneous petrogenesis and tectonic setting of granitic rocks from the eastern Blue Ridge and Inner Piedmont, Alabama Appalachians: Boulder, Colorado, Geological Society of America Memoir 191, p. 147-164.

Eilu, P.K., Mathison, C.I., Groves, D.I., and Allardyce, W.J., 1999, Atlas of alteration assemblages, styles and zoning in orogenic lode-gold deposits in a variety of host

rock and metamorphic settings: The University of Western Australia Publication, v. 30, 80 p.

Gebre-Mariam, M., Hagemann, S.G., and Groves, D.I., 1995, A classification scheme for epigenetic Archean lode-gold deposits: Mineralium Deposita, v. 30, p. 408-410.

Goldfarb, R.J., Groves, D.I., and Gardoll, S., 2001, Orogenic gold and geologic time: a global synthesis: Ore Geology Reviews, v. 18, p. 1-75.

Goldfarb, R.J., Baker, T., Dube, B., Groves, D.I., Hart, C.J.R., and Gosselin, P., 2005, Distribution, character, and genesis of gold deposits in metamorphic terranes: Economic Geology 100th Anniversary Volume, p. 407-450.

Goldfarb, R.J., Taylor, R.D., Collins, G.S., Goryachev, N.A., and Orlandini, O.F., 2014, Phanerozoic continental growth and gold metallogeny of Asia: Gondwana Research 25, p. 48-102.

Goldfarb, R.J., and Groves, D.I., 2015, Orogenic gold: common or evolving fluid and metal sources through time: Lithos, v. 233, p. 2-26.

Goltrant, O., Cordier, P., and Doukhan, J.C., 1991, Planar deformation features in shocked quartz: a transmissinon electron microscopy investigation: Earth and Planetary Science Letters, v. 106, p. 103-115.

Green, N.L., A.K., Sinha, A.K., and Lesher, C.M., 1988, Gold associated with retrograded shear zones: An Alleghanian episode of mineralization in the southern Appalachians (abs.): Geological Society of America Abstracts with Programs, v. 21, no. 7, p. A277.

Groves D.I., Goldfarb R.J., Gebre-Mariam M., Hagemann S.G., and Robert F., 1998, Orogenic gold deposits: A proposed classification in the context of their crustal distribution and relationship to other gold deposit types: Ore Geology Reviews, v. 13, p. 7-27.

Groves, D.I., Goldfarb, R.J., Robert, F., and Hart, C.J.R., 2003, Gold deposits in metamorphic belts: Overview of current understanding, outstanding problems, future research, and exploration significance: Economic Geology, v. 98, p. 1-29.

Groves, D.I., and Santosh, M., 2015, The giant Jiaodong gold province: The key to a unified model for orogenic gold deposits: Geoscience Frontiers, p. 1-9.

Groves, D.I., Goldfarb, R.J., Santosh, M., 2015, The conjunction of factors that lead to the formation of giant gold provinces and deposits in non-arc settings: Geoscience Frontiers, http://dx.doi.org/10.1016/j.gsf.2015.07.001.

Guthrie, G.M., 1989, Geology and marble resources of the Sylacauga marble district: Alabama Geological Survey Bulletin 131, 81 p.

Guthrie, G.M., and Dean, L.S., 1989, Geology of the New Site 7.5-Quadrangle, Tallapoosa and Clay Counties, Alabama: Alabama Geological Survey Quadrangle Map 9, 41 p.

Guthrie, G.M., and Lesher, C.M., 1989, Geologic setting of lode gold deposits in the Northern Piedmont and Brevard zone, Alabama: Geological Survey of Alabama Bulletin 136, p. 11-32.

Hagemann, S.G., and Brown, P.E., 2000, Gold in 2000: An introduction: SEG Reviews, v. 13, p. 1-7.

Hatcher, R.D., Jr., Osberg, P.H., Drake, A.A., Jr., Robinson, P., Thomas, W.A., 1990, Tectonic map of the U.S. Appalachians: Geological Society of America, Geology of North America, v. F-2, plate 2.

Hooper, R.J., and Hatcher. R.D., Jr., 1988, Pine Mountain terrane, a complex window in the Georgia and Alabama Piedmont, evidence from the eastern termination: Geology, v. 16, p. 307-310.

Kerrich, R., and Cassidy, K.F., 1994, Temporal relationships of lode gold mineralization to accretion, magmatism, metamorphism and deformation-Archean to present: A review: Ore Geology Reviews, v. 9, p. 263-310.

Kerrich,R., and Wyman, D., 1990, The geodynamic setting of mesothermal gold deposits: An association with accretionary tectonic regimes: Geology, v. 18, p. 882-885.

Lambe, R.L., 1982, Hog Mountain Gold Project Alabama: Phase 2 Exploration Program, unpublished report, 13 p.

Lindgren, W., 1933, Mineral deposits, 4th ed.: New York, McGraw-Hill, 930 p.

Neathery, T. L., and Reynolds, J. W., 1975, Geology of the Lineville East, Ofelia, Wadley North, and Mellow Valley Quadrangles: Alabama Geological Survey Bulletin 109, 120 p.

Osborne, W. E., Szabo, M. W., Neathery, T. L., and Copeland, C. W., Jr., compilers, 1988, Geologic map of Alabama, northeast sheet (1:250,000): Alabama Geological Survey Special Map 220.

Pardee, J.T., and Park, C.F., Jr., 1948, Gold deposits of the southern Piedmont: U.S. Geological Survey Professional Paper 213, 156 p.

Park, C.F., 1935, Hog Mountain gold district, Alabama: American Institute of Mining and Metallurgical Engineers Transactions, Mining Geology, v. 115, p. 209-228.

Phillips, G.N., and Powell, R., 2015, A practical classification of gold deposits, with a theoretical basis: Ore Geology Reviews, v. 65, p. 568-573.

Raymond, D.E., Osborne, W.E., Copeland, C.W., and Neathery T.L., 1988, Alabama Stratigraphy: Alabama Geological Survey Circular 140, 97 p.

Ridley, J., 2013, Ore Deposits Geology, Cambridge: Cambridge University Press pp. 201-216.

Robert, F., Poulsen, K.H., and Dube, B., 1997, Gold deposits and their geological classification: Exploration Geochemistry, v. 29, p. 209-220.

Russell, G.S., 1978, U-Pb, Rb-Sr, and K-Ar isotopic studies bearing on the development of the southernmost Appalachian orogen, Alabama: Unpublished Ph.D. thesis, Tallahassee, Florida, Florida State University, 197 p.

Sapp C.D., and Emplaincourt J., 1975, Physiographic regions of Alabama: Alabama Geological Survey Special Map 168, scale 1:100.000.

Saunders, J., Steltenpohl, M., and Cook, R.B., 2013, Gold exploration and potential of the Appalachian Piedmont of Eastern Alabama: SEG Newsletter 94, p. 13-19.

Saunders, J.A., Hofstra A.H., Goldfarb R.J. and Reed M.H., 2014, Geochemistry of Hydrothermal Gold Deposits. In: Holland H.D. and Turekian K.K. (eds) Treatise on Geochemistry, second edition, v. 13. p. 383-424.

Seifert, W., Rhede, D., Thomas, R., Forster, H.J., Lucassen, F., Dulski, P., and Wirth, R., 2011, Distinctive properties of rock-froming blue quartz: inferences from a multi-anaytical study of submicron mineral inclusion: Mineralogical Magazine, v. 75(4), pp. 2519-2534.

Steltenpohl, M.G., Heatherington, A.L., and Guthrie, G.M., 1995, Geologic setting and Alleghanian development of the Alabama and southwest Georgia inner and southern Piedmonts, in Guthrie, G.M., ed., The timing and tectonic mechanism of the Alleghanian orogeny, Alabama Piedmont: Alabama Geological Society Fieldtrip Guidebook, p. 17-41.

Stowell, H.H., Lesher, C.M., Green, N.L., Sha, P., Guthrie, G.M. and Sinha, A.K., 1996, Metamorphism and gold mineralization in the Blue Ridge, southernmost Appalachians: Economic Geology, v. 91, p. 1115-1144.

APPENDIX

RE12110603 - Finalized																							
CLIENT : " MINWEL - Wellborn Mining Company LLC"																							
# of SAMPLES: 96																							
DATE RECEIVED : 2012-05-17 DATE FINALIZED : 2012-06-02																							
CERTIFICATE COMMENTS: " Hg-CV41:Detection limits on samples requiring dilutions due to interferences or high concentration levels have been increased according to the dilution factor. ME-MS61r :REE's may not be totally soluble in this r																							
	WEI-21	Au-AA23	ME-MS61r	ME-MS61r	ME-MS61r	ME-MS61r	ME-MS61r	ME-MS61r	ME-MS61r	ME-MS61r	ME-MS61r	ME-MS61r	ME-MS61r	ME-MS61r	ME-MS61r	ME-MS61r	ME-MS61r	ME-MS61r	ME-MS61r	ME-MS61r	ME-MS61r	ME-MS61r	ME-MS61r	ME-MS61r
SAMPLE	Recvd Wt.	Au	Ag	Al	As	Ba	Be	Bi	Ca	Cd	Ce	Co	Cr	Cs	Cu	Fe	Ga	Ge	Hf	In	K	La	
DESCRIPTION	kg	ppm	ppm	%	ppm	ppm	ppm	ppm	%	ppm	ppm	ppm	ppm	ppm	ppm	%	ppm	ppm	ppm	ppm	%	ppm	
HM-1 175-180	0.02	0.202	0.59	7.78	7.6	520	3.44	8.05	1.88	0.16	44.4	5.7	49	6.73	188.5	3.88	23.8	0.15	0.9	0.071	1.76	20.7	
HM-1 180-185	0.02	0.72	1.45	7.13	19.8	550	3.44	28.2	1.57	0.25	48.6	7.6	134	4.98	607	4.54	23.2	0.14	0.8	0.093	1.88	23.7	
HM-1 185-190	0.02	0.194	0.22	7.56	4.4	500	2.72	7.48	1.91	0.14	42	5.7	55	6.24	118.5	3.3	23.2	0.13	0.8	0.054	1.63	19.5	
HM-1 190-195	0.02	5.39	1.31	3.94	786	300	1.83	169	0.7	2.53	20.1	27.5	122	2.75	714	7.52	12.6	0.18	0.4	0.045	1.12	9.6	
HM-1 215-220	0.02	2.11	3.03	5.36	4.1	380	2.88	133.5	1.19	0.75	32.9	8.6	95	6.31	137.5	4.5	16.4	0.13	0.6	0.046	1.47	15.7	
HM-1 220-224	0.02	0.033	0.41	7.82	5	540	3.3	3.23	1.99	0.32	42.4	6	76	9.27	78.1	3.06	23.2	0.13	0.9	0.043	1.88	19.6	
HM-1 271-275	0.02	1.735	1.16	2.98	5.1	270	1.4	64.7	0.37	4.92	15.8	23.6	130	3.13	815	10.3	10.35	0.23	0.3	0.069	1.05	7.6	
HM-1 275-280	0.02	0.401	0.25	7.49	2.5	520	3.3	17.65	1.75	0.16	41.9	6.2	80	6.12	129	3.68	22.8	0.14	0.9	0.079	1.84	19.6	
HM-2 190-195	0.02	0.041	0.19	7.73	16.7	540	3.54	2.71	1.67	0.26	38.8	5.5	104	10.05	114.5	2.93	23	0.14	1.1	0.039	2.22	18	
HM-2 195-200	0.02	0.07	0.46	7.2	27.6	510	3.12	8.45	1.44	0.19	42.3	5.6	79	9.21	126.5	3.22	21.6	0.13	1	0.055	2.21	19.8	
HM-2 200-205	0.02	5.88	0.82	6.5	108	480	2.74	67.1	1.38	0.14	37.1	7.7	110	7.45	161	4.3	19.35	0.14	0.9	0.06	1.98	17.8	
HM-2 205-210	0.02	0.114	0.26	7.7	493	570	3.7	5.28	1.62	0.78	39.7	5.1	70	11.1	138	2.99	23.1	0.13	1.2	0.061	2.65	18	
HM-2 210-212	0.02	0.128	0.39	7.94	43.2	580	3.43	6.98	1.66	0.33	43.6	5.4	78	10.35	185	3.26	24.2	0.15	1.2	0.07	2.36	20.2	
HM-4 95-100	0.02	5.44	2.16	1.61	38.1	190	0.99	333	0.26	0.46	13.15	8.4	164	1.29	464	4.47	7.35	0.11	0.1	0.035	0.68	6.2	
HM-4 100-105	0.02	0.814	0.26	7.48	1.4	580	3.29	24.9	1.6	0.3	50.3	6.6	81	8.48	171	3.62	26.1	0.14	0.7	0.094	2.28	24.5	
HM-4 105-110	0.02	0.281	0.15	7.85	1.5	520	3.29	14.35	1.49	0.29	51.2	6.1	62	5.96	95.1	3.64	25	0.14	0.8	0.076	1.76	24.4	
HM-4 110-113	0.02	0.041	0.09	7.8	1.3	560	3.29	2.22	2.04	0.36	48.6	5.7	58	7.57	81.8	3.19	24.8	0.14	0.9	0.057	1.8	22.7	
HM-4 233-235	0.02	0.112	0.19	7.57	1	530	4.37	6.39	1.5	0.23	43.2	6.1	77	10.1	158	3.35	24.6	0.16	1	0.061	2.27	20.5	
HM-4 235-240	0.02	0.113	0.29	7.58	2.2	570	3.81	6.67	1.48	0.2	43.9	10.2	71	8.83	267	4.82	23.4	0.19	0.9	0.058	2.32	20.7	
HM-4 240-245	0.02	5.25	1.24	3.84	7.2	330	1.7	135.5	0.78	0.28	27.3	14.2	139	3.27	423	5.66	14.15	0.18	0.4	0.028	1.05	13.3	
HM-4 245-250	0.02	>10.0	1.62	1.1	3.8	150	0.42	204	0.09	0.13	6.01	13.1	188	0.75	281	5.28	5.69	0.13	0.1	0.014	0.45	2.9	
HM-4 250-255	0.02	4.28	1.34	4.53	3.6	540	2.03	134	0.68	0.17	36.3	11.4	146	3.6	342	4.85	18.65	0.17	0.6	0.048	1.61	17.4	
HM-4 255-260	0.02	0.586	0.3	6.51	1.7	610	2.66	11.85	1.38	0.16	37.6	7.1	102	5.06	205	3.48	22.7	0.13	0.8	0.048	1.86	17.9	
HM-4 290-295	0.02	0.103	0.18	7.51	1	550	3.14	4.21	1.93	0.15	41.1	5.4	75	8.04	97.8	2.83	22.5	0.15	1.1	0.05	1.95	18.9	
HM-4 295-300	0.02	0.071	0.19	7.44	5.1	540	3.03	2.82	1.93	0.23	41.6	6	72	9.23	94.3	2.91	22.9	0.15	1.1	0.043	1.93	19	
HM-4 300-305	0.02	3.51	2.17	3.5	8.9	270	1.26	85.1	0.66	0.12	19.25	12.7	137	3.28	347	5.39	11.85	0.15	0.4	0.028	0.89	9.2	
HM-4 305-310	0.02	2.43	0.96	6.09	2.1	610	2.26	72.1	1.57	0.19	45.6	10.7	124	6.85	312	4.42	22.7	0.15	1	0.056	2.4	22.2	
HM-4 310-315	0.02	0.422	0.51	5.46	31.1	460	1.77	11.4	1.02	0.25	29.5	20.2	98	6.91	434	7.68	18.55	0.2	0.8	0.032	1.52	14	
HM-4 315-319	0.02	0.126	0.18	7.52	0.9	620	3.07	3.58	1.59	0.2	41.1	5.2	61	9.2	82.8	2.82	23.9	0.13	1.1	0.05	2.05	19	
HM-5 101-105	0.02	0.47	0.19	6.57	1.6	690	3.97	18.95	0.62	0.12	37.3	5.9	110	4	175.5	2.98	29.3	0.14	1.6	0.067	2.74	18.2	
HM-5 105-110	0.02	1.01	0.27	5.6	1.7	560	3.47	37.3	0.4	0.11	22.2	6.6	161	3.58	159.5	3.18	22.9	0.12	1.4	0.07	2.2	11.1	
HM-5 110-115	0.02	0.395	0.22	6.28	1.6	620	3.32	15.3	0.57	0.12	23.6	11.8	131	4.03	341	5.09	19.35	0.12	1.6	0.055	2.4	11.1	
HM-5 115-120	0.02	0.664	0.35	8.62	0.6	940	4.7	24	0.6	0.15	36.1	8.6	74	6.51	438	4.08	29.3	0.16	2	0.087	3.7	16.6	
HM-5 120-125	0.02	8.1	0.63	9.44	6.2	940	4.35	129	1.13	0.19	44.4	19.4	69	6.46	715	7.28	36.9	0.21	2.1	0.083	3.34	20.3	
HM-5 125-130	0.02	1.39	0.23	9.34	0.9	1000	4.89	45.1	0.73	0.06	37.7	7.3	77	6.24	188.5	3.6	33.4	0.11	2.2	0.08	3.54	17.3	
HM-6 175-180	0.02	0.131	0.06	8.6	4.9	560	2.39	4.58	2.41	0.07	45.2	6.8	97	4.15	88.5	3.39	23.6	0.13	1	0.059	1.63	19.9	
HM-6 180-185	0.02	0.095	0.09	8.6	3.6	540	2.69	3.31	2.34	0.04	43.5	6.5	74	4.46	118.5	3.4	23.3	0.11	1	0.049	1.65	19.1	
HM-6 185-190	0.02	0.104	0.06	8.68	3.5	520	2.98	4.73	2.45	0.06	45.2	6	81	4.54	72	3.43	22.3	0.11	1	0.047	1.53	19.7	
HM-6 190-195	0.02	0.883	0.3	6.71	>10000	530	2.91	42.7	1.42	0.13	37.2	24	98	4.6	161	4.77	21.7	0.12	0.8	0.085	1.96	16.8	
HM-6 195-200	0.02	0.064	0.16	8.65	18.8	540	3.43	5.98	2.19	0.1	46.7	6.6	91	5.8	226	3.63	24.3	0.12	1.1	0.062	1.85	21.2	
HM-6 200-203.5	0.02	0.235	0.1	8.57	80.5	530	2.84	8.11	2.38	0.07	45.9	6.5	71	4.59	112	3.54	23.4	0.12	1	0.057	1.55	20.2	
HM-6 276-280	0.02	1.085	0.35	8.35	4.7	830	4.2	38.2	1.27	1.33	48.2	8.5	86	6.35	188	4.34	30	0.16	1.2	0.119	2.85	21.8	
HM-6 280-285	0.02	1.045	0.18	8.61	12.4	810	3.51	29.4	1.56	0.16	48.7	8.8	71	5.39	222	4.2	30.8	0.14	1.6	0.121	2.89	21.7	
HM-7 245-250	0.02	0.25	0.89	7.81	38.3	670	3.21	10.2	1.58	0.18	36.8	4.9	83	4.88	287	2.95	22.3	0.13	1.9	0.047	1.96	16.9	
HM-7 250-255	0.02	0.111	1.48	8.88	12.2	800	3.87	10.25	1.73	10.9	43	5.3	78	9.03	97.4	2.9	26.8	0.15	2.2	0.144	2.66	19.8	
HM-7 255-260	0.02	2.73	5.17	5.86	6650	530	2.48	55.6	1.1	0.41	27.3	11.2	85	5.37	284	4.92	19	0.13	1.3	0.051	1.78	12.9	
HM-7 260-265	0.02	1.965	0.7	6.89	48.2	600	3.1	57.4	1.2	0.26	32	6.2	97	5.03	176.5	3.46	21.3	0.11	1.5	0.05	1.99	15	
HM-7 265-270	0.02	0.026	0.21	8.18	6.4	660	3.78	3.81	1.77	0.34	37.6	5.2	47	7.09	106.5	2.87	22.2	0.1	1.9	0.044	2.01	17.3	
HM-7 270-273	0.02	0.055	0.21	8.17	7	640	3.68	4.53	1.78	0.22	38.3	4.6	58	7.31	69.7	2.55	21.5	0.14	1.8	0.03	1.95	17.7	
HM-8 121-125	0.02	0.129	3.17	7.54	64.3	680	4.61	18.7	1.28	1.86	36.5	4.3	64	6.97	109	2.87	25.1	0.12	2.1	0.116	2.27	17.1	
HM-8 125-131	0.02	0.304	1.71	7.96	8040	760	5.78	19.55	0.95	0.49	34.2	3.9	72	7.93	72.8	2.84	28.8	0.13	2.2	0.104	2.88	15.9	
HM-8 140.5-145	0.02	0.976	0.22	7.47	18.2	730	3.83	51.8	1.21	0.89	35.7	6.6	57	3.59	161	3.31	24	0.13	2.1	0.101	1.95	16.6	
HM-8 145-150	0.02	1.515	0.48	7.04	53.3	670	4.21	83.8	1.17	12	35.4	8.5	77	3.48	179	3.81	23	0.15	2	0.163	1.9	16.8	
HM-8 150-155	0.02	0.595	0.21	7.97	5.6	730	4.28	36.3	1.33	0.16	37.4	7.8	81	3.41	175.5	3.55	25.9	0.13	2.2	0.1	2.02	17.6	
HM-8 155-160	0.02	0.739	0.2	7.77	9.6	750	3.85	40.3	1.28	0.2	38.7	7.7	84	3.31	174.5	3.33	26	0.13	2.2	0.103	2	18.1	
HM-8 160-165	0.02	1.145	0.37	6.86	8.5	740	3.74	68.2	0.76	0.05	25.9	8.2	116	2.78	177.5	3.75	29.4	0.14	1.9	0.076	2.33	12.1	
HM-8 165-170	0.02	0.632	0.18	7.4	5.2	780	3.75	34.9	1.09	0.09	32.4	10	81	3.19	235	4.08	27.7	0.17	2	0.098	2.23	15.3	
HM-8 170-175	0.02	0.38	0.09	7.65	2.3	670	4.03	24.7	1.42	0.04	37.6	6.8	66	3.07	164	3.21	24.3	0.16	2.2	0.087	1.8	17.8	
HM-8 175-180	0.02	0.579	0.14	7.64	3.7	720	3.59	34.6	1.24	0.12	38.7	8	76	2.82	205	3.45	26.6	0.14	2.3	0.11	2.09	18.2	
HM-8 277-280	0.02	0.671	1.14	7.27	6.2	530	3.65	61.3	1.61	0.82	33.3	6	76	4.97	137.5	3.48	20.3	0.14	1.9	0.059	1.49	15.6	
HM-8 280-285	0.02	0.401	0.23	7.54	5.1	660	3.18	22.8	1.75	0.06	32.4	4.5	67	5.71	78.4	2.74	20.5	0.13	2.2	0.04	1.7	15	
HM-8 285-290	0.02	1.5	0.97	5.66	19.7	550	3.62	109.5	0.74	26	23.7	11.6	92	3.2	281	5.55	18.2	0.17	1.3	0.302	1.89	11.2	
HM-8 290-296	0.02	0.95	0.48	6.23	4.8	570	3.65	52.5	0.93	0.32	25.8	9.1	107	3.36	189.5	4.32	21.7	0.15	1.7	0.082	1.88	12.4	
HM-9 110-115	0.02	1.245	0.28	6.21	22.8	520	3.4	57.1	1.05	0.65	28.2	4.9	88	5.33	99.1	2.95	21.1	0.13	1.3	0.053	1.55	13.2	
HM-9 115-120	0.02	1.225	0.32	5.99	20.7	450	3	54.3	1.05	0.15	28.8	5.3	105	6.77	120	3.1	17.45	0.11	1.4	0.028	1.31	13.5	
HM-9 120-125	0.02	0.238	0.22	7.84	45.1	610	3.67	10.05	1.42	0.19	39	5	78	10.25	102.5	2.68	21.5	0.13	1.8	0.033	1.87	18	
HM-9 125-131	0.02	0.107	3.68	7.36	8630	570	3.54	17.75	2.14	4.42	32.5	8.8	55	11	123.5	3.03	21.3	0.16	1.6	0.052	1.93	15.4	
HM-9 211-215	0.02	0.091	0.38	8.54	12.2	520	4.31	5.46	2.15	0.31	46.9	4	72	11.65	95.5	3.29	23.8	0.15	0.9	0.055	1.93	21.6	
HM-9 215-220	0.02	0.636	0.71	7.9	67.5	540	3.76	27.3	1.76	0.35	45.1	4.6	80	10.75	169.5	3.39	23.7	0.16	0.8	0.061	1.97	21.3	
HM-9 220-225	0.02	1.42	1.43	7.63	12	640	3.48	48.9	3.4	0.31	37.7	10.3	67	8.03	192	5.86	24.3	0.2	0.7	0.071	2.25	17.6	
HM-9 225-230	0.02	1.945	2.07	3.78	15.6	310	1.38	76.8	3.57	0.13	19.25	7.8	140	3.88	229	4.17	11.8	0.15	0.3	0.035	1.05	9.3	
HM-9 230-235	0.02	0.107	0.46	7.95	3.8	480	3.49	5.06	2.12	0.28	43.8	4.5	86	10.5	75.9	3.21	22.8	0.17	0.9	0.046	1.61	20.2	
HM-9 235-239	0.02	0.076	0.54	8.19	7.7	490	4.14	5.96	2.15	0.99	45	3.9	86	11	56.2	3	22.6	0.17	0.9	0.057	1.78	20.5	
HM-10 113-115	0.02	0.053	0.1	7.87	3.5	550	3.19	3.2	2.16	28.3	33	3	76	7.14	48.6	2.56	20.1	0.14	1.6	0.477	1.48	15.5	
HM-10 115-120	0.02	0.038	0.06	7.66	12.1	560	2.96	1.31	1.96	0.24	33.9	3.1	67	7.48	25.3	2.34	20.9	0.14	1.7	0.034	1.43	15.6	
HM-10 120-125	0.02	0.583	0.24	7.49	3.5	580	3.4	23.6	1.79	0.57	35.1	4.3	61	6.66	105	2.8	20.8	0.17	1.5	0.05	1.66	16.8	
HM-10 125-130	0.02	0.303	5.01	7.74	5.5	580	2.86	26	1.86	0.28	32.7	4.6	80	6.61	67.5	2.9	19.75	0.16	1.6	0.034	1.47	15.8	
HM-10 130-135	0.02	0.18	0.63	7.66	295	570	3.26	14	1.78	0.22	35.7	6.5	60	7.87	58.3	2.67	21.8	0.14	1.7	0.043	1.72	17	
HM-10 135-142	0.02	0.028	1.4	7.55	3.3	590	3.31	5.41	1.9	3.33	33.7	4	52	7.71	65.9	2.48	21	0.16	1.6	0.058	1.78	16	
HM-11 107.5-110	0.02	0.088	0.09	7.91	439	610	2.96	3.46	1.9	0.15	37.7	5.2	56	5.37	32.7	2.5	21.7	0.15	1.7	0.035	1.57	18	
HM-11 110-115	0.02	0.397	0.35	7.49	6.3	570	3.07	28.2	1.63	0.17	36.5	4	65	5.53	66.4	2.57	21	0.14	1.6	0.036	1.56	17.5	
HM-11 115-120	0.02	0.084	0.15	8.14	1745	640	3	3.69	1.93	0.13	39.7	7.7	65	6.17	40.5	2.68	21.3	0.17	1.8	0.03	1.78	18.6	
HM-11 120-127	0.02	0.158	0.16	8.03	7	640	3.01	7.58	1.87	0.08	38.3	3.7	62	4.88	56.3	2.53	21.8	0.15	1.8	0.035	1.67	18.2	
HM-11 253-260	0.02	0.177	0.34	8	9	640	2.78	8.5	1.91	0.28	36.9	3.9	69	6.09	61.2	2.67	21.3	0.16	1.7	0.039	1.51	17.7	
HM-11 260-265	0.02	0.153	0.13	8.17	1.5	690	2.88	4.35	1.94	0.13	35.4	3.6	46	5.73	55.7	2.44	20.9	0.14	1.9	0.036	1.58	17	
HM-11 265-272	0.02	0.939	0.33	7.61	332	600	3.14	40.9	1.68	2.04	33.3	4.6	58	5.36	116.5	2.75	19.75	0.14	1.7	0.065	1.51	16.3	
HM-12 42-50	0.02	0.882	2.33	7.64	336	570	3.71	37.6	0.9	0.32	39.6	5.1	85	10.7	147	3.67	21.2	0.17	0.7	0.05	2.11	19.1	
HM-12 50-55	0.02	0.056	0.1	9.03	8.1	590	2.86	2.6	2.21	0.08	47.1	5	73	8.19	42	3.59	23.5	0.19	0.9	0.051	1.81	21.5	
HM-12 55-60	0.02	0.039	0.14	9.26	6.7	610	2.88	2.78	2.27	0.22	46.6	5.6	86	7.41	31.4	3.41	23	0.15	0.9	0.037	1.74	21.2	
HM-12 60-62.5	0.02	0.018	0.09	8.4	3.1	540	2.81	1.35	2.18	0.15	45.8	5	65	8.19	29.7	3.04	22.3	0.2	0.8	0.041	1.6	20.8	
HM-12 111-118.5	0.02	0.091	0.12	8.47	5.9	610	2.97	4.61	2.13	0.16	49.3	6.1	76	9.24	70	3.3	25	0.19	0.8	0.047	1.82	22.5	
HM-12 119-120	0.02	6.44	1	2.46	131.5	240	1.24	113.5	0.36	0.16	8.44	18.4	168	1.51	325	6.88	8.78	0.19	0.3	0.011	0.64	4	
HM-12 120-125	0.02	0.284	0.18	8.41	3.2	640	3.43	5.49	1.76	0.08	49.9	7	82	6.88	198	3.55	27.7	0.18	0.8	0.036	2.07	23.5	
HM-12 125-130	0.02	8.12	1.2	5.05	3.7	460	1.6	117.5	1.06	0.12	29.1	15.2	81	3.58	329	6.19	17.7	0.19	0.5	0.025	1.36	13.8	
HM-12 130-135	0.02	0.411	0.17	7.77	1.9	480	2.83	21.9	2.01	0.2	44.6	6.2	81	7.14	104.5	3.41	22.1	0.18	0.8	0.036	1.59	20.4	
HM-12 135-140	0.02	0.211	0.12	8.52	5.3	580	3.02	10.65	2.2	0.26	45.6	6.1	63	7.61	76	3.59	22.9	0.18	0.8	0.045	1.82	20.8	

Appendix (part 1)

RE12110603 - Finalized																							
CLIENT : " MINWEL - Wellborn Mining Company LLC"																							
# of SAMPLES: 96																							
DATE RECEIVED: 2012-05-17 DATE FINALIZED: 2012-06-02																							
CERTIFICATE COMMENTS: " Hg-CV41:Detection limits on samples requiring dilutions due to interferences or high concentration levels have been increased according to the dilution factor.. ME-MS61r:REE's may not be totally soluble in this r																							
	ME-MS61r	ME-MS61r	ME-MS61r	ME-MS61r	ME-MS61r	ME-MS61r	ME-MS61r	ME-MS61r	ME-MS61r	ME-MS61r	ME-MS61r	ME-MS61r	ME-MS61r	ME-MS61r	ME-MS61r	ME-MS61r	ME-MS61r	ME-MS61r	ME-MS61r	ME-MS61r	ME-MS61r	ME-MS61r	ME-MS61r	ME-MS61r
SAMPLE	Li	Mg	Mn	Mo	Na	Nb	Ni	P	Pb	Rb	Re	S	Sb	Sc	Se	Sn	Sr	Ta	Te	Th	Ti	Tl	
DESCRIPTION	ppm	%	ppm	ppm	%	ppm	ppm	ppm	ppm	ppm	ppm	%	ppm	ppm	ppm	ppm	ppm	ppm	ppm	ppm	%	ppm	
HM-1 175-180	73.9	0.59	526	15.65	2.07	8.2	56.6	530	42.4	107.5	0.002	0.75	1.3	7.6	1	20.4	551	0.47	0.64	4.8	0.258	0.63	
HM-1 180-185	70.9	0.58	416	10.25	1.57	7.4	10.5	530	61.8	112.5	0.002	1.45	4.05	7.3	2	40.2	440	0.48	3.16	4.8	0.25	0.51	
HM-1 185-190	73.1	0.61	464	4.48	2.19	7.5	6	550	24.5	91.7	<0.002	0.62	0.59	7.4	1	11.6	570	0.45	0.61	4.5	0.274	0.47	
HM-1 190-195	39.6	0.27	222	8.02	0.76	3.8	6.8	270	38	67.9	<0.002	3.46	0.92	3.5	3	15.1	204	0.23	20.4	2.3	0.127	0.28	
HM-1 215-220	55.7	0.38	367	9.47	1.18	5.4	5.7	460	83.1	100.5	0.002	1.55	0.5	5	2	31.7	306	0.36	18.4	3.4	0.179	0.43	
HM-1 220-224	84.4	0.62	581	5.85	2.22	7.8	6.2	600	40.1	107	<0.002	0.41	0.41	7.9	1	43.9	549	0.49	0.28	4.5	0.284	0.56	
HM-1 271-275	34.3	0.19	176	8.23	0.39	3	7.7	190	13.2	64.3	<0.002	4.55	0.39	2.9	4	11.7	103	0.19	8	1.7	0.097	0.25	
HM-1 275-280	73.7	0.56	412	5.77	1.86	7.3	6.1	520	17.1	107.5	<0.002	0.9	0.39	7.4	1	20.1	488	0.51	1.48	4.4	0.25	0.48	
HM-2 190-195	81.7	0.58	538	6.84	1.9	6.6	5.9	620	29.8	135.5	<0.002	0.68	0.39	7.7	1	53.2	451	0.49	0.22	4.2	0.232	0.62	
HM-2 195-200	73.6	0.52	432	5.37	1.44	5.8	5.7	550	37.1	138.5	<0.002	0.92	0.4	7.1	1	37.4	364	0.46	0.53	4.3	0.213	0.61	
HM-2 200-205	62.3	0.45	435	7.64	1.27	5.4	5.8	510	30.2	122	<0.002	1.5	0.39	6.2	2	27.9	327	0.43	7.58	3.7	0.19	0.48	
HM-2 205-210	85.9	0.55	481	4.85	1.43	6.2	5.3	590	30.2	157	<0.002	0.87	0.31	7.2	1	50.2	367	0.47	0.45	4.3	0.228	0.68	
HM-2 210-212	75	0.58	482	5.55	1.69	7.3	5.6	610	36.2	144.5	0.002	0.86	0.33	7.6	1	37.7	426	0.56	0.63	4.5	0.247	0.65	
HM-4 95-100	19.6	0.09	117	10.8	0.07	1.1	5.8	280	96.8	43.5	0.002	1.97	1.16	1.5	2	9.4	27.7	0.05	44.2	1.2	0.043	0.19	
HM-4 100-105	72.4	0.66	486	6.85	1.9	7.9	6	660	19.1	137.5	<0.002	1.09	0.35	7.6	1	18.1	316	0.43	3.89	5.1	0.3	0.68	
HM-4 105-110	65.9	0.7	499	4.71	2.63	7.9	6.2	690	15.8	103.5	0.002	0.59	0.28	7.8	1	10.9	399	0.47	1.09	5.5	0.315	0.51	
HM-4 110-113	73.9	0.66	537	4.92	2.23	8.1	5.6	630	13.4	105	<0.002	0.6	0.21	8.1	1	24.1	625	0.5	0.23	5.4	0.303	0.53	
HM-4 233-235	80.7	0.58	354	5.65	1.73	6.9	5.5	540	16.3	143	<0.002	1.01	0.21	7.4	1	31.6	464	0.46	0.51	4.6	0.257	0.61	
HM-4 235-240	74.4	0.56	414	5	1.51	6.1	6.1	520	40.1	139.5	0.002	1.95	0.18	7	2	32.4	401	0.4	0.67	4.5	0.243	0.56	
HM-4 240-245	35.4	0.25	190	9.89	0.74	3	8.1	270	9.8	61.7	0.002	2.58	0.34	3.5	2	11	202	0.17	17.9	2.4	0.11	0.25	
HM-4 245-250	11.9	0.06	90	10.15	0.06	1	6.5	70	4.9	25	<0.002	2.34	0.44	1	2	4	19.8	<0.05	29.5	0.8	0.029	0.09	
HM-4 250-255	42.3	0.24	200	10.65	0.62	4.1	5.6	310	13.2	91.6	<0.002	2.1	0.35	4.2	2	12	158.5	0.23	17.45	3.3	0.134	0.29	
HM-4 255-260	53.4	0.37	242	6.54	1.32	5.5	4.9	480	18.5	107.5	0.002	1.22	0.19	5.9	1	12.2	348	0.37	1.49	3.8	0.199	0.4	
HM-4 290-295	68.4	0.49	485	5.41	2.14	7.3	6.5	610	23	112	0.002	0.66	0.23	7.1	1	28.2	494	0.63	0.45	4.3	0.247	0.55	
HM-4 295-300	69.9	0.55	569	5.44	2.3	7.9	5.9	660	26.7	104.5	0.002	0.61	0.28	7.3	1	22	533	0.6	0.33	4.3	0.274	0.55	
HM-4 300-305	35.3	0.26	223	10.4	0.79	3.4	7.2	250	28.7	53.4	<0.002	2.31	0.83	3	2	24.7	211	0.22	12.7	2	0.11	0.25	
HM-4 305-310	63.5	0.5	324	9.12	0.63	6.7	5.7	500	11.8	123	0.002	2.18	0.33	5.8	2	29.1	168	0.48	9.5	4.2	0.201	0.44	
HM-4 310-315	48.7	0.38	291	6.91	1.34	6.3	8.1	430	18.3	89.3	<0.002	3.91	0.29	5.1	2	10.5	258	0.42	1.64	3	0.173	0.36	
HM-4 315-319	71.7	0.61	447	4.38	2.23	7.9	6	610	26	114	0.002	0.54	0.23	7.2	1	21.5	509	0.56	0.4	4.3	0.26	0.58	
HM-5 101-105	76.1	0.32	162	7.98	0.47	3.9	4.1	360	6.3	156.5	<0.002	1.12	0.17	4	1	27	119.5	0.23	2.25	4.2	0.129	0.44	
HM-5 105-110	61.9	0.28	146	12.15	0.52	3.3	5.8	320	10.2	129	0.002	1.31	0.32	3.8	1	24.2	126	0.22	4.44	3.1	0.111	0.35	
HM-5 110-115	61.3	0.33	186	7.58	0.72	2.7	7	380	5.9	124	<0.002	2.47	0.22	3.9	2	32.8	163	0.16	1.8	3	0.116	0.39	
HM-5 115-120	91.3	0.47	216	54.1	0.59	4	5.4	440	6.6	195	0.002	1.67	0.29	6	2	71.9	123.5	0.25	2.68	4.2	0.171	0.65	
HM-5 120-125	73.6	0.47	264	5.33	1.69	7.3	6.9	670	11.6	165	<0.002	3.43	0.34	7.1	2	39.9	284	0.43	16.3	4.8	0.236	0.66	
HM-5 125-130	78.5	0.48	218	6	1.44	5.2	4.8	620	10.6	185.5	0.005	1.29	0.62	6.1	2	54.2	174	0.3	5.48	4.4	0.195	0.73	
HM-6 175-180	70.2	0.65	555	6.74	2.93	7.2	6.1	650	10.2	63.8	0.002	0.44	0.23	7.6	1	6.4	698	0.49	0.39	4.5	0.295	0.39	
HM-6 180-185	68.8	0.66	446	5.29	2.93	7	6.3	650	14.4	67.9	<0.002	0.54	0.97	7.5	1	10.9	684	0.51	0.3	4.6	0.296	0.42	
HM-6 185-190	67	0.69	421	5.73	2.96	6.9	5.7	680	11.1	68	<0.002	0.53	0.55	7.6	1	6.4	714	0.52	0.23	4.7	0.305	0.42	
HM-6 190-195	60.8	0.48	356	8.11	1.35	5.6	5.9	860	10.3	97.2	0.002	1.98	1.61	5.8	2	22.6	365	0.37	6.3	3.7	0.223	0.41	
HM-6 195-200	72	0.64	553	6.03	2.53	7	7.6	810	19.1	90.2	0.002	0.85	0.44	7.6	1	21.7	642	0.48	0.47	4.7	0.286	0.46	
HM-6 200-203.5	70.2	0.66	496	5.1	2.85	7.2	5.9	690	10.5	66.4	0.002	0.62	0.26	7.7	1	7	688	0.49	0.81	4.6	0.299	0.39	
HM-6 276-280	82	0.54	291	9.79	1.04	6.7	5.5	1010	8.8	149	0.002	1.6	0.29	7	2	34.3	299	0.52	3.39	4.6	0.245	0.54	
HM-6 280-285	78.4	0.54	282	25.9	1.35	7.8	5.2	2210	7.5	137	<0.002	1.56	0.25	7.2	2	23.6	362	0.64	3.41	4.6	0.286	0.52	
HM-7 245-250	59.2	0.45	449	5.81	2.31	6.4	4.7	450	64	111	0.002	0.58	1.14	5.3	1	21.3	433	0.49	0.65	4.2	0.208	0.51	
HM-7 250-255	82.4	0.47	454	6.68	2.05	7.1	4.2	610	106.5	153	0.002	0.75	0.29	5.7	1	55.1	408	0.54	0.79	4.7	0.224	0.64	
HM-7 255-260	54.1	0.31	282	7.22	1.19	4.6	5	510	131	98.5	<0.002	2.18	0.96	3.8	2	23.6	250	0.33	10.1	2.9	0.144	0.39	
HM-7 260-265	63.7	0.38	306	7.04	1.51	5.6	5.2	450	33.2	107.5	0.002	1.16	0.32	4.6	1	21.6	324	0.44	8.3	3.6	0.178	0.41	
HM-7 265-270	68.1	0.47	406	3.41	2.55	6.7	4.7	500	27.3	104	<0.002	0.75	0.34	5.2	1	24.6	485	0.57	0.32	4.3	0.214	0.5	
HM-7 270-273	69.3	0.47	411	4.11	2.68	6.8	4.8	500	23	104.5	0.002	0.53	0.2	5.3	1	24	468	0.59	0.49	4.3	0.217	0.5	
HM-8 121-125	63.2	0.31	332	4.01	1.66	5.7	3.2	320	263	124.5	<0.002	0.91	1.58	3.6	1	23.7	340	0.46	0.64	4.4	0.136	0.46	
HM-8 125-131	82.7	0.37	305	5.36	1.28	5.5	3.4	300	116.5	163.5	<0.002	0.93	1.63	3.7	1	83.2	268	0.44	1.9	4.4	0.139	0.59	
HM-8 140.5-145	49.1	0.3	265	6.68	1.78	5.7	3.9	330	13.3	95.4	<0.002	1	0.67	3.3	1	16.4	367	0.49	3.82	4.4	0.135	0.35	
HM-8 145-150	49	0.29	234	7.76	1.6	5.3	4.1	290	13	96.5	0.002	1.51	0.52	3.2	2	22.8	336	0.46	7.65	4.3	0.127	0.36	
HM-8 150-155	49.7	0.32	255	9.63	1.98	6.3	4.2	330	13	102.5	0.002	1.23	0.48	3.6	1	14.4	404	0.53	1.57	4.6	0.143	0.38	
HM-8 155-160	48.2	0.31	215	9.93	1.88	6.2	4.1	330	10.4	99.5	<0.002	1.18	0.46	3.7	1	11	383	0.53	2.14	4.7	0.139	0.36	
HM-8 160-165	56.5	0.29	186	9.79	1.09	4.6	6	260	8.1	113	0.002	1.41	0.48	2.6	1	21.1	229	0.44	6.45	4	0.125	0.36	
HM-8 165-170	50	0.3	214	7.4	1.54	5.7	4.9	320	10.8	105.5	0.002	1.61	0.71	3.3	2	16.5	316	0.51	2.61	4.5	0.137	0.36	
HM-8 170-175	45.4	0.31	224	5.72	2.07	6.2	3.9	290	9.9	89.2	0.002	1	0.29	3.3	1	8.6	425	0.51	1.13	4.8	0.14	0.32	
HM-8 175-180	49.6	0.31	221	6.43	1.76	6.7	4.3	400	9.6	99	<0.002	1.23	0.25	3.7	1	11.3	371	0.56	1.54	4.8	0.145	0.35	
HM-8 277-280	52.8	0.37	326	4.93	2.36	5.3	4.6	480	45.5	80.2	<0.002	1.01	0.56	4	1	8.8	446	0.47	4.96	3.8	0.17	0.37	
HM-8 280-285	60	0.37	339	4.47	2.61	5.5	4.2	440	19.4	85.1	<0.002	0.72	0.39	4.1	1	26.7	449	0.48	1.88	3.7	0.176	0.39	
HM-8 285-290	57	0.26	197	6.57	1.21	3.7	5.6	320	16	98.1	<0.002	2.65	0.48	3	2	37.2	196.5	0.27	13.6	2.8	0.121	0.35	
HM-8 290-296	56.8	0.29	205	8.23	1.33	4.4	6.4	380	13	101.5	<0.002	1.78	0.38	3.4	2	28.8	250	0.32	5.87	3.2	0.136	0.37	
HM-9 110-115	60.1	0.34	262	10.6	1.62	5	5.7	370	10.8	87.8	<0.002	0.8	0.36	4.2	1	15.5	327	0.34	7.14	3.2	0.157	0.36	
HM-9 115-120	57.6	0.34	268	6.88	1.87	4.6	5.4	340	11	80.5	<0.002	0.82	0.48	3.8	1	15.7	337	0.33	7.05	3.3	0.162	0.35	
HM-9 120-125	80.2	0.44	373	5.44	2.39	5.8	4.5	440	23.5	114	<0.002	0.58	0.34	5	1	50.9	437	0.43	1.31	4.3	0.204	0.56	
HM-9 125-131	80.5	0.44	681	4.05	2.03	5.5	4.4	430	255	112	0.002	1.03	0.92	4.9	1	68.8	435	0.42	1.76	3.7	0.191	0.57	
HM-9 211-215	98.6	0.66	656	4.58	2.6	7.1	5.6	570	43.8	107	0.002	0.58	0.29	7.2	1	34.7	636	0.54	0.56	4.9	0.305	0.63	
HM-9 215-220	99.7	0.61	548	5.08	1.95	6.5	5.7	540	47.4	113.5	<0.002	0.67	0.25	6.9	1	44.3	508	0.53	3.31	4.7	0.275	0.59	
HM-9 220-225	94	0.64	460	5.69	1.54	6.2	5.8	500	40.8	102.5	0.002	4.24	0.31	6.3	3	43.3	456	0.46	5.34	4.1	0.261	0.53	
HM-9 225-230	45.3	0.29	319	9.46	0.77	2.8	5.6	220	22.6	52.6	<0.002	2.82	0.36	3	2	22.4	303	0.2	10.95	1.9	0.115	0.26	
HM-9 230-235	91.7	0.62	517	5.72	2.54	6.5	5.8	510	48.8	93.5	<0.002	0.48	0.29	6.9	1	16.1	630	0.49	0.65	4.5	0.277	0.6	
HM-9 235-239	99.2	0.64	675	5.57	2.56	6.8	7.6	530	58.9	103.5	0.002	0.3	0.26	7.1	1	40.3	634	0.53	0.67	4.7	0.292	0.63	
HM-10 113-115	66.4	0.46	450	4.7	3.06	6.4	5.1	540	16	75.3	<0.002	0.39	0.23	5	1	12.7	616	0.58	0.36	3.9	0.218	0.46	
HM-10 115-120	66.1	0.44	436	4.36	3.12	6.7	8	510	15.9	74	<0.002	0.13	0.21	5.1	1	6.4	591	0.63	0.14	3.9	0.22	0.46	
HM-10 120-125	68.1	0.41	413	4.39	2.35	6.3	5.2	470	19.7	89.3	0.002	0.68	0.26	5.1	1	22.2	467	0.59	3.08	3.9	0.202	0.45	
HM-10 125-130	59.3	0.42	378	5.36	2.79	6.3	5.6	560	109.5	75.9	<0.002	0.57	0.32	4.9	1	9.3	539	0.59	2.33	3.8	0.211	0.42	
HM-10 130-135	68.2	0.44	444	4.51	2.58	6.7	5.6	530	43.1	93.6	<0.002	0.46	0.36	5.2	1	19.4	516	0.65	1.2	4.1	0.216	0.51	
HM-10 135-142	66.5	0.42	558	4.04	2.49	6.5	5.4	520	57	99.5	0.002	0.46	0.26	5.1	1	26.6	491	0.62	0.43	4	0.208	0.56	
HM-11 107.5-110	67.3	0.45	426	4.17	3.01	6.6	4.3	500	21.2	72.4	<0.002	0.25	0.37	5.3	1	8.1	586	0.59	0.4	4.1	0.215	0.45	
HM-11 110-115	65.7	0.43	482	5.37	2.71	6.3	8.1	470	19.8	75.6	<0.002	0.39	0.25	5	1	16.1	524	0.55	3.46	4	0.205	0.43	
HM-11 115-120	68.1	0.47	573	4.31	3.05	6.7	4.3	510	19.9	82.1	<0.002	0.35	0.35	5.2	1	17.7	571	0.6	0.39	4.3	0.23	0.48	
HM-11 120-127	66	0.45	399	4.25	3.07	6.6	4.4	460	14.5	73.7	0.002	0.29	0.23	5.2	1	6.7	574	0.57	0.69	4.3	0.216	0.42	
HM-11 253-260	61.9	0.44	414	4.72	2.98	6.6	4.7	480	34.6	73.5	0.002	0.42	0.25	5.1	1	8.8	583	0.56	0.75	4.1	0.209	0.44	
HM-11 260-265	60.7	0.43	398	3.6	3.15	6.4	3.9	460	20.5	70.8	0.002	0.33	0.21	4.8	1	10	589	0.57	0.43	4.1	0.21	0.43	
HM-11 265-272	57.2	0.39	362	4.25	2.68	5.8	4.6	450	16.3	76.3	0.002	0.64	0.3	4.4	1	15.7	500	0.51	5.29	3.7	0.185	0.42	
HM-12 42-50	86.6	0.57	522	5.29	1.43	6	4.8	570	70.4	118.5	0.002	0.66	0.25	6.6	1	61.6	344	0.45	3.51	4.3	0.269	0.64	
HM-12 50-55	89.9	0.7	583	4.45	3.02	7.3	6	720	21.1	76.6	<0.002	0.3	0.33	7.8	1	14.4	735	0.56	0.22	4.6	0.33	0.49	
HM-12 55-60	89.2	0.72	622	5.13	3.09	7.3	6	690	14.2	70.5	<0.002	0.18	0.24	7.7	1	8.4	752	0.54	0.22	4.6	0.332	0.46	
HM-12 60-62.5	87.1	0.65	556	4.37	2.91	6.8	5.9	640	20.4	73.2	0.002	0.21	0.25	7.6	1	10.6	695	0.51	0.11	4.7	0.296	0.49	
HM-12 111-118.5	89.6	0.66	540	5.09	2.63	7	5.9	640	19	87.9	0.002	0.42	0.22	7.8	1	10.5	643	0.53	0.39	4.9	0.309	0.5	
HM-12 119-120	23.9	0.14	151	14.45	0.55	2.2	6.3	140	5.3	30.2	0.002	3.24	0.34	1.8	3	4.5	119.5	0.16	19	0.9	0.085	0.13	
HM-12 120-125	86.9	0.66	311	5.25	2.27	7.2	5.5	640	8.2	102	0.002	0.9	0.18	7.9	1	9.9	569	0.54	0.84	5.3	0.309	0.46	
HM-12 125-130	51.4	0.37	218	5.81	1.11	3.9	5.7	350	4.9	64.1	0.002	2.8	0.32	4.5	3	5.2	317	0.29	23.9	2.9	0.177	0.31	
HM-12 130-135	79.4	0.62	439	5.06	2.48	6.6	6	580	12.1	79.6	<0.002	0.72	0.32	7.1	1	9	647	0.48	2.7	4.6	0.289	0.47	
HM-12 135-140	84.2	0.68	517	4.12	2.78	6.9	6.4	630	14.2	82.2	<0.002	0.61	0.25	7.3	1	12.4	698	0.5	0.82	4.6	0.316	0.5	

Appendix (part 2)

RE12110603 - Finalized																					
CLIENT : "MINWEL - Wellborn Mining Company LLC"																					
# of SAMPLES: 96																					
DATE RECEIVED : 2012-05-17 DATE FINALIZED : 2012-06-02																					
CERTIFICATE COMMENTS: " Hg-CV41:Detection limits on samples requiring dilutions due to interferences or high concentration levels have been increased according to the dilution factor. ME-MS61r:REE's may not be to																					
	ME-MS61r	ME-MS61r	ME-MS61r	ME-MS61r	ME-MS61r	ME-MS61r	ME-MS61r	ME-MS61r	ME-MS61r	ME-MS61r	ME-MS61r	ME-MS61r	ME-MS61r	ME-MS61r	ME-MS61r	ME-MS61r	ME-MS61r	ME-MS61r	ME-MS61r	ME-MS61r	Hg-CV41
SAMPLE	U	V	W	Y	Zn	Zr	Dy	Er	Eu	Gd	Ho	Lu	Nd	Pr	Sm	Tb	Tm	Yb	Hg		
DESCRIPTION	ppm	ppm	ppm	ppm	ppm	ppm	ppm	ppm	ppm	ppm	ppm	ppm	ppm	ppm	ppm	ppm	ppm	ppm	ppm		
HM-1 175-180	1.3	49	6.4	16.3	77	25.5	2.79	1.5	1.03	3.75	0.53	0.2	19.9	4.9	4.02	0.54	0.22	1.37	0.2		
HM-1 180-185	1.4	52	12.7	15.5	92	23.2	2.63	1.37	0.93	3.72	0.5	0.18	21.4	5.39	4.15	0.52	0.2	1.21	0.1		
HM-1 185-190	1	52	6.8	14.4	71	22.4	2.53	1.3	1	3.43	0.48	0.17	19.1	4.73	3.82	0.48	0.19	1.19	<0.1		
HM-1 190-195	0.7	27	48.5	7.5	133	11.4	1.28	0.67	0.43	1.72	0.25	0.1	8.9	2.21	1.77	0.24	0.1	0.62	<0.1		
HM-1 215-220	1.2	34	16.7	11.7	79	15.6	1.97	1.03	0.72	2.73	0.38	0.13	14.5	3.62	2.88	0.39	0.15	0.95	<1		
HM-1 220-224	1.1	53	5.4	15.3	93	24.3	2.66	1.39	1.04	3.61	0.52	0.18	19.6	4.8	4.01	0.52	0.2	1.28	0.04		
HM-1 271-275	0.5	21	5.5	5.9	200	8.2	0.96	0.53	0.28	1.33	0.2	0.07	7	1.74	1.39	0.19	0.08	0.49	0.01		
HM-1 275-280	1.5	48	10.8	15.3	96	23.1	2.63	1.4	0.95	3.55	0.52	0.19	19	4.68	3.78	0.51	0.21	1.34	0.02		
HM-2 190-195	1.4	50	15.9	14.5	77	28.8	2.45	1.31	0.92	3.3	0.47	0.18	17.5	4.34	3.59	0.47	0.19	1.22	0.04		
HM-2 195-200	1.5	43	7.5	14.2	59	25.9	2.47	1.27	0.88	3.41	0.47	0.17	18.8	4.77	3.79	0.48	0.18	1.16	0.02		
HM-2 200-205	1.3	40	12.4	12.8	52	24	2.19	1.14	0.79	2.99	0.42	0.15	16.3	4.12	3.26	0.43	0.17	1.08	<0.1		
HM-2 205-210	1.4	48	14.1	14.3	88	29.8	2.55	1.33	0.85	3.42	0.5	0.18	18.3	4.51	3.77	0.5	0.2	1.26	0.02		
HM-2 210-212	1.6	49	25.2	15.2	74	31.1	2.63	1.4	0.9	3.57	0.51	0.19	19.9	4.96	3.97	0.51	0.2	1.29	<0.1		
HM-4 95-100	0.3	14	166	4.5	19	4.4	0.77	0.38	0.14	1.02	0.14	0.04	5.7	1.43	1.14	0.15	0.05	0.3	<1		
HM-4 100-105	0.9	57	12.5	14	80	22.8	2.43	1.19	0.9	3.45	0.46	0.15	22.2	5.61	4.08	0.47	0.18	1.08	0.01		
HM-4 105-110	1	57	8.9	14.2	100	22.2	2.59	1.3	1.03	3.76	0.49	0.16	22.8	5.73	4.25	0.51	0.18	1.14	<0.1		
HM-4 110-113	1.1	57	5.7	15.9	86	27.1	2.79	1.46	1.12	3.97	0.54	0.19	22.2	5.5	4.34	0.56	0.21	1.3	0.01		
HM-4 233-235	1.2	51	34.2	15.2	67	25.6	2.6	1.39	0.96	3.51	0.5	0.18	19.2	4.78	3.9	0.52	0.2	1.24	0.01		
HM-4 235-240	1.2	48	30.7	15.2	71	23.3	2.6	1.38	0.91	3.6	0.5	0.18	19.5	4.89	3.89	0.51	0.2	1.27	0.01		
HM-4 240-245	0.7	26	124.5	9	26	11.7	1.62	0.82	0.46	2.08	0.3	0.11	11.7	2.96	2.21	0.29	0.12	0.77	<1		
HM-4 245-250	0.2	11	5.5	2.9	9	3.3	0.43	0.27	0.07	0.5	0.09	0.04	2.7	0.65	0.51	0.07	0.04	0.28	<1		
HM-4 250-255	0.8	31	11.7	11	19	15.6	1.86	0.97	0.4	2.68	0.36	0.13	15.7	3.97	2.98	0.37	0.14	0.9	<1		
HM-4 255-260	1.1	41	11.1	15	31	22.1	2.38	1.29	0.68	3.13	0.47	0.17	16.7	4.16	3.35	0.45	0.19	1.21	0.01		
HM-4 290-295	1.5	47	98.1	15.1	45	28.5	2.61	1.39	0.96	3.43	0.51	0.19	18.5	4.63	3.75	0.5	0.2	1.29	<0.1		
HM-4 295-300	1.3	52	9.1	14.7	71	30.1	2.59	1.37	1	3.52	0.5	0.18	18.8	4.67	3.82	0.51	0.21	1.3	0.03		
HM-4 300-305	0.7	24	5.9	6.8	36	11.7	1.12	0.58	0.42	1.55	0.22	0.08	8.4	2.12	1.65	0.22	0.09	0.55	<0.1		
HM-4 305-310	1.4	39	12.8	13	41	26.5	2.2	1.07	0.56	3.31	0.42	0.14	20.4	5.08	3.87	0.44	0.16	0.95	<0.1		
HM-4 310-315	1	35	7.7	11.4	39	24.2	1.84	1.01	0.55	2.41	0.36	0.13	13	3.28	2.66	0.35	0.15	0.92	0.01		
HM-4 315-319	1.3	50	7.2	14.5	67	28.8	2.47	1.31	0.92	3.34	0.49	0.17	18.3	4.63	3.72	0.48	0.2	1.21	0.01		
HM-5 101-105	1.3	31	16.3	10.4	29	53	1.73	0.88	0.38	2.46	0.33	0.13	15.7	4.05	2.95	0.35	0.14	0.89	0.01		
HM-5 105-110	1.1	27	20.4	7.2	31	49.5	1.14	0.61	0.27	1.58	0.22	0.1	9.3	2.37	1.86	0.23	0.1	0.62	<0.1		
HM-5 110-115	1.1	28	15.3	7.8	24	57.4	1.45	0.85	0.34	1.76	0.28	0.12	10.3	2.57	2.07	0.27	0.11	0.73	0.01		
HM-5 115-120	1.4	41	21.9	11.2	34	68.6	2.12	1.25	0.46	2.73	0.41	0.18	15.9	3.98	3.2	0.41	0.17	1.05	0.01		
HM-5 120-125	1.5	52	163.5	14.6	32	73.7	2.87	1.68	0.63	3.43	0.56	0.22	20	4.99	4.03	0.54	0.23	1.46	<1		
HM-5 125-130	1.5	45	449	12.3	32	74.8	2.39	1.42	0.49	2.89	0.47	0.19	16.8	4.16	3.38	0.46	0.19	1.25	<0.01		
HM-6 175-180	1.2	56	6.1	15.4	59	26.8	3.05	1.76	1.08	3.77	0.59	0.21	21.6	5.22	4.57	0.58	0.22	1.39	0.02		
HM-6 180-185	1.3	55	9.1	15	47	27	2.98	1.68	1.02	3.71	0.58	0.21	20.9	5.04	4.35	0.56	0.22	1.35	0.01		
HM-6 185-190	1.3	57	3.4	14.7	32	26.6	2.96	1.64	1.04	3.81	0.57	0.2	21	5.15	4.44	0.57	0.22	1.34	0.01		
HM-6 190-195	1.1	42	9.3	13	44	20.6	2.45	1.43	0.68	2.97	0.48	0.16	17	4.16	3.5	0.46	0.18	1.14	<0.01		
HM-6 195-200	1.3	54	5.3	16.4	71	27.1	3.13	1.84	1.04	3.86	0.61	0.21	22	5.43	4.48	0.6	0.23	1.42	0.01		
HM-6 200-203.5	1.2	56	3.6	15.9	56	27.1	3.16	1.82	1.09	3.81	0.61	0.21	21.7	5.26	4.55	0.6	0.23	1.43	0.02		
HM-6 276-280	1.7	49	18.1	14.8	75	30.8	2.92	1.6	0.67	3.61	0.56	0.21	21.9	5.42	4.39	0.56	0.21	1.32	0.01		
HM-6 280-285	2.3	51	20.2	17.9	40	40.8	3.49	1.92	0.78	4.23	0.66	0.24	23	5.62	4.98	0.67	0.26	1.61	0.01		
HM-7 245-250	1.3	38	6	11.3	49	65.5	2.17	1.21	0.73	2.78	0.41	0.16	16.3	4.07	3.36	0.43	0.16	0.99	0.01		
HM-7 250-255	1.7	39	10.6	12.5	678	75.9	2.39	1.37	0.77	3.19	0.47	0.17	18.9	4.75	3.8	0.47	0.18	1.14	0.01		
HM-7 255-260	1	27	52.1	7.9	38	44.2	1.52	0.82	0.49	1.99	0.28	0.11	11.9	2.99	2.43	0.3	0.11	0.67	<0.1		
HM-7 260-265	1.2	33	8.8	9.6	51	52.3	1.8	0.99	0.55	2.33	0.34	0.13	13.9	3.48	2.83	0.35	0.13	0.84	<0.1		
HM-7 265-270	1.5	36	7.4	11.3	92	65.1	2.25	1.26	0.81	2.85	0.43	0.16	16.9	4.18	3.38	0.44	0.17	1.04	0.01		
HM-7 270-273	1.5	36	6	11.5	85	64.8	2.13	1.2	0.81	2.83	0.41	0.16	16.9	4.22	3.45	0.42	0.16	1.01	0.01		
HM-8 121-125	1.5	20	12.9	7.9	123	76.7	1.5	0.79	0.6	2.26	0.28	0.11	15.3	3.96	3.02	0.31	0.11	0.68	0.02		
HM-8 125-131	1.6	22	12.1	7.3	58	77.3	1.46	0.78	0.54	2.13	0.26	0.11	14.5	3.71	2.81	0.3	0.1	0.68	0.01		
HM-8 140.5-145	2	18	8.2	8.3	78	72.3	1.63	0.87	0.63	2.34	0.3	0.12	15.2	3.91	3	0.35	0.12	0.74	<0.01		
HM-8 145-150	1.5	17	126	8.1	544	71.7	1.59	0.82	0.6	2.27	0.29	0.11	15.1	3.8	2.92	0.33	0.11	0.71	<0.1		
HM-8 150-155	1.7	20	13.9	9.1	32	79	1.75	0.92	0.68	2.49	0.32	0.13	15.8	4.06	3.15	0.34	0.12	0.79	0.01		
HM-8 155-160	1.7	20	10.1	8.8	28	77.3	1.74	0.94	0.63	2.56	0.31	0.13	16.2	4.15	3.28	0.36	0.12	0.78	0.01		
HM-8 160-165	1.5	20	10.9	7	27	66.7	1.34	0.76	0.39	1.78	0.25	0.11	11.2	2.84	2.23	0.27	0.1	0.67	<0.01		
HM-8 165-170	1.7	19	55.3	8.6	26	73.9	1.67	0.92	0.58	2.3	0.31	0.12	13.9	3.54	2.82	0.33	0.12	0.77	0.01		
HM-8 170-175	1.8	18	6.7	8.8	17	79.6	1.72	0.91	0.74	2.49	0.31	0.12	16.2	4.07	3.15	0.36	0.12	0.76	0.01		
HM-8 175-180	2	20	10.4	8.8	26	80.1	1.79	0.9	0.65	2.7	0.32	0.12	16.3	4.2	3.31	0.38	0.12	0.76	0.02		
HM-8 277-280	1.3	29	5.6	8.8	72	70	1.73	0.93	0.69	2.39	0.32	0.12	14.5	3.61	2.86	0.35	0.12	0.78	0.01		
HM-8 280-285	1.4	30	6.7	8.8	47	79	1.77	0.93	0.72	2.42	0.33	0.13	14.3	3.57	2.94	0.36	0.12	0.81	0.01		
HM-8 285-290	1	23	21.1	6.4	1470	46.4	1.26	0.66	0.39	1.67	0.23	0.1	10	2.55	2	0.25	0.08	0.58	<0.1		
HM-8 290-296	1.1	25	21.7	7.5	49	60.7	1.4	0.79	0.41	1.84	0.27	0.11	11	2.79	2.26	0.27	0.1	0.67	0.01		
HM-9 110-115	1	30	8.7	7.9	81	49.1	1.53	0.84	0.49	2.03	0.29	0.11	12.1	3.03	2.43	0.3	0.1	0.69	<0.1		
HM-9 115-120	1	30	6	7.9	57	52.2	1.53	0.87	0.56	2.05	0.29	0.11	12.5	3.14	2.51	0.3	0.11	0.73	<0.1		
HM-9 120-125	1.3	35	6.1	10.6	83	68.1	2.08	1.15	0.78	2.76	0.4	0.16	16.9	4.26	3.45	0.42	0.15	0.96	0.01		
HM-9 125-131	1	33	6.2	9.6	270	54.7	1.92	0.93	0.73	2.33	0.36	0.13	14.8	3.71	3.02	0.35	0.14	0.88	0.01		
HM-9 211-215	1	54	5.1	16.3	129	24.4	3.16	1.67	1.09	3.55	0.61	0.22	22.2	5.55	4.57	0.55	0.25	1.55	0.01		
HM-9 215-220	1.1	48	6.4	14.7	116	22.4	2.84	1.48	0.99	3.39	0.55	0.18	21.2	5.28	4.33	0.52	0.21	1.28	0.01		
HM-9 220-225	1	46	7	13	107	19.2	2.58	1.31	0.78	2.96	0.49	0.16	18.1	4.43	3.7	0.44	0.19	1.12	<0.1		
HM-9 225-230	0.5	25	4	6.6	40	10.3	1.16	0.61	0.39	1.41	0.24	0.08	9	2.26	1.78	0.21	0.09	0.55	<0.1		
HM-9 230-235	1.1	50	3.9	14.5	105	24.3	2.87	1.49	1.03	3.36	0.56	0.19	20.8	5.15	4.3	0.5	0.21	1.31	0.01		
HM-9 235-239	1.2	52	4.5	14.6	179	26.1	2.91	1.46	1.05	3.37	0.55	0.18	21.4	5.27	4.36	0.51	0.21	1.28	0.01		
HM-10 113-115	1.4	38	7.4	11.5	1830	55.5	2.18	1.16	0.86	2.48	0.43	0.16	15.4	3.84	3.21	0.39	0.17	1.08	0.04		
HM-10 115-120	1.4	38	3.2	12	71	57.7	2.37	1.22	0.88	2.74	0.46	0.18	15.6	3.86	3.27	0.41	0.18	1.16	0.01		
HM-10 120-125	1.5	36	5.1	11.6	87	50.9	2.22	1.14	0.82	2.56	0.42	0.16	16.1	4.03	3.32	0.39	0.16	1.06	0.01		
HM-10 125-130	1.4	36	4.3	11.5	59	53	2.19	1.11	0.8	2.54	0.43	0.15	14.9	3.78	3.14	0.38	0.16	1.04	0.03		
HM-10 130-135	1.5	38	31	11.7	86	55.7	2.24	1.14	0.82	2.63	0.43	0.15	16.2	4.06	3.38	0.41	0.17	1.06	0.02		
HM-10 135-142	1.4	36	145.5	11.7	195	53.2	2.22	1.13	0.8	2.56	0.42	0.15	15.5	3.9	3.29	0.4	0.17	1.04	0.02		
HM-11 107.5-110	1.4	37	2.9	12	59	56.4	2.31	1.13	0.89	2.62	0.43	0.15	17.3	4.4	3.6	0.41	0.17	1.05	0.02		
HM-11 110-115	1.4	35	5.6	11.5	64	52	2.21	1.13	0.86	2.62	0.42	0.15	16.7	4.21	3.47	0.41	0.16	1.07	<0.1		
HM-11 115-120	1.4	39	3.4	12.2	57	56.7	2.39	1.23	0.97	2.87	0.46	0.16	18	4.54	3.75	0.44	0.18	1.1	0.01		
HM-11 120-127	1.4	37	4	11.7	46	59	2.31	1.15	0.91	2.72	0.43	0.15	17.4	4.41	3.62	0.41	0.16	1.05	0.01		
HM-11 253-260	1.3	35	3	11.7	75	58.7	2.24	1.12	0.88	2.65	0.42	0.16	16.9	4.32	3.47	0.4	0.17	1.03	0.01		
HM-11 260-265	1.3	33	3.8	10.8	60	62.9	2.05	1.09	0.85	2.57	0.4	0.15	15.9	4.03	3.26	0.38	0.16	0.97	0.01		
HM-11 265-272	1.3	30	145.5	10.3	168	57.4	1.94	1.01	0.76	2.34	0.38	0.14	14.9	3.81	3.14	0.36	0.14	0.89	<0.1		
HM-12 42-50	1.2	50	45.4	13.1	124	19	2.66	1.37	0.91	3.08	0.51	0.18	19.2	4.91	3.89	0.48	0.2	1.23	0.01		
HM-12 50-55	1.3	61	4.4	16.1	82	22.9	3.17	1.62	1.16	3.66	0.61	0.2	22.5	5.61	4.75	0.56	0.23	1.4	0.01		
HM-12 55-60	1.2	61	4.8	16.1	90	23.1	3.16	1.62	1.19	3.7	0.61	0.2	22.3	5.54	4.59	0.56	0.24	1.45	0.01		
HM-12 60-62.5	1.2	55	2.9	15.6	89	22.3	3.21	1.67	1.14	3.63	0.61	0.2	21.9	5.42	4.56	0.56	0.23	1.42	0.01		
HM-12 111-118.5	1.2	58	75.6	16.1	69	22.9	3.19	1.64	1.15	3.7	0.62	0.2	23.7	5.84	4.88	0.57	0.23	1.41	0.01		
HM-12 119-120	0.3	17	10.8	5.7	12	6.4	0.96	0.59	0.18	0.82	0.2	0.08	3.9	0.97	0.85	0.14	0.09	0.56	<1		
HM-12 120-125	1.3	57	9.5	16.6	40	22	3.28	1.71	1.03	3.77	0.63	0.21	23.8	5.94	4.86	0.59	0.24	1.45	0.02		
HM-12 125-130	0.8	34	46.1	9.5	22	12.2	1.88	0.97	0.52	2.21	0.35	0.12	13.6	3.39	2.75	0.33	0.13	0.84	<1		
HM-12 130-135	1.1	53	6.6	14.8	60	21.1	2.93	1.52	1.03	3.4	0.57	0.19	21.2	5.22	4.33	0.53	0.22	1.35	0.02		
HM-12 135-140	1	58	5.2	14.9	93	21.9	2.93	1.54	1.07	3.39	0.58	0.19	21.8	5.39	4.55	0.52	0.22	1.37	0.01		

Appendix (part 3)